State of California
California Natural Resources Agency
DEPARTMENT OF WATER RESOURCES

Methodology for Flow and Salinity Estimates in the Sacramento-San Joaquin Delta and Suisun Marsh

36th Annual Progress Report to the
State Water Resources Control Board in
Accordance with Water Right Decisions 1485 and 1641

June 2015

Edmund G. Brown Jr.	**John Laird**	**Mark W. Cowin**
Governor	Secretary for Natural Resources	Director
State of California	California Natural Resources Agency	Department of Water Resources

Foreword

This is the 36th annual progress report of the California Department of Water Resources San Francisco Bay-Delta Evaluation Program, which is carried out by the Delta Modeling Section. This report is submitted annually by the section to the California State Water Resources Control Board pursuant to its Water Right Decision 1485, Term 9, which is still active pursuant to its Water Right Decision 1641, Term 8.

This report documents progress in the development and enhancement of computer models for the Delta Modeling Section of the Bay-Delta Office. It also reports the latest findings of studies conducted as part of the program. This report was compiled under the direction of Tara Smith, program manager for the Bay-Delta Evaluation Program.

Online versions of previous annual progress reports are available at:

http://baydeltaoffice.water.ca.gov/modeling/deltamodeling/annualreports.cfm.

For more information contact:

Tara Smith

Chief, Delta Modeling Section
Bay-Delta Office
California Department of Water Resources

tara@water.ca.gov
(916) 653-9885

State of California
Edmund G. Brown Jr., Governor

California Natural Resources Agency
John Laird, Secretary for Natural Resources

Department of Water Resources
Mark W. Cowin, Director

Laura King Moon, Chief Deputy Director

Office of the Chief Counsel
Cathy Crothers

Public Affairs Office
Ed Wilson, Director

Security Operations
Bill Croyle

Policy Advisor
Waiman Yip

Legislative Affairs Office
Kasey Schimke, Ass't Dir.

Deputy Directors

Gary Bardini	**Integrated Water Management**
Carl Torgersen	**State Water Project**
John Pacheco	**California Energy Resources Scheduling**
Kathie Kishaba	**Business Operations**
Bill Croyle	**Statewide Emergency Preparedness and Security**
Jeffrey Ingles	**Internal Audits Office**
Stephanie Varrelman	**Office of Workforce Equality**

Bay Delta Office
Paul A. Marshall, Chief

Modeling Support Branch
Francis Chung, Chief

Delta Modeling Section
Tara Smith, Chief

Edited by

Min Yu, Bay-Delta Office
See individual chapters for authors.

Editorial review
Supervisor of Technical Publications,
Patricia Cornelius
Jeff Woled, Research Writer

Contents

Foreword ..... **iii**
Preface ..... **x**

1 PTM Fish Behavior Development Workshop **1-1**

1.1 INTRODUCTION 1-1
1.2 BACKGROUND 1-1
1.3 GOALS AND OBJECTIVES 1-1
1.4 METHODOLOGIES 1-1
1.4.1 Swimming Velocity Calibration 1-2
1.4.2 Particle Route Selection Submodel 1-2
1.4.3 Particle Survival Submodel 1-3
1.5 COLLABORATION PLAN 1-3

2 New Reservoir Implementation in DSM2 V8.1.3 ..... **2-1**

2.1 INTRODUCTION 2-1
2.2 DESCRIPTION 2-1
2.3 RESULTS COMPARISON 2-8
2.4 SUMMARY 2-15

3 Estimating the Impact of Groundwater on Delta Channel Depletions **3-1**

3.1 BACKGROUND 3-1
3.1.1 Delta channel depletion relates to model EC in the summers of critical and dry years 3-1
3.1.2 Existing problems in modeling Delta channel depletion 3-1
3.2 LITERATURE REVIEW 3-2
3.2.1 Delta Upland findings 3-2
3.2.2 Delta Lowlands findings 3-2
3.3 DETAW-CD METHODOLOGY 3-3
3.3.1 Groundwater for Delta Uplands irrigation 3-3
3.3.2 Groundwater for Delta Lowlands irrigation 3-3
3.3.3 Deep percolation 3-3
3.4 IMPACTS OF INCORPORATING GROUNDWATER ON CHANNEL DEPLETION, DELTA OUTFLOW AND EC MODELING 3-3
3.4.1 Impact on Channel Depletion 3-3
3.4.2 Impact on Net Delta Outflow (NDO) 3-4
3.4.3 Impact on EC Simulation 3-4
3.5 CONCLUSION 3-6
3.6 REFERENCES 3-6

4 Modeling Physical Barriers (Gates) as Engineering Solutions to Satisfy National Marine Fisheries Services Biological Opinion Reasonable Prudent Alternative Action IV.1.3 ..... **4-1**

4.1 INTRODUCTION 4-1

4.2 THE SIMULATION MODEL 4-1

4.3 METHODOLOGY 4-1
4.3.1 Description of Existing Condition 4-2
4.3.2 Description of Modeling Scenarios 4-3
4.4 MODEL RESULTS 4-7
4.4.1 Full Flow Blockage to Delta Channels 4-10
4.4.2 Partial Flow Blockage to Delta Channels 4-11
4.4.3 Flow Blockage used in other Projects 4-11
4.5 CONCLUSION 4-28
4.6 REFERENCES 4-36

5 Visualizing DSM2 Simulation Results with ArcMap 5-1

5.1 INTRODUCTION 5-1
5.1.1 Python 5-1
5.1.2 ArcGIS 5-1
5.1.3 DSM2 Output 5-1
5.1.4 NetCDF 5-1
5.2 STEPS TO CREATE ANIMATION IN ARCMAP 5-2
5.3 EXAMPLES 5-9
5.4 CONCLUSIONS 5-10
5.5 REFERENCES 5-10

6 Rating Clifton Court 6-1

6.1 SUMMARY 6-1
6.2 CLIFTON COURT FOREBAY 6-1
6.3 PROJECT DATA 6-3
6.4 PRIOR GATE RATINGS 6-4
6.5 DYNAMIC RESPONSE TO RADIAL GATES 6-5
6.6 THE NEW RATING 6-6
6.7 SYNTHESIZING HEIGHTS 6-8
6.8 VALIDATION THROUGH FLOW BALANCE 6-8
6.9 DSM2 EXPERIMENTS WITH FULL AND LIMITED DATA 6-16
6.10 OLD VERSUS NEW RATING 6-16
6.11 DATA GRANULARITY 6-19
6.12 BANKS DATA GRANULARITY 6-21
6.13 GATE TIMING: SCHEDULED PRIORITY 3 VS HISTORICAL 6-21
6.14 CONCLUSION 6-22
6.15 REFERENCES 6-22

7 Calibrating the Martinez Boundary Salinity Generator Using PEST 7-1

7.1 INTRODUCTION 7-1
7.2 BACKGROUND 7-1
7.2.1 G Model 7-2
7.2.2 Tidal Signal Incorporation 7-3
7.2.3 Model Calibration and Problems 7-3
7.3 METHODOLOGY AND STUDY CONFIGURATION 7-5
7.3.1 Theory 7-6
7.3.2 Configuration Setup 7-6

7.4 RE-CALIBRATION RESULTS AND DISCUSSION 7-8
7.4.1 Calibration for year 1991-1993 7-8
7.4.2 Model Improvement and Re-calibration 7-8
7.4.3 Re-Calibration with Other Periods 7-11
7.5 SUMMARY AND FUTURE WORKS 7-12
7.6 REFERENCE 7-13

8 Bay-Delta SCHISM Model Developments and Applications 8-1

8.1 INTRODUCTION 8-1
8.2 PUBLIC RELEASE 8-1
8.3 APPLICATIONS 8-2
8.3.1 Drought modeling and emergency barriers 8-2
8.3.2 Temperature calibration 8-2
8.3.3 Flood Robustification 8-4
8.3.4 Liberty Island and Yolo County 8-4
8.4 ALGORITHMIC IMPROVEMENTS 8-4
8.5 REFERENCES 8-6

Preface

Chapter 1. PTM Fish Behavior Development Workshop

This chapter summarizes the Particle Tracking Model (PTM) Fish Behavior Development Workshop held at DWR on January 8, 2015. This workshop was attended by PTM developers from National Marine Fisheries Service (NMFS), U.S. Geological Survey (USGS), and California Department of Water Resources (DWR). The leads for the three agencies were Doug Jackson (NMFS), Russel Perry (USGS), and Xiaochun Wang (DWR).

Chapter 2. New Reservoir Implementation in DSM2 V8.1.3

This chapter describes a modification for the Delta Simulation Model 2 (DSM2) open water areas to include changing bathymetry with elevations. Previously, open water areas were treated as a constant area with a bottom elevation. This change will help to better model Liberty Island in addition to other open water areas in the Delta. The elevation-area-storage curves for reservoirs can be calculated using geographic information system (GIS) tools like ArcMap. The model has been tested and new results have been evaluated.

Chapter 3. Estimating the Impact of Groundwater on Delta Channel Depletions

This chapter describes the study that integrated the consumptive use, hydrodynamics, and water quality models and also calibrated the groundwater supply and electric conductivity together by using the correlation between Delta outflow and EC. With the estimated groundwater contribution, EC, in the summers of the critical and dry years, could be estimated close to the measured field data.

Chapter 4. Modeling Physical Barriers (Gates) as Engineering Solutions to Satisfy NMFS BiOp RPA Action IV.1.3

This chapter provides detailed modeling information on the potential impact on flow, water quality, and water level throughout the Delta of physical barriers (gates) as engineering solutions to deter fish from entering the Delta. The modeling was performed to provide information to support decision-making for engineering solutions to satisfy the National Marine Fisheries Service Biological Opinion Reasonable Prudent Alternative (NMFS-BiOp RPA) Action IV.1.3 (Action). The Action objective is to prevent emigrating salmonids from entering into the Interior of the Delta and southern Delta, and to reduce exposure to the Central Valley Project (CVP) and State Water Project (SWP) export facilities. Delta Simulation Model II (DSM2) was used to simulate gates on the Delta channels: Georgiana Slough, Head of Old River, Turner Cut, and Columbia Cut. The modeling results have been evaluated for impact analysis of flow, water quality, and water level throughout the Delta.

Chapter 5. Visualizing DSM2 Simulation Results with ArcMap

The Delta Simulation Model II has been widely used for three types of Delta simulations: historical conditions, near- and long-term forecasting, and planning studies. DSM2 simulations have been applied for various purposes. Some examples include forecasting water quality in the Delta and the California Aqueduct system, generating hydrologic information for a permit application, and providing support for litigation. Since DSM2 simulation results can be presented to members of the public coming from various backgrounds, it is vital to present simulation results tailored to meet the needs of different audiences. In the past, the visualization of DSM2 electric conductivity results was readily accepted. Even so, it takes many steps to prepare an animation, and the process relies on a program called Tecplot.

Tecplot was fairly uneconomical to purchase, especially considering that Tecplot has been rarely used by other staff in the Bay-Delta Office.

This chapter presents several ways to visualize DSM2 simulation results with ArcMap, a product of Environmental Systems Research Institute (ESRI). A programming language, Python, is used to convert DSM2 output to ArcGIS geodatabase or NetCDF files.

Chapter 6. Rating Clifton Court

With the help of staff at California Department of Water Resources (DWR) Operations and Maintenance (O&M), Delta Field Division (DFD), and North Central Region Office (NCRO), the Delta Modeling Section has developed a new rating for the Clifton Court radial gates — a formula for estimating flow into the forebay based on gate heights and water levels inside and outside the gates. The new rating is suitable for operational and modeling purposes. Clifton Court Forebay is included explicitly in our models, DSM2 and SCHISM. In addition to presenting the new rating, we describe DSM2 modeling experiments that show the role the gates play in the local balance and where modeling error tends to manifest. Although our main results are obtained with detailed gate data and pumping data, we also address situations, such as planning scenarios, where detailed time series of gate heights and exports are not available.

The main potential impact of the work presented in this chapter is on water levels in the forebay, where the Clifton Court gate characterization and modeling practices have an enormous impact on results. There are more minor impacts as well on exterior water levels in the South Delta, on high tide, on water quality, and residence time in the forebay.

Chapter 7. Calibrating the Martinez Boundary Salinity Generator using PEST

Martinez represents the stage-and-salinity boundary and the location for applying the Delta Simulation Model 2 (DSM2). The salinity at this location is estimated using the Net Delta Outflow (NDO) and stage. This chapter presents a re-calibration effort for the Martinez boundary salinity generator, with a mathematically based calibration software named PEST. This new calibration improves the performance of the model by better matching the historical salinity data, particularly at the higher value range. The performance of the current calibration has been a concern of water resources management, especially in the current drought crisis.

This chapter describes the background of the Martinez boundary salinity generator, explains the methodology and configuration of PEST for model calibration, and presents some preliminary findings.

Chapter 8. Bay-Delta SCHISM Model Developments and Applications

The Bay-Delta SCHISM project is an application of the 3D SCHISM (Semi-Implicit Cross-Scale Hydroscience Integrated System Model) that offers the capability to study cross-scale, multidimensional flow and transport in the Bay-Delta. SCHISM is an open source, 3D computational model derivative from an earlier model, SELFE. We have incorporated into SCHISM practical details needed to model the Bay-Delta, such as agricultural sources and sinks, gates and seasonal gates, and barriers. Work on the model has been collaborative with the Virginia Institute of Marine Science and other users.

The model has been deployed for studies over the full domain of two years by DWR, and we have begun offering institutional support through workshops. The model has also been used as the estuary hydrodynamic component of multidisciplinary collaborations with National Aeronautics and Space Administration (NASA), National Marine Fisheries Service/National Oceanic and Atmospheric Administration (NMFS/NOAA), and San Francisco State University, including the SESAME project, a full

life cycle model for fish, and NASA-HICO, a remote sensing and nutrient modeling analysis of human impacts.

Development in the past year has emphasized a public release, drought applications, and algorithm improvements. Progress has been made towards diverse capabilities such as robust flood modeling and temperature calibration. Chapter 8 surveys some of the work, much of which is in progress.

Methodology for Flow and Salinity Estimates in the Sacramento-San Joaquin Delta and Suisun Marsh

36th Annual Progress Report

June 2015

Chapter 1
PTM Fish Behavior Development Workshop

Author: Xiaochun Wang
Delta Modeling Section
Bay-Delta Office
California Department of Water Resources

Contents

1 PTM Fish Behavior Development Workshop 1-1
1.1 INTRODUCTION 1-1
1.2 BACKGROUND 1-1
1.3 GOALS AND OBJECTIVES 1-1
1.4 METHODOLOGIES 1-1
1.4.1 Swimming Velocity Calibration 1-2
1.4.2 Particle Route Selection Submodel 1-2
1.4.3 Particle Survival Submodel 1-3
1.5 COLLABORATION PLAN 1-3

1 PTM Fish Behavior Development Workshop

1.1 Introduction

This chapter summarizes the Particle Tracking Model (PTM) Fish Behavior Development Workshop held at DWR on January 8, 2015. This workshop was attended by PTM developers from National Marine Fisheries Service (NMFS), U.S. Geological Survey (USGS), and California Department of Water Resources (DWR). The leads for the three agencies were Doug Jackson (NMFS), Russel Perry (USGS), and Xiaochun Wang (DWR).

1.2 Background

NMFS and DWR staff, for the most part, have been independently developing fish behavior PTMs with USGS staff providing expertise on developing methodologies for calibration and fish behavior submodels. The purpose of this technical workshop was to establish a plan for coordinating NMFS and DWR PTM behavior development efforts.

In the workshop, the participants from the three agencies learned the background of the development efforts, reviewed differences in the development goals and objectives between NMFS and DWR, discussed technical details of methodologies, provided updates on development status, and identified opportunities for collaboration.

1.3 Goals and Objectives

NMFS and DWR both seek to develop a PTM with fish behaviors assigned to the neutrally buoyant particles to evaluate possible impacts on fish migration through the Delta because of project operations and new construction in the Delta. However, the NMFS and DWR PTM behavior developments differ in scope. The NMFS PTM behavior development has a specific goal and a targeted species. As a part of the NMFS Central Valley Chinook Life Cycle Model, the NMFS PTM will provide smolt mortality rate for the life cycle model during smolt migration through the Delta. Therefore, its development is focused on Chinook smolts. In addition, because of the tight time frame for the scheduled release of the Chinook Life Cycle Model in March 2015, and the specifically targeted fish species, model reusability, flexibility, and scalability are not emphasized.

DWR intends to develop a PTM with fish behaviors that is more flexible and scalable, that is a model that accommodates various species and environmental conditions and is more accessible to the general public. In addition, because fish behavior research is an active field, DWR's model development will take into consideration reusability for future development.

Although NMFS and DWR have differences in the scope of the development, the workshop participants agreed that coordinating development efforts of the two agencies would be mutually beneficial. Therefore, it was decided that NMFS and DWR will merge the current development and work collaboratively in the future to produce a single set of behavior submodels for Chinook smolts.

1.4 Methodologies

The methodologies being used by the two agencies to calibrate the behavior submodels are being developed primarily by USGS (Russell Perry's group). Three types of behaviors are needed to make a particle "fish-like": swimming, survival, and route selection. The following sections provide brief explanations of the methods used to implement the three behaviors into PTM.

1.4.1 Swimming Velocity Calibration

Both NMFS and DWR calibrate the particle swimming velocities from field-observed acoustic telemetry tag data using optimization techniques. However, there are major differences in the optimization methods and swimming behavior submodels.

NMFS employs an optimization method that is based on a Bayesian framework and a Markov Chain Monte Carlo algorithm. This method requires repeated sampling, on the order of thousands of samples, of PTM outputs under different parameterizations. Generating this large number of PTM realizations by running the PTM directly would be impracticable. To address this issue, emulators of the PTM outputs are constructed. Once these emulators are constructed, they allow for nearly instantaneous estimates of the PTM outputs for any arbitrary parameterization. However, there is a substantial upfront cost to generate the emulators, as it requires the PTM to be run numerous times across a range of parameter values. There is also significant expertise required to tailor this framework to a specific data set, making this approach inaccessible to most DSM2 users.

In contrast, DWR's method allows users to couple an optimization routine with PTM simulations. Users can plug in a specific set of observed data and obtain the swimming parameters tailored for this set of data. This will be a powerful tool for fish biologists who are interested in finding behavior patterns for a specific fish species under specific environmental conditions. Then again, there is a cost for the flexibility. It requires more development effort, and it is computationally more expensive. Currently, USGS and DWR are working on applying an efficient optimization method called Particle Swarm Optimization (PSO) to PTM. PSO is a population-based stochastic optimization technique. Since its development in 1995, PSO has demonstrated it can find a global optimum faster and cheaper than many other optimization methods.

Two holding behavior submodels are used to calibrate swimming velocities. They are selective tidal stream transport (STST), where there is fish hold position if the upstream flow exceeds a specified threshold, and diel-holding submodels. NMFS' STST submodel uses 1) a velocity threshold, 2) the net direction of flow over one or more tidal cycles, and 3) a probability of confusion, which is a function of a signal-to-noise ratio (the mean flow over the standard deviation of flow), to decide whether a particle is holding or swimming. In contrast, DWR's submodel only uses a velocity threshold (a fitting parameter) to make this decision.

For the holding behavior during a diel period, NMFS' submodel only allows particles to swim during a specified period centered on midnight. DWR's submodel uses sunrise and sunset to determine daytime and nighttime. All particles swim during nighttime. During daytime, whether or not a particle swims is determined by a probability calculated from the percentage of the particles allowed to swim. The percentage is a fitting parameter.

1.4.2 Particle Route Selection Submodel

In the original PTM, the probability of a particle selecting a certain route, either a branch or the main stem of a river, at a river junction is based on the flow split proportion to the route. The higher the flow into the route, the higher the probability a particle selects the route. When a particle's swimming velocity is superimposed on a river velocity, the net velocity, which decides the direction of the particle's movement, may not be in the same direction as the river flow. In turn, this may cause numerical errors and the PTM to crash. To solve this problem, NMFS' route selection submodel prohibits the particle from selecting the route when there is a directional conflict in the net velocity and the river flow. DWR's submodel has a different approach; a swimming flow (swimming velocity multiplied by the channel cross-sectional area) is superimposed on the river flow. The probability of the route selection is then calculated using the original flow split method. By superimposing swimming flow, the higher the

combined river and swimming flows, which relate to the swimming velocity and channel cross-sectional area, the higher probability a particle will enter the route.

Using flow splits to calculate route selection probabilities is a simple model that may not match actual fish routing dynamics, but is general enough to be used at any river junction. In contrast, generalized linear models fit to telemetry data at a specific junction may describe routing dynamics well, but cannot be generalized across junctions. Therefore, DWR, NMFS, and USGS are working toward developing a set of routing models that are general enough to apply to river junctions where no telemetry data exists, but are specific enough to capture the primary mechanisms affecting migration routing.

1.4.3 Particle Survival Submodel

NMFS uses an XT model to calculate smolt survival rates. The XT model relates smolt survival through the Delta to the smolt travel distance (X) and time (T). The XT model is implemented in PTM and the two model parameters, λ and ω, are calibrated using acoustic telemetry tag data.

DWR implements a survival model developed by USGS that relates the smolt survival rates to river discharge. The parameters were estimated from observed acoustic telemetry tag data.

1.5 Collaboration Plan

The workshop participants carefully examined the different methodologies and discussed technical details of each method. The discussion took into consideration the two agencies' goals and objectives. It was decided that the current development work from NMFS and DWR will be integrated by taking the best of both efforts and only one set of behavior submodels for Chinook smolts will be developed. After weighing the pros and cons in terms of ecological, fish-biological, and software developmental merits for the different methods, the participants agreed that NMFS will adapt DWR's route selection and diel holding submodels. DWR will use NMFS' STST and calibrated XT submodels.

Because of the differences in development goals, it was also agreed that both NMFS and DWR will keep their own optimization method so that DWR will have a general, data-driven model to release to the public domain while NMFS will have a more specific PTM for the life cycle model to meet the release schedule. The other added benefit to using different optimization methods to calibrate the PTM parameters is that the parameters can be compared from the different methods to ensure the consistency and quality of the PTM calibration.

The workshop action items for USGS, NMFS, and DWR were:

1) DWR and NMFS will exchange and review the PTM codes.

2) NMFS will implement DWR's route selection and diel-period-holding submodels.

3) DWR will implement NMFS' STST and calibrated XT submodels.

4) USGS will develop a PSO routine to be implemented in PTM.

The timeline for completing the above list is April-May, 2015. For future collaboration, DWR will schedule quarterly technical meetings so that the involved parties can be updated on each other's development status.

In summary, the PTM Behavior Development Workshop was very productive. The technical issues, arising from the development of the software to simulate smolt behaviors, were thoroughly discussed, the tasks were finalized and assigned, the timeline to complete the tasks was set, and future collaborations were planned. The group will submit a proposal for future PTM development at the next meeting.

Methodology for Flow and Salinity Estimates in the Sacramento-San Joaquin Delta and Suisun Marsh

36th Annual Progress Report
June 2015

Chapter 2
New Reservoir Implementation in DSM2 V8.1.3

Authors: Lianwu Liu and Prabhjot Sandhu
Delta Modeling Section
Bay-Delta Office
California Department of Water Resources

Contents

2 New Reservoir Implementation in DSM2 V8.1.3 2-1
2.1 INTRODUCTION 2-1
2.2 DESCRIPTION 2-1
2.3 RESULTS COMPARISON 2-8
2.4 SUMMARY 2-15

Figures

Figure 2-1 Liberty Island Storage Area Map 2-3
Figure 2-2 Flow at Sacramento River at Rio Vista 2-9
Figure 2-3 Stage at Sacramento River at Rio Vista 2-10
Figure 2-4 Flow at San Joaquin River at Jersey Point (RSAN018) 2-11
Figure 2-5 Stage at San Joaquin River at Jersey Point (RSAN018) 2-12
Figure 2-6 Stage at San Joaquin River at Jersey Point (RSAN018) 2-13
Figure 2-7 Simulated EC at San Joaquin River at Jersey Point (RSAN018) 2-13
Figure 2-8 Simulated EC at Old River at Bacon Island (ROLD024) 2-14
Figure 2-9 Simulated EC at Clifton Court Forebay 2-14

Tables

Table 2-1 Calculated Reservoir Elevation-Area-Volume at Liberty Island 2-2
Table 2-2 New RESERVOIR_VOL Table 2-4
Table 2-3 Calculated Reservoir Elevation-Area-Volume at Clifton Court Forebay 2-5
Table 2-4 Calculated Reservoir Elevation-Area-Volume at Franks Tract 2-6
Table 2-5 Calculated Reservoir Elevation-Area-Volume at Bethel 2-7
Table 2-6 Calculated Reservoir Elevation-Area-Volume at Mildred 2-7
Table 2-7 Calculated Reservoir Elevation-Area-Volume at Discovery Bay 2-8

2 New Reservoir Implementation in DSM2 V8.1.3

2.1 Introduction

This chapter describes a modification in the Delta Simulation Model 2 (DSM2) open water areas algorithm to include changing bathymetry with elevations. Previously, open water areas were treated as a constant area with a bottom elevation. This change will help to better model Liberty Island in addition to other open water areas in the Delta. The elevation-area-storage curves for reservoirs can be calculated using geographic information system (GIS) tools like ArcMap. The model has been tested and new results have been evaluated.

2.2 Description

Originally, DSM2 implemented reservoirs with constant area and bottom elevation; a reservoir volume can be easily calculated as a product of area and depth. A more realistic implementation of reservoirs using elevation against area and volume relationship is described here and added to version 8.1.3,

$$\frac{dV}{dt} = \sum Q = Q_s - Q_c,$$

Where

V is the reservoir volume,

t is time,

dV/dt is the derivative of Volume with respect to time,

Qs is external (source) flow into or out of a reservoir, including transfer flow, Delta Island Consumtive Use (DICU), or pumping,

Qc is the (connection) flow between the reservoir and connected channel (out of reservoir is positive).

Following the FourPt hydrodynamic model procedures, numerical integration in time can be written as

$$V_{t_2} - V_{t_1} = \left(\theta(Q_s)_{t_2} + (1-\theta)(Q_s)_{t_1}\right)\Delta t - \left(\theta(Q_c)_{t_2} + (1-\theta)(Q_c)_{t_1}\right)\Delta t.$$

with the numerals 1 and 2 indicating the volumes and flows at two different points in time and Δt representing the difference in time. Linearization with truncated Taylor series, in terms of incremental changes of variables *Q* and *Z,* can be written as

$$V_{t_2}^* + \frac{\partial V_{t_2}^*}{\partial Z}\Delta Z - V_{t_1} = \left(\theta(Q_s)_{t_2} + (1-\theta)(Q_s)_{t_1}\right)\Delta t - \left(\theta Q_{c_{t_2}}^* + \theta\Delta Q_c + (1-\theta)(Q_c)_{t_1}\right)\Delta t,$$

where the superscript "*" indicates values from the preceding iteration, Z is the water surface elevation, and θ is a time-weighted paramenter, which varies from 0.5 to 1.0 in the four point implicit scheme. Rearranging the equation by moving terms known from the preceding iteration to the right-hand side is

$$\theta\Delta Q_c + \frac{1}{\Delta t}\frac{\partial V_{t_2}^*}{\partial Z}\Delta Z = \frac{-(V_{t_2}^* - V_{t_1})}{\Delta t} + \left(\theta(Q_s)_{t_2} + (1-\theta)(Q_s)_{t_1}\right) - \left(\theta Q_{c_{t_2}}^* + (1-\theta)(Q_c)_{t_1}\right).$$

In the old model, a constant area was used, then

$$\frac{\partial V_{t_2}^*}{\partial Z} = A = constant.$$

When using the new elevation-area-storage curve,

$$\frac{\partial V_{t_2}^*}{\partial Z} = A_{t_2}^*.$$

$A_{t_2}^*$ is the area, which varies with elevation.

Reservoir elevation-area-volume curves can be generated using the 3D Analyst Tools in ArcMap. Table 2-1 shows the calculated reservoir elevations areas, and volumes of Liberty Island at roughly a 0.5 meter interval. The table shows the inundated area of Liberty Island changes greatly from low elevation to high elevation, about 3,032 acres at 1.64 ft. North American Vertical Datum of 1988 (NAVD) and 5,190 acres at 6.562 ft. NAVD. This calculation included some storage areas outside Liberty Island (Figure 2-1), e.g., Little Holland Tract, as shown in the Figure 2-1. Channels were kept out of the storage area calculation.

Liberty Island		
Elevation(ft. NAVD)	Area(acre)	Volume(acre-feet.)
-61.975	0.000	0.000
-32.808	2.478	12.020
-16.404	16.220	114.969
-3.281	272.328	1154.224
-1.640	1017.270	2023.584
0.000	1999.522	4448.286
1.640	3031.999	8456.815
3.281	4209.851	14598.662
4.921	4584.028	21795.491
6.562	5190.456	29734.639
8.202	6359.679	39288.629
9.843	6636.050	50043.149
13.123	6731.118	72015.036
16.404	6830.894	94276.839
19.685	6876.916	116780.976
22.966	6890.138	139391.916

Table 2-1 Calculated Reservoir Elevation-Area-Volume at Liberty Island

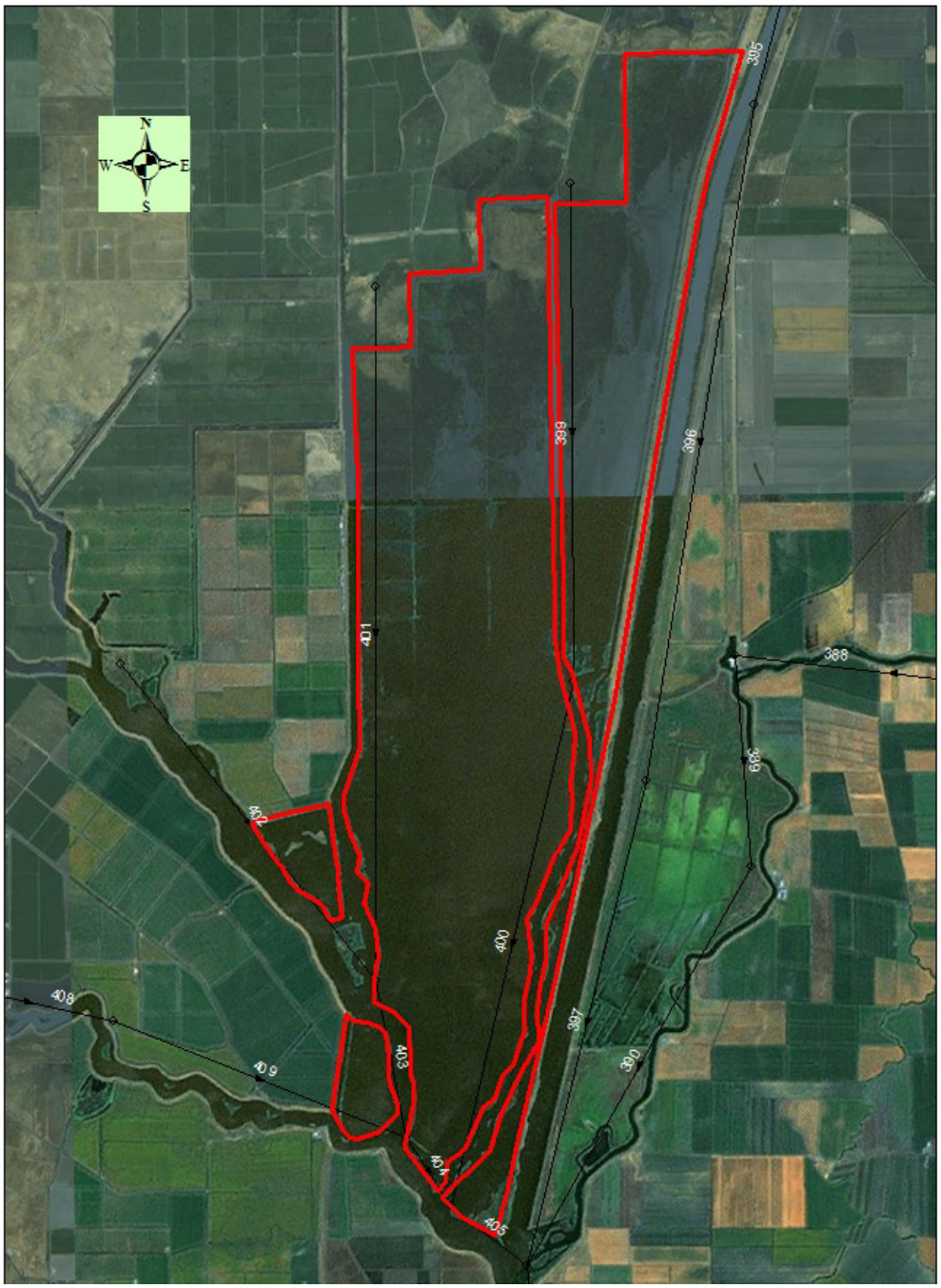

Figure 2-1 Liberty Island Storage Area Map

2.2.1 Calculation of $A^*_{t_2}$ and $V^*_{t_2}$

Within each layer, between two specified elevations in the Table 2-2, if we assume the area changes linearly from the bottom to the top, the volume can be calculated as

$$\Delta V = \frac{1}{2}(A_1 + A_2)(Z_2 - Z_1).$$

Where A is area, Z is the elevation, and ΔV is the calculated volume between specified (designated as 1 and 2) areas and elevations.

But this calculated volume is not equal to the real volume as defined in the elevation-area-volume table (Table 2-1 or Table 2-2), i.e.,

$$\Delta V \neq V_2 - V_1.$$

A correction factor is defined as

$$\alpha = \frac{V_2 - V_1}{\Delta V}.$$

At any elevation *Z*, the area (A) and volume (V) can be calculated as

$$A = \frac{A_2 - A_1}{Z_2 - Z_1}(Z - Z_1) + A_1$$

$$V = \alpha \frac{A + A_1}{2}(Z - Z_1) + V_1$$

and

$$\frac{\partial V}{\partial Z} = \alpha \cdot A.$$

This way, the calculated volume using area exactly matches the specified volumes in the elevation-area-volume in tables 2-3, 2-4, 2-5, 2-6, and 2-7.

The only change for the input files is a new table added to the original reservoir input file. In the new RESERVOIR_VOL table (Table 2-2), the area unit is acre and volume unit is acre-feet. No change was made to the original RESERVOIR table, which used million square feet for the area. The new executable V8.1.3 (not released yet) is backward compatible with V8.1.2 so that V8.1.2 input files can still run using V8.1.3 without any changes. If no elevation-area-volume values were specified for a reservoir, the original constant area would be used.

```
RESERVOIR_VOL
RES_NAME        ELEV        AREA       VOLUME
liberty       -61.975       0.000       0.000
liberty       -32.808       2.478      12.020
liberty       -16.404      16.220     114.969
liberty        -3.281     272.328    1154.224
liberty        -1.640    1017.270    2023.584
liberty         0.000    1999.522    4448.286
liberty         1.640    3031.999    8456.815
END
```

Table 1-2 New RESERVOIR_VOL Table

2.2.2 Other Reservoir Elevation-Area-Volume Tables

Clifton Court Forebay		
Elevation(ft. NAVD)	Area(acre)	Volume(acre-feet)
-41.864	0.000	0.000
-32.808	0.232	0.685
-16.404	2.641	19.749
-3.281	1721.648	3634.879
-1.640	2060.266	6766.577
0.000	2167.212	10261.804
1.640	2189.206	13837.950
3.281	2202.368	17439.877
4.921	2213.733	21063.314
6.562	2222.305	24701.898
8.202	2228.793	28350.774
9.843	2233.958	32007.171
13.123	2243.772	39346.372
16.404	2255.195	46730.970
19.685	2258.395	54155.385
22.966	2258.395	61564.824

Table 2-2 Calculated Reservoir Elevation-Area-Volume at Clifton Court Forebay

Franks Tract		
Elevation(ft. NAVD)	Area(acre)	Volume(acre-feet)
-37.664	0.000	0.000
-32.808	0.077	0.097
-16.404	15.458	81.712
-3.281	2863.623	6347.693
-1.640	3053.221	11229.356
0.000	3108.659	16289.292
1.640	3135.313	21414.532
3.281	3148.853	26569.405
4.921	3157.061	31739.000
6.562	3162.805	36920.426
8.202	3167.736	42112.172
9.843	3173.686	47313.134
13.123	3179.422	57750.586
16.404	3179.431	68181.904
19.685	3179.431	78613.118

Table 2-3 Calculated Reservoir Elevation-Area-Volume at Franks Tract

Bethel		
Elevation(ft. NAVD)	Area(acre)	Volume(acre-feet)
-10.433	0.000	0.000
-3.281	220.520	386.621
-1.640	274.450	804.670
0.000	286.141	1264.891
1.640	293.217	1740.520
3.281	296.166	2224.650
4.921	297.149	2712.450
6.562	297.198	3199.959
8.202	297.230	3687.516
9.843	297.252	4175.117
13.123	297.268	5150.659
16.404	297.268	6125.948

Table 2-4 Calculated Reservoir Elevation-Area-Volume at Bethel

Mildred		
Elevation(ft. NAVD)	Area(acre)	Volume(acre-feet)
-27.592	0.000	0.000
-16.404	30.433	43.056
-3.281	955.409	7648.080
-1.640	960.074	9217.757
0.000	964.188	10794.926
1.640	967.400	12377.913
3.281	969.247	13966.830
4.921	971.128	15559.504
6.562	972.641	17157.774
8.202	973.281	18755.206
9.843	973.874	20353.688
13.123	974.667	23553.121
16.404	974.977	26754.369
19.685	974.979	29953.415
22.966	974.979	33152.168

Table 2-5 Calculated Reservoir Elevation-Area-Volume at Mildred

Discovery Bay		
Elevation(ft. NAVD)	Area(acre)	Volume(acre-feet)
-7.612	0.000	0.000
-3.281	379.378	855.693
-1.640	409.827	1494.922
0.000	436.020	2180.971
1.640	460.503	2909.906
3.281	485.850	3683.030
4.921	516.216	4499.517
6.562	588.874	5395.956
8.202	649.454	6408.017
9.843	696.445	7502.144
13.123	906.898	10038.752
16.404	1134.594	13533.369
19.685	1141.429	17278.161
22.966	1141.429	21023.010

Table 2-6 Calculated Reservoir Elevation-Area-Volume at Discovery Bay

From the tables, it can be seen that other reservoir areas are fairly constant over the tidal range, and are very close to the constant area values used in V8.1.2.

2.3 Results Comparison

Historical simulations from 2000 to 2008 were done with the new reservoir specifications and results were compared with the V8.1.2 calibration. The change of the Liberty Island storage affected flow around the lower Sacramento River and even the San Joaquin River. Small adjustments of Manning's coefficients were made to a few channels for calibration. The recalibrated flow and stage results were generally very close to the V8.1.2 calibration. Obvious differences were seen only at Rio Vista; the phase difference for flow changed from 25 to 35 minutes (Figure 2-2), and stage amplitude became larger (Figure 2-3). There were almost no differences at Jersey Point and the entire South Delta (Figures 2-4 to 2-5). Electrical Conductivity (EC) results are almost identical to the V8.1.2 calibration. EC results at key stations: RSAC081, RSAN018, ROLD024 are shown in Figures 2-6 to 2-8 and at Clifton Court in Figure 2-9.

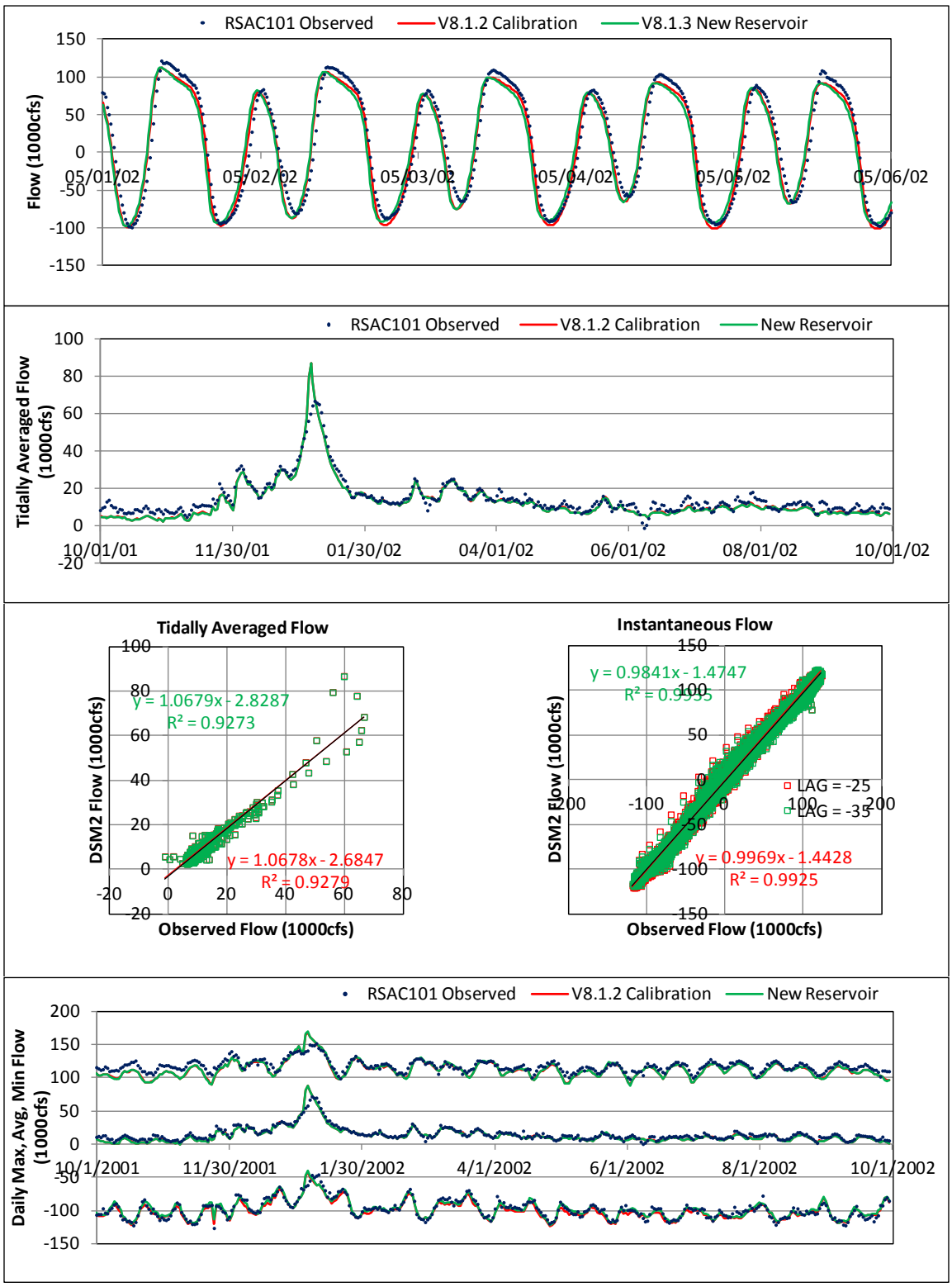

Figure 2-2 Flow at Sacramento River at Rio Vista

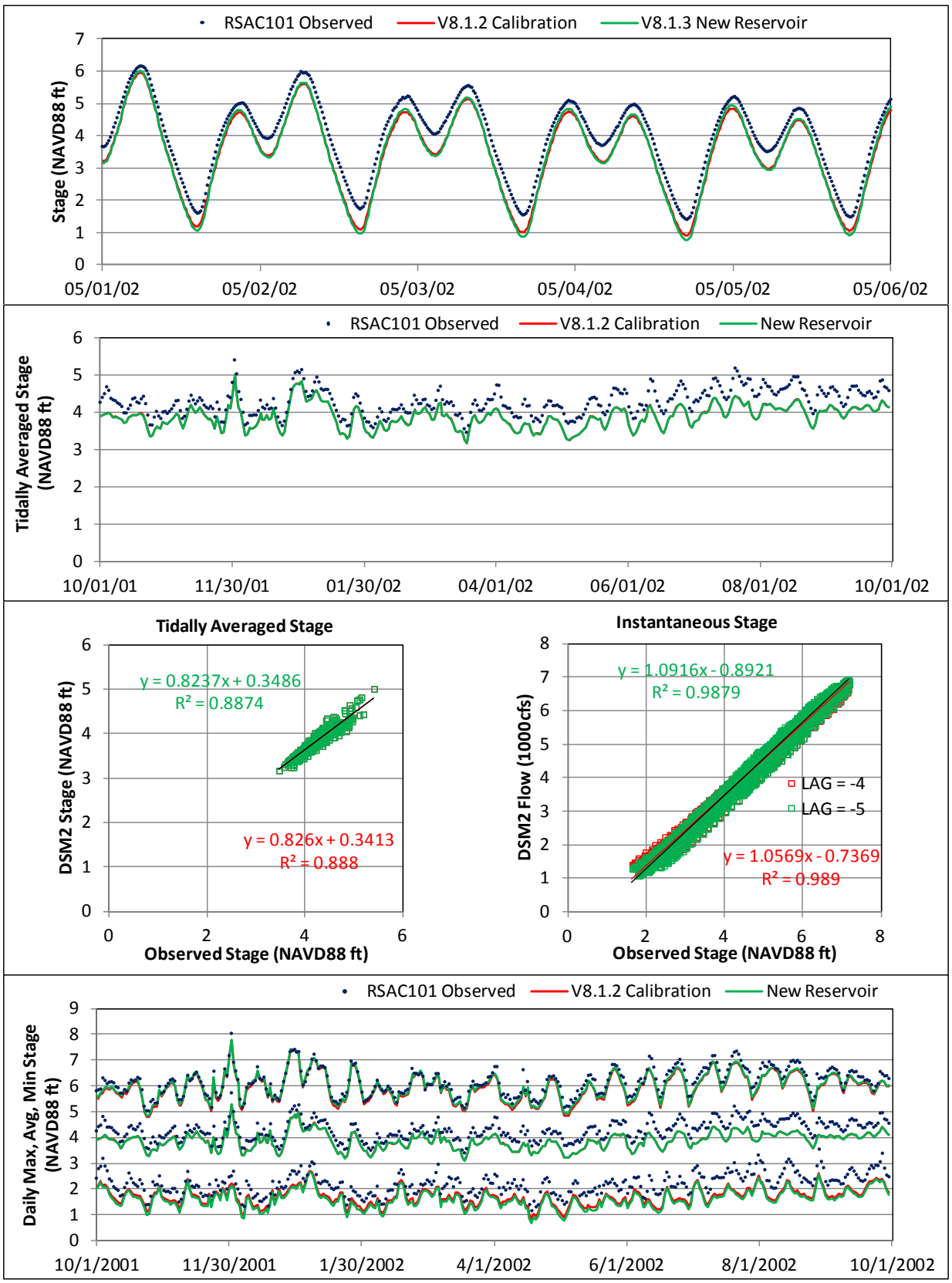

Figure 2-3 Stage at Sacramento River at Rio Vista

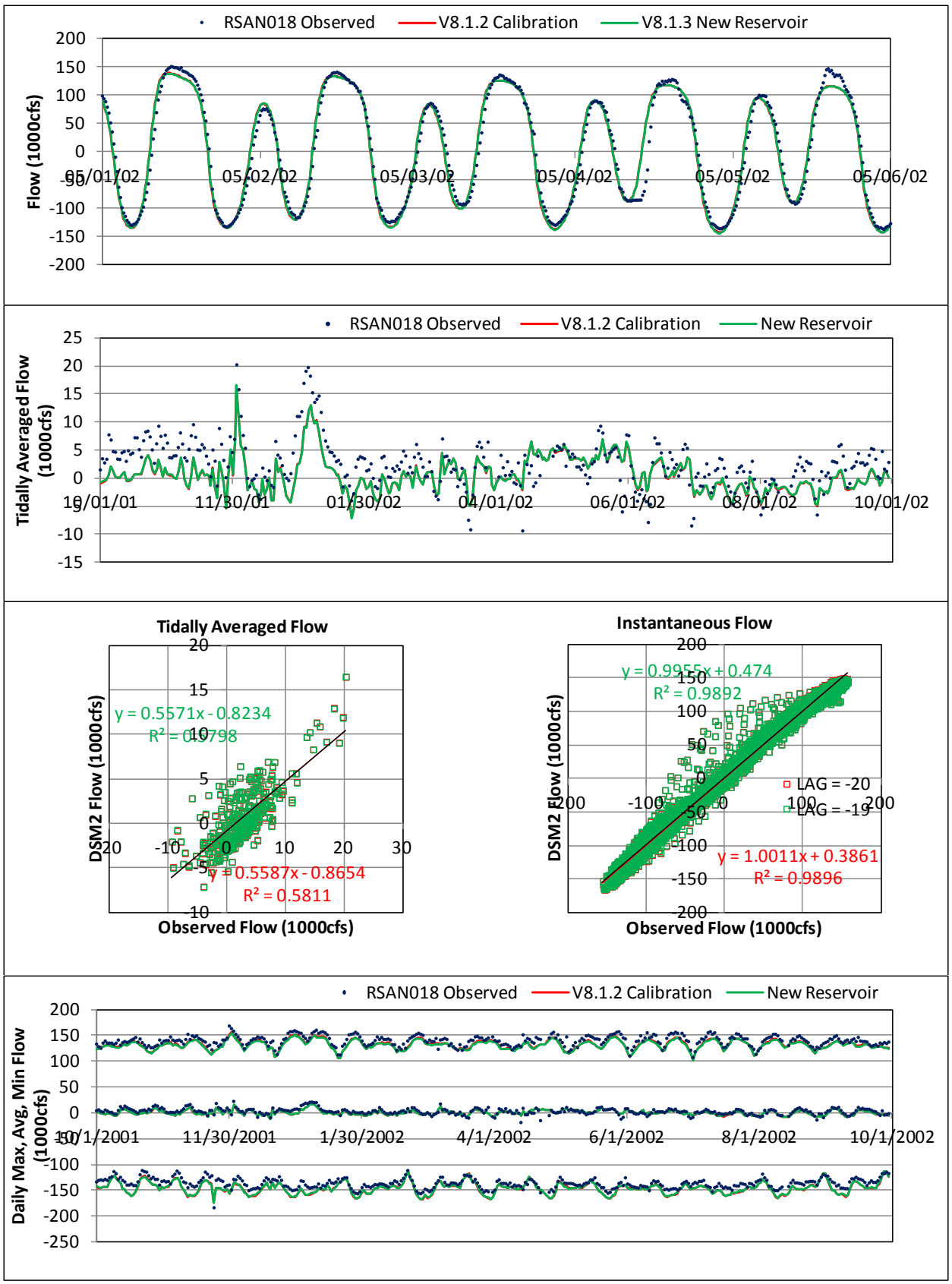

Figure 2-4 Flow at San Joaquin River at Jersey Point (RSAN018)

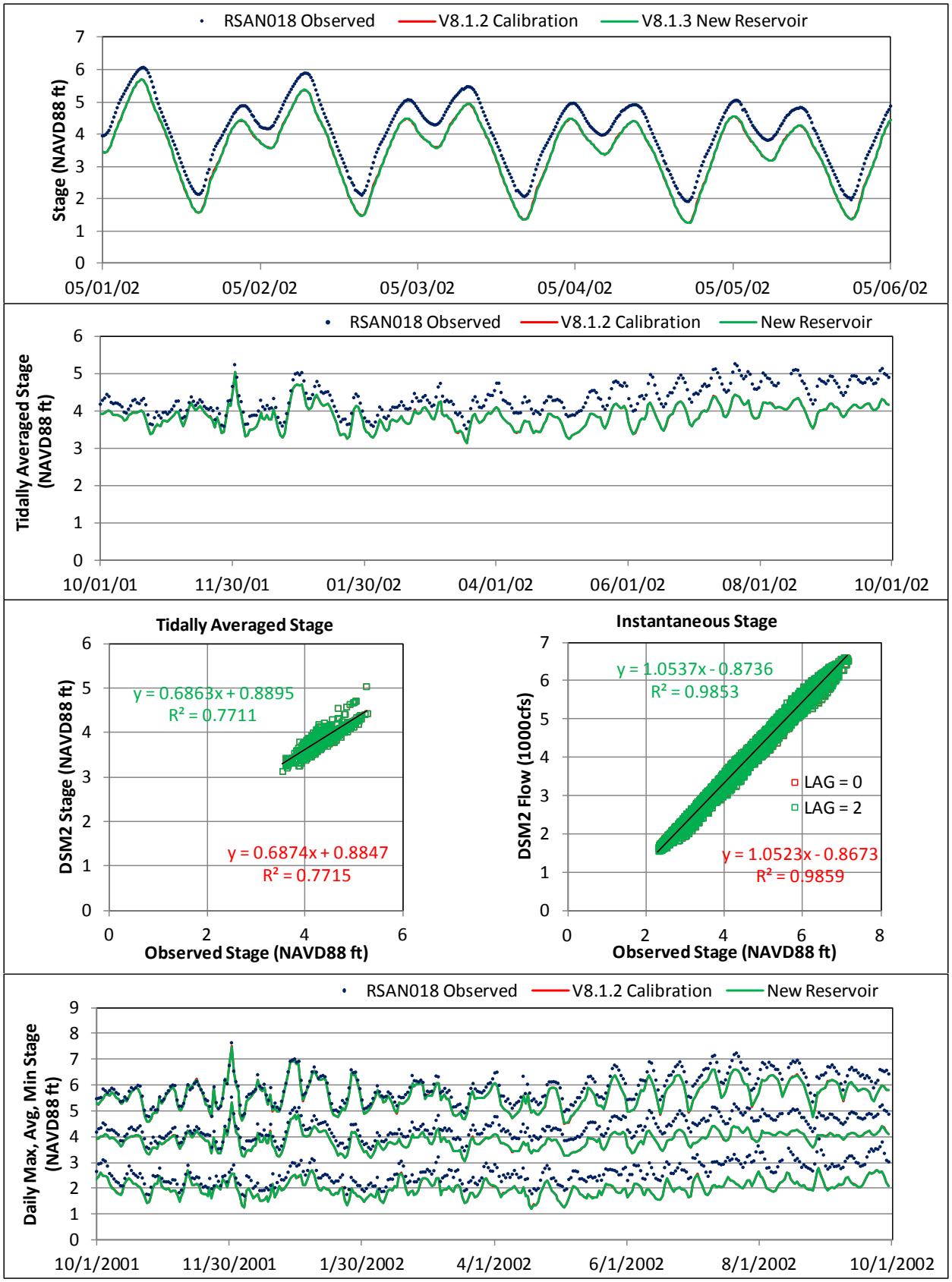

Figure 2-5 Stage at San Joaquin River at Jersey Point (RSAN018)

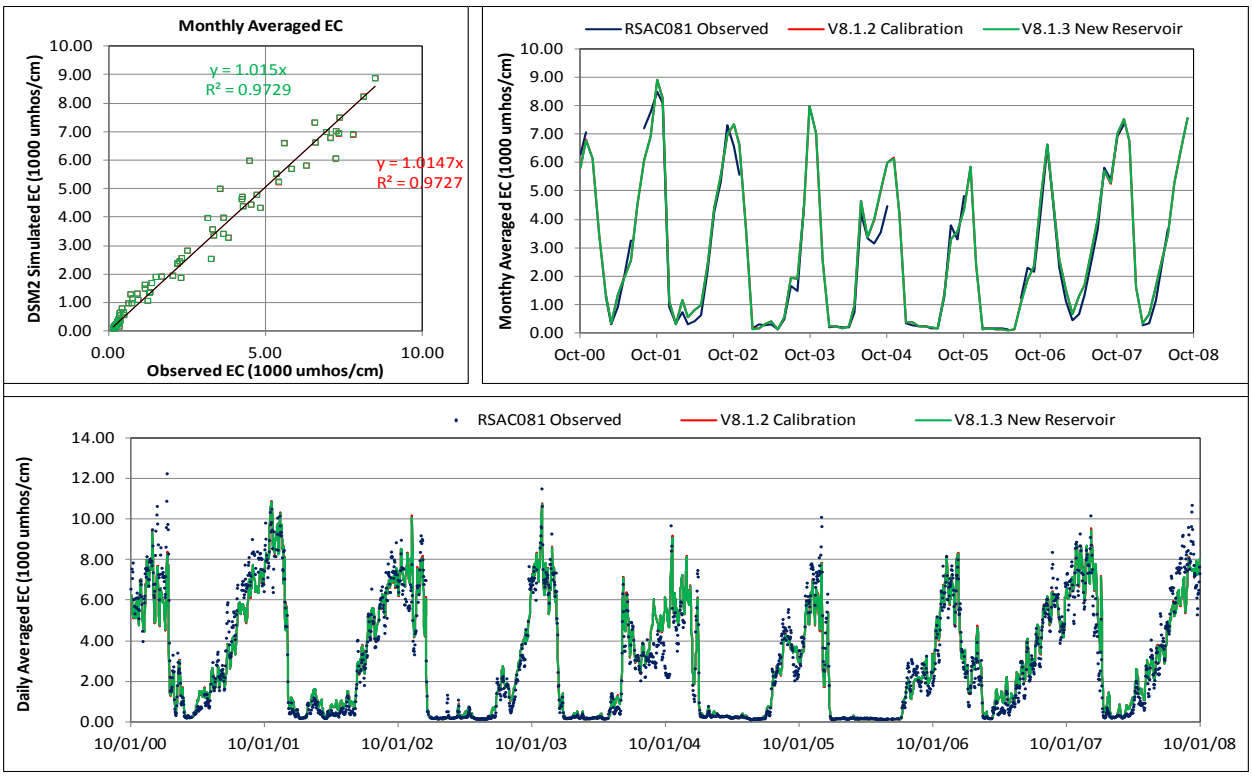

Figure 2-6 Stage at San Joaquin River at Jersey Point (RSAN018)

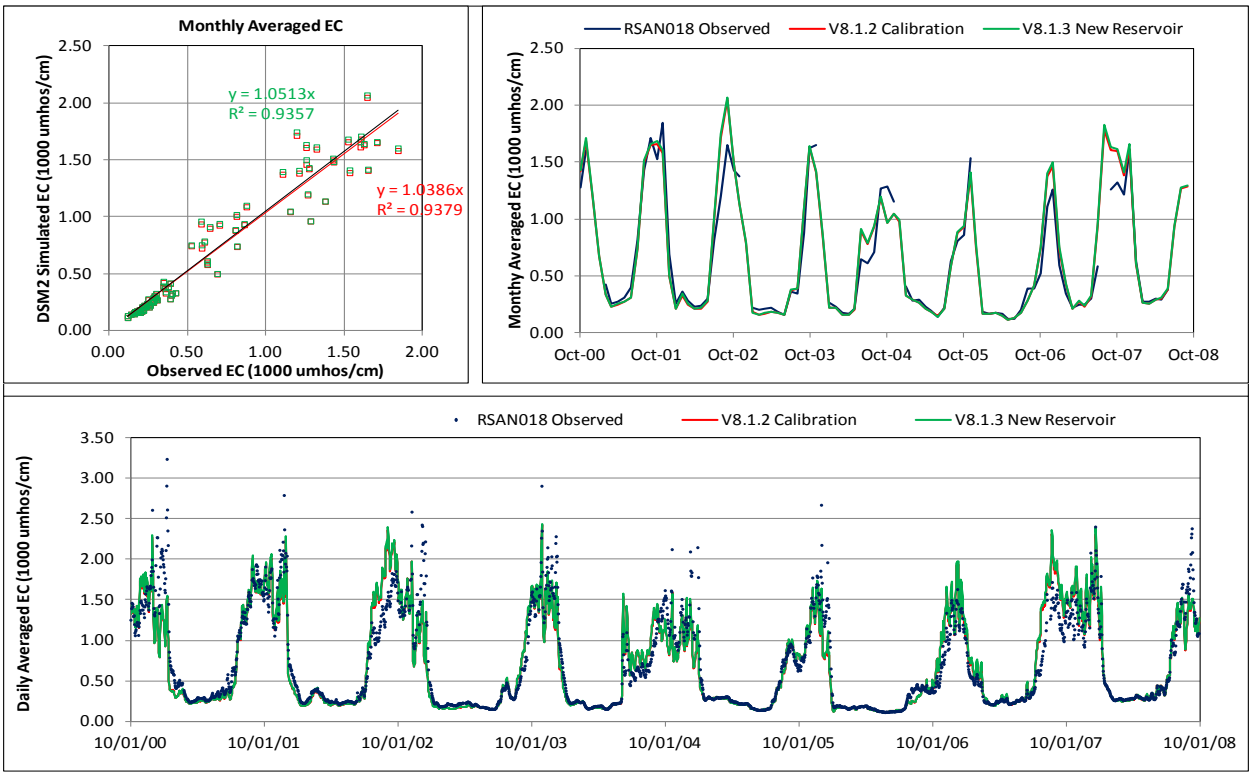

Figure 2-7 Simulated EC at San Joaquin River at Jersey Point (RSAN018)

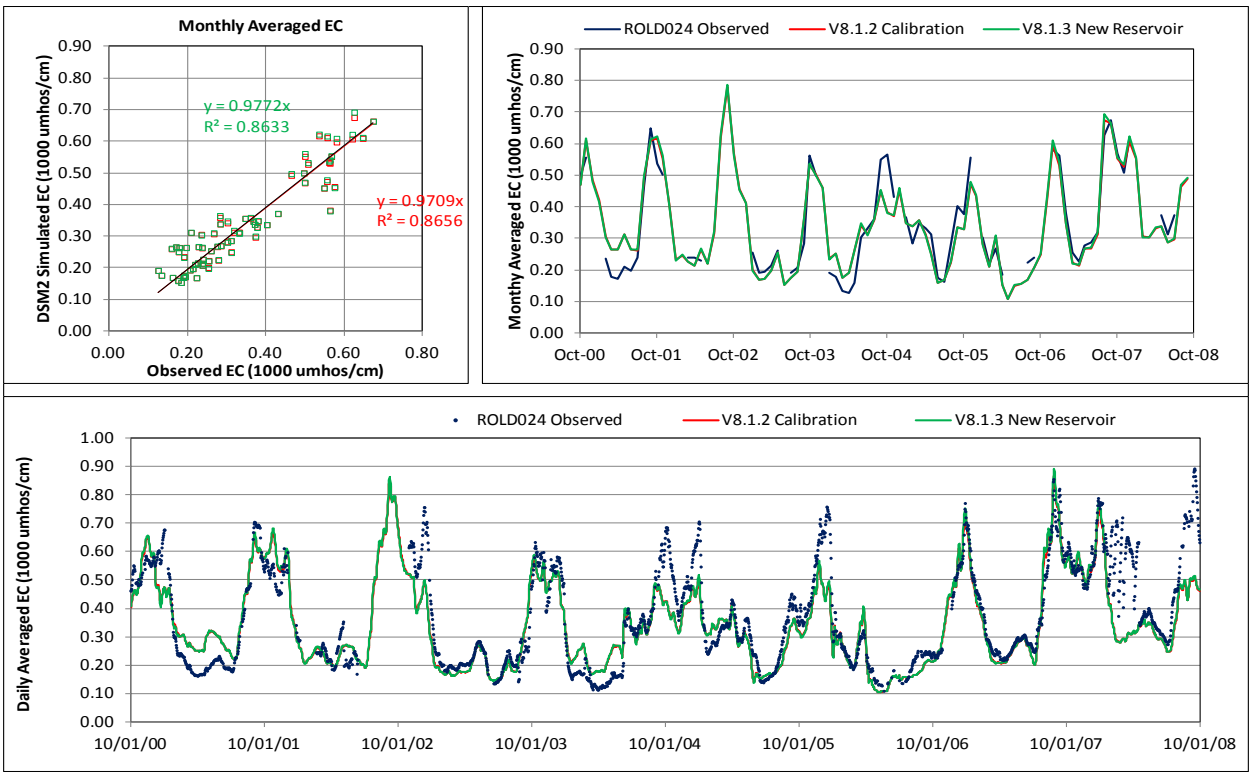

Figure 2-8 Simulated EC at Old River at Bacon Island (ROLD024)

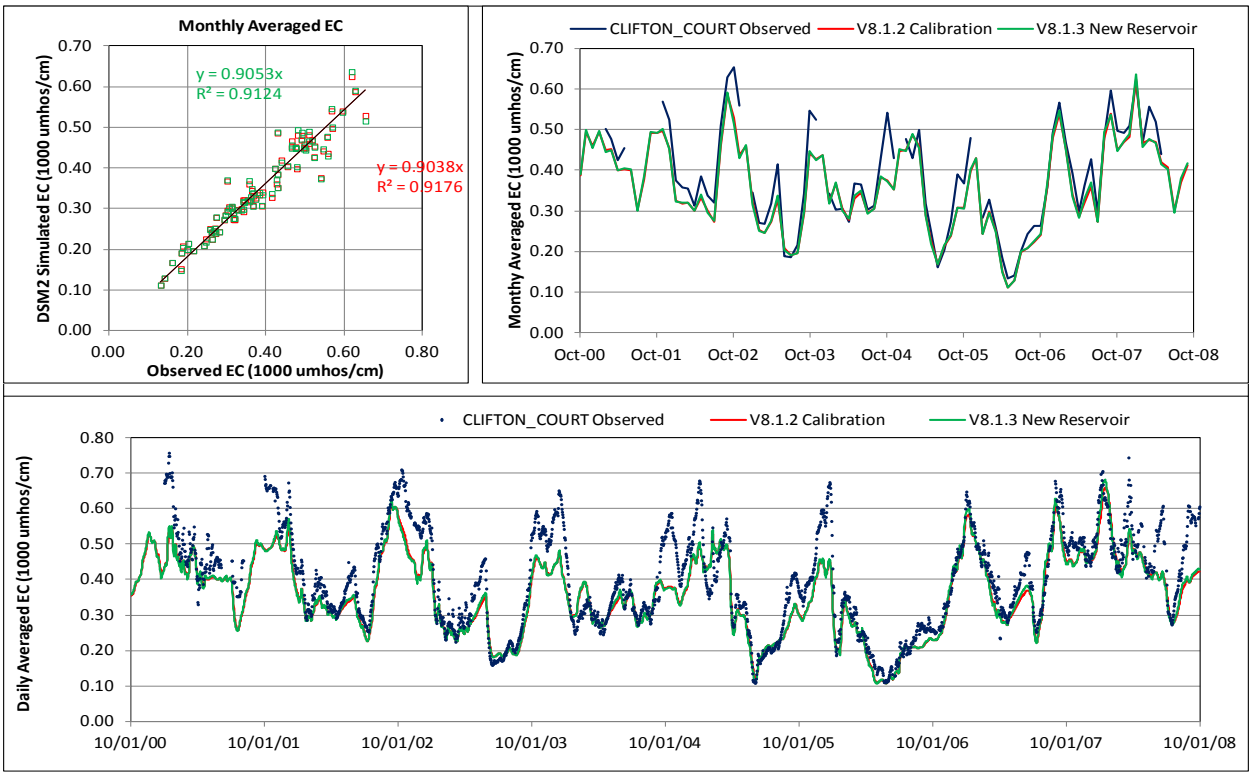

Figure 2-9 Simulated EC at Clifton Court Forebay

2.4 Summary

A new input table to use elevation-area-volume curve for reservoirs was added. The modifications were tested for stability and accuracy. This feature is useful to better model Liberty Island and other potential tidal-marsh restoration areas where the inundated area changes significantly with tidal elevations. This change prompted a recalibration in the region of Liberty Island, and the resulting differences using the new reservoir specifications were not significant.

A new information message was added for accumulated volume balance errors of reservoirs at the end of a Qual run and those errors are listed in the end of the output file (*.qof).

Methodology for Flow and Salinity Estimates in the Sacramento-San Joaquin Delta and Suisun Marsh

36th Annual Progress Report
June 2015

Chapter 3
Estimating the Impact of Groundwater on Delta Channel Depletions

Authors: **Lan Liang and Bob Suits**
Delta Modeling Section
Bay-Delta Office
California Department of Water Resources

Contents

3 Estimating the Impact of Groundwater on Delta Channel Depletions 3-1
3.1 BACKGROUND 3-1
3.1.1 Delta Channel Depletion Relates to Model EC in the Summers of Critical and Dry Years. 3-1
3.1.2 Existing Problems in Modeling Delta Channel Depletion 3-1
3.2 LITERATURE REVIEW 3-2
3.2.1 Delta Uplands Findings 3-2
3.2.2 Delta Lowlands Findings 3-2
3.3 DETAW-CD METHODOLOGY 3-3
3.3.1 Groundwater for Delta Uplands Irrigation 3-3
3.3.2 Groundwater for Delta Lowlands Irrigation 3-3
3.3.3 Deep Percolation 3-3
3.4 IMPACTS OF INCORPORATING GROUNDWATER ON CHANNEL DEPLETION, DELTA OUTFLOW, AND EC MODELING 3-3
3.4.1 Impact on Channel Depletion 3-3
3.4.2 Impact on Net Delta Outflow (NDO) 3-4
3.4.3 Impact on EC Simulation 3-4
3.5 CONCLUSION 3-6
3.6 REFERENCES 3-6

Figures

Figure 3-1 Examples of EC Comparison of DSM2-DICU, DSM2-DETAW-wo-CD and Observation 3-2
Figure 3-2 Average Monthly Delta Channel Depletion from WY 1975 to WY 2010 3-4
Figure 3-3 Monthly Average NDO under DAYFLOW, DETAW-wo-CD, and DETAW-CD Compared with DICU 3-5
Figure 3-4 EC Comparisons of DSM2-DICU, DSM2-DETAW-CD, and the Observed Data from IEP 3-5

3 Estimating the Impact of Groundwater on Delta Channel Depletions

3.1 Background

3.1.1 Delta Channel Depletion Relates to Model EC in the Summers of Critical and Dry Years.

Historical Delta electric conductivity (EC) during critical and dry years, simulated by Delta Simulation Model 2 (DSM2), has been investigated since DSM2 was developed in the 1990s. In the 2006 Annual Report, Myint Thein and Parviz Nader-Tehrani noted large discrepancies between observed and DSM2-simulated EC during summers of dry periods, 1975-1989. Similar accuracy concerns of modeled EC have been noted during drought years after 1989. Figure 3-1 shows the Delta Island Consumptive Use (DICU)-based DSM2-simulated EC and the observed EC in the Delta confluence area during the critical years, 1990 and 1991. DSM2-DETAW-wo-CD, Delta Evapotranspiration of Applied Water without groundwater assumption, is also shown in Figure 3-1 and will be explained in more detail later in this chapter.

The EC estimation in the west Delta is strongly related to Delta outflow. Low Delta outflow for a sufficiently long duration will cause salinity intrusion, while high Delta outflow will eventually push salinity out of the Delta. Calculated Delta outflow is the total Delta inflow less exports and channel depletions. Errors in modeled historical channel depletions will result in errors in modeled Delta outflow, which, in turn, cause errors in the modeled extent of seawater intrusion. Potential errors in modeled salinity intrusion are highly sensitive to Delta outflow. When Delta outflow is low, particularly over an extended period, the simulated location of high salinity gradient in the west Delta can vary widely for relatively small changes in estimated outflow. The significant overestimation of DSM2-modeled historical EC in critical and dry years is most likely the result of overestimating channel depletions. Sufficiently accurate estimations of Delta channel depletion are crucial to producing meaningful DSM2 simulations of salinity intrusion when the Delta outflow is low.

3.1.2 Existing Problems in Modeling Delta Channel Depletion

Delta island consumptive use is the island water lost mostly because of crop evapotranspiration (ET). Related to consumptive use, Delta channel depletion is the water gained or lost in the Delta channels. The consumptive-use models, such as DICU and Delta Evapotranspiration of Applied Water (DETAW), estimate crop ET on Delta islands and the water sources to supply the water demands. These water sources include rainfall, seepage, and applied water. To model Delta hydrodynamics and water quality, DICU has a post-processing computer program that computes the channel depletion, based on the assumptions representing the correlations between the water sources and the channel depletion. DETAW does not have this post-processing program.

In the initial phase of implementing DETAW for the Delta, the same assumptions used with DICU were applied to take estimated island consumptive use and generate channel depletion. Similar to the DICU-based DSM2 simulation, the DETAW-based DSM2 simulation of EC generated considerably higher EC than the observed data in the critical years (Figure 3-1). Attempting to improve the DSM2 simulation of EC during extended low outflow periods, the allocation of sources of water to meet Delta consumptive use was reexamined.

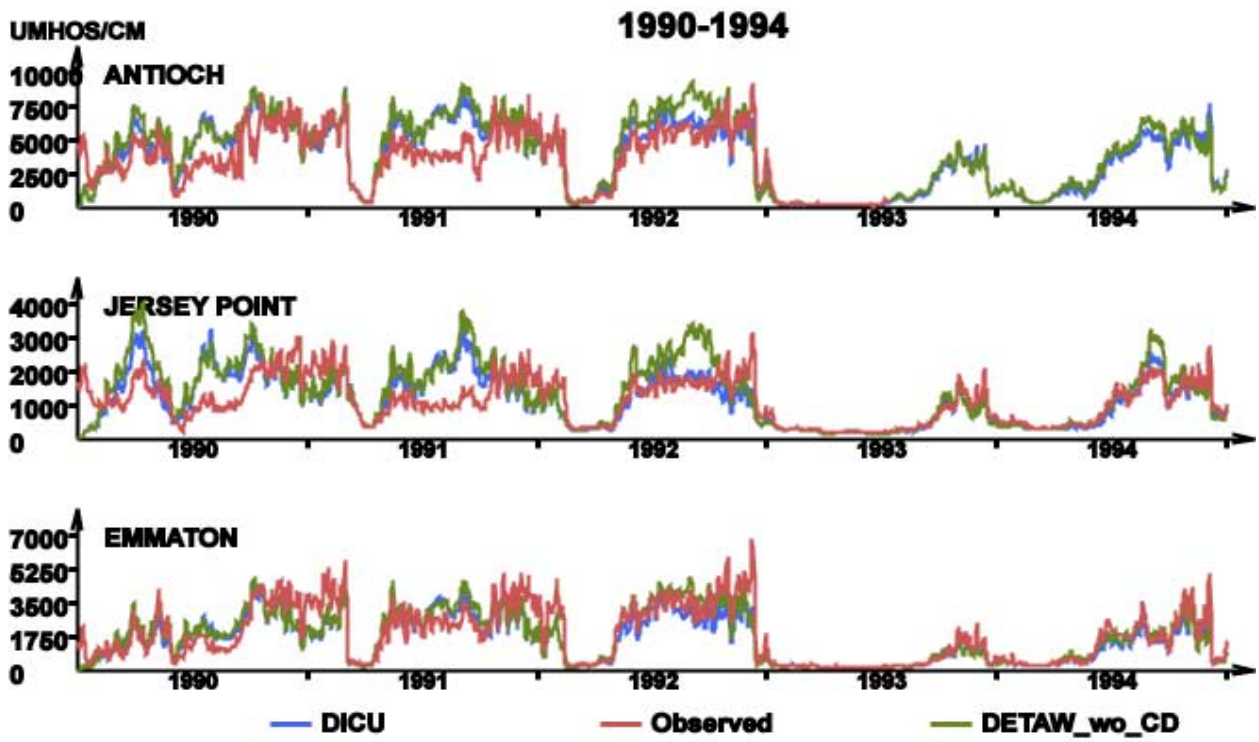

Figure 3-1 Examples of EC Comparison of DSM2-DICU, DSM2-DETAW-wo-CD and Observation

3.2 Literature Review

A literature review was conducted to explore past assumptions and study conclusions of the water sources that contributed to meeting the island consumptive use demands. The findings are described in the following two sections.

3.2.1 Delta Uplands Findings

The *Draft Environmental Impact Report/Environmental Impact Statement Bay Delta Conservation Plan* (California Department of Water Resources 2013) summarizes the domestic and irrigation wells in the Delta and indicates there are at least 3,693 domestic wells and 420 municipal and irrigation wells in the Delta. Although the actual pumping yield is unknown, the amount of wells proves that some groundwater is pumped for irrigation and urban use.

In addition, the California Department of Water Resources (DWR) North Central Region Office maintains a database of the groundwater wells in the Delta. Projecting the well locations on a geographic information system map indicates that most wells are located in Delta Uplands.

3.2.2 Delta Lowlands Findings

A basic assumption of using island consumptive use to calculate the channel depletion in DICU and DETAW is that the channel water is the sole water source to meet demands in the Delta, excluding precipitation and soil moisture. Nonetheless, a literature review revealed that groundwater is a significant source of water in the Delta. From 1956 to 1959, DWR published four reports about the investigation of groundwater in the Sacramento-San Joaquin Delta. Reports No. 2 (Kabakov et al. 1956b) and No. 3 (Kabakov et al. 1959) found that applied water on Medford and McDonald islands was composed of approximately 80 percent of San Joaquin River and 20 percent of Mokelumne River area groundwater and connate water.

It is apparent that the estimation of the Delta channel depletion should be modified by including groundwater as a source to meet island water demands.

3.3 DETAW-CD Methodology

Since DETAW has been developed to replace DICU to estimate consumptive use in the Delta, DETAW now also accounts for groundwater in calculating Delta channel depletions. Using this new post-processing, DETAW-Produced Channel Depletion (DETAW-CD), simulates not only the water interactions between channels and ground surface, but also those interactions between groundwater and ground surface. Three water interactions between groundwater and ground surface have been added in DETAW-CD. These are the groundwater pumping for the Delta Uplands irrigation, groundwater interaction with ground surface in the Delta Lowlands, and deep percolation.

3.3.1 Groundwater for Delta Uplands Irrigation

The groundwater contribution is assumed to be a constant fraction of the applied water. The groundwater rate of each year is determined based on the accumulated number of irrigation wells of that year. The annual number of irrigation wells from the 1940s to the present was obtained from the groundwater well database maintained by the DWR North Central Region Office. No irrigation wells were recorded before the 1950s, so the groundwater rate in the Delta Uplands then was assumed to be zero. After 1950, the rate gradually increased as the number of recorded wells increased. In 2009 and later, the portion of consumptive-use demands met by groundwater in Delta Uplands is set at 40 percent.

3.3.2 Groundwater for Delta Lowlands Irrigation

Based on the studies of the chemical makeup of agricultural drainage, which DWR conducted in the 1950s, the main water supply to two islands in the Delta lowlands — Medford and McDonald islands — consisted of 20 percent groundwater from the areas surrounding the Delta and the connate water, and 80 percent from channel surface water. Due to the significant subsidence in the Delta Lowlands since that time, it is assumed that the groundwater in the past several decades contributed more to the island consumptive use. The portion of consumptive-use demands met by groundwater in the Delta Lowlands is set at 25 percent for all years.

3.3.3 Deep Percolation

In the new implementation of DETAW-CD, deep percolation of precipitation is assumed to be 25 percent of the residue of the precipitation after supplying the evapotranspiration.

3.4 Impacts of Incorporating Groundwater on Channel Depletion, Delta Outflow, and EC Modeling

3.4.1 Impact on Channel Depletion

Figure 3-2 presents the average monthly Delta channel depletion from water year (WY) 1975 to WY 2010 by different consumptive-use models: DICU, DETAW-wo-CD, and DETAW-CD. DETAW-wo-CD represents DETAW without the groundwater assumption. DETAW-CD generates lower channel depletion than DICU because of groundwater supply. The difference between the DETAW-wo-CD and DETAW-CD for each month is the amount of groundwater supply. The groundwater contribution in spring and summer is driven by the consumptive use, so it varies in a similar pattern like the consumptive use does. The maximum average groundwater supply is about 1,500 cubic feet per second (cfs) in July.

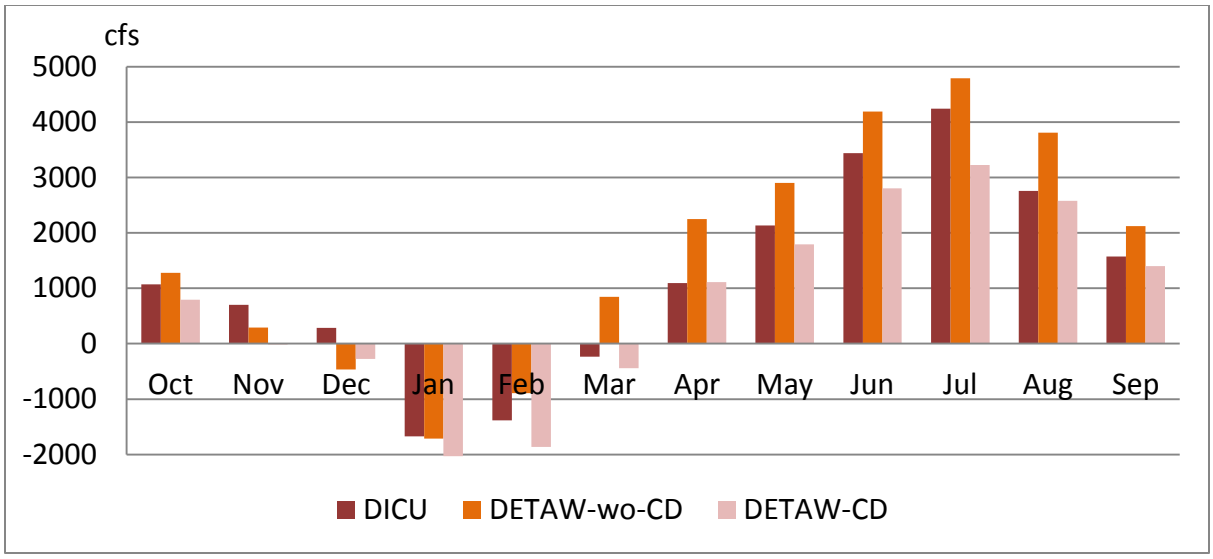

Figure 3-2 Average Monthly Delta Channel Depletion from WY 1975 to WY 2010

3.4.2 Impact on Net Delta Outflow (NDO)

Since the channel depletion of DETAW-CD is less than that of DICU and DETAW-wo-CD, the net Delta outflow (NDO) of DETAW-CD is higher than for the other models. Figure 3-3 compares monthly average NDO by DICU, DAYFLOW, DETAW-wo-CD, and DETAW-CD when DICU NDOs are less than 6,000 cfs. Salinity intrusion under these low outflows is sensitive to small changes in NDO. DICU, DAYFLOW, and DETAW-wo-CD produced more or less similar NDOs, but DETAW-CD generally has a higher NDO than other models.

3.4.3 Impact on EC Simulation

Simulated historical EC for models DSM2-DICU and DSM2-DETAW-CD are shown in Figure 3-4, along with the Interagency Ecological Program (IEP) observed data. The models DSM2-DICU and DSM2-DETAW-CD use the same DSM2 setup, but with different channel depletions. With the consideration of groundwater, the EC simulation matches well with the field data. Most of the large EC overestimations by DICU and DETAW-wo-CD shown in Figure 3-1 have been eliminated.

Nonetheless, the discrepancies between DETAW-CD and the field data for some fall and winter periods still exist. During the transition period from the irrigation season to the nonirrigation season, the groundwater interaction with the ground surface in the Delta is probably related to many random farming activities and water environment variation, and both are hard to predict.

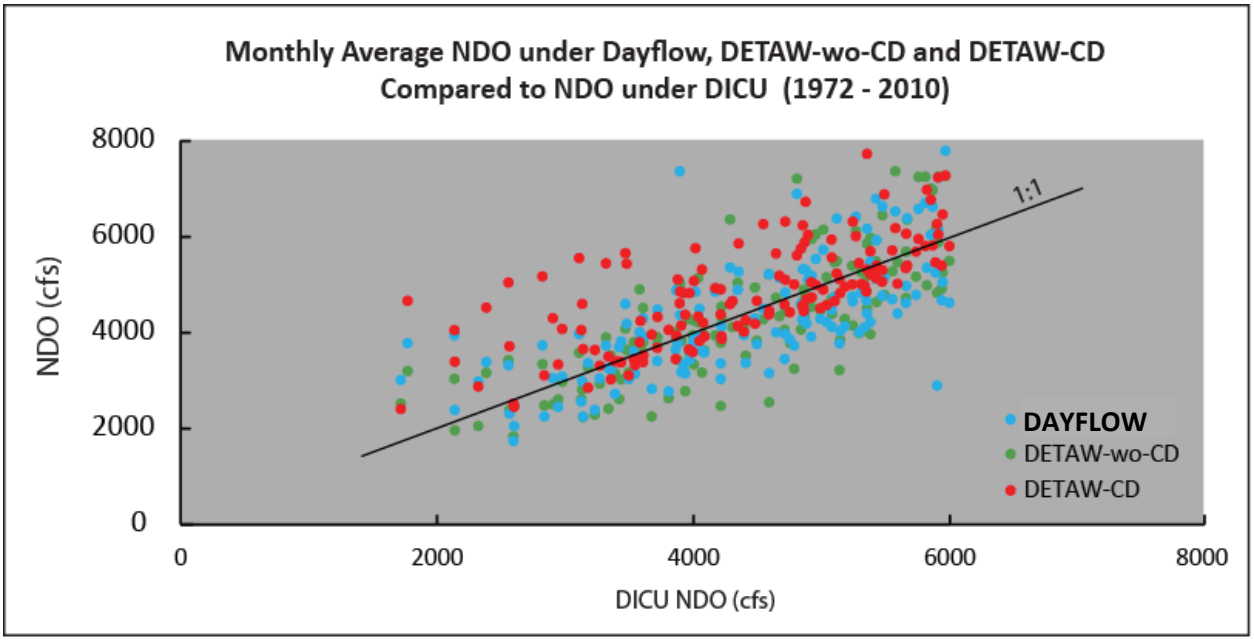

Figure 3-3 Monthly Average NDO under DAYFLOW, DETAW-wo-CD, and DETAW-CD Compared with DICU

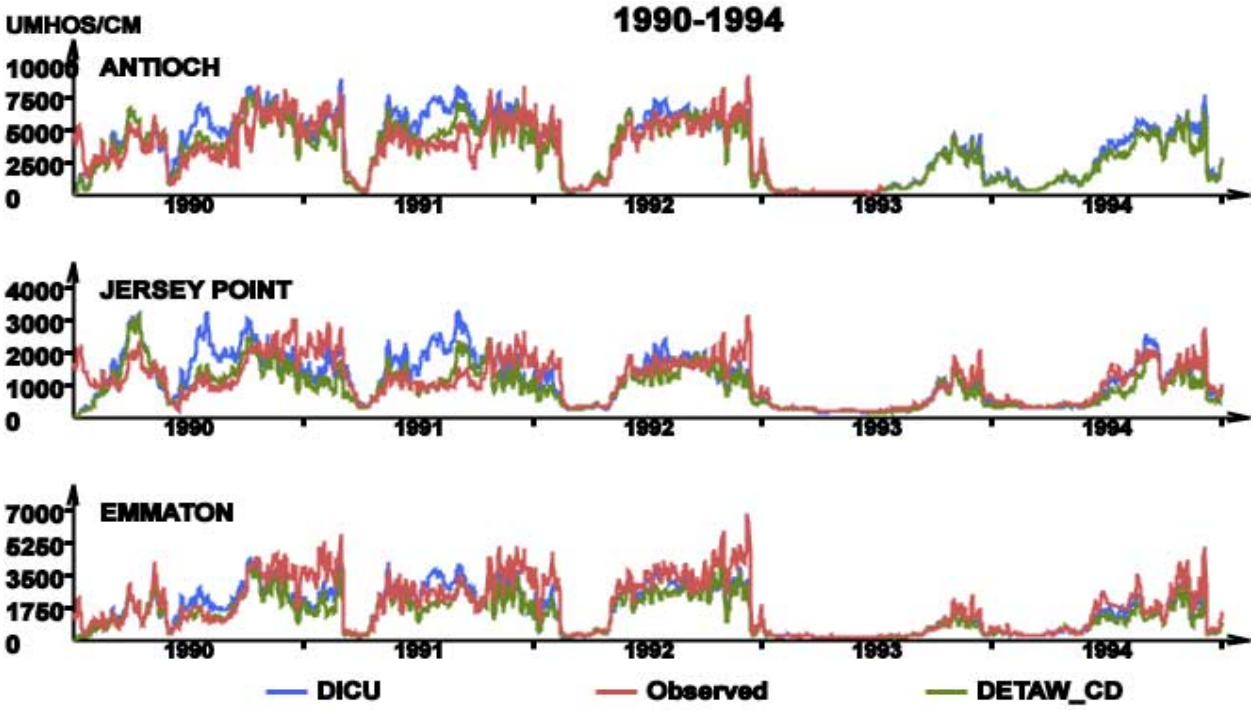

Figure 3-4 EC Comparisons of DSM2-DICU, DSM2-DETAW-CD, and the Observed Data from IEP

3.5 Conclusion

Although the concept of groundwater contributing to the Delta consumptive use has been recognized in the past, the quantifying of groundwater supply is still at the starting point. This study integrated consumptive use, hydrodynamics, and water quality models, and then calibrated the groundwater supply and EC together by using the correlations between Delta outflow and EC. With the estimated groundwater contribution, EC in the summers of the critical and dry years can be estimated to be close to the measured field data. Nonetheless, factors contributing to EC during the transition period from irrigation season to nonirrigation season seem more random. More data describing the flow interactions among channels, groundwater, and ground surface during those periods should help further understand the Delta groundwater supply.

3.6 References

California Department of Water Resources. 2013. *Draft Environmental Impact Report/Environmental Impact Statement Bay Delta Conservation Plan.* Viewed online at: http://baydeltaconservationplan.com/Libraries/Dynamic_Document_Library/EIR-EIS_Chapter_7_%E2%80%93_Groundwater_5-10-13.sflb.ashx.

Kabakov S, et al. 1956a. *Investigation of the Sacramento-San Joaquin Delta. Report No. 1. Ground Water Geology*. Sacramento (CA): Water Project Authority of the State of California.

———.1956b. *Investigation of the Sacramento-San Joaquin Delta. Report No. 2. Water Supply and Water Utilization on Medford Island*. Sacramento (CA): Water Project Authority of the State of California.

———.1956c. *Investigation of the Sacramento-San Joaquin Delta. Report No. 4. Quantity and Quality of Waters Applied to and Drained from the Delta Lowlands.* Sacramento (CA): California Department of Water Resources.

———.1959. *Investigation of the Sacramento-San Joaquin Delta. Report No. 3. Water Supply and Water Utilization on McDonald Island*. Sacramento (CA): California Department of Water Resources.

Myint T and Nader-Tehrani P. 2006. "Chapter 9: DSM2 Simulation of Historical Delta Conditions over the 1975-1990 Period." In: *Methodology for Flow and Salinity Estimates in the Sacramento-San Joaquin Delta and Suisun Marsh. 27th Annual Progress Report to the State Water Resources Control Board*. Sacramento (CA): California Department of Water Resources. Bay-Delta Office.

Methodology for Flow and Salinity Estimates in the Sacramento-San Joaquin Delta and Suisun Marsh

36th Annual Progress Report
June 2015

Chapter 4
Modeling Physical Barriers (Gates) as Engineering Solutions to Satisfy National Marine Fisheries Service Biological Opinion Reasonable Prudent Alternative Action IV.1.3

Author: **Subir Saha**
Delta Modeling Section
Bay-Delta Office
California Department of Water Resources

Contents

4 Modeling Physical Barriers (Gates) as Engineering Solutions to Satisfy National Marine Fisheries Service Biological Opinion Reasonable Prudent Alternative Action IV.1.3 4-1

4.1 INTRODUCTION 4-1

4.2 THE SIMULATION MODEL 4-1

4.3 METHODOLOGY 4-1

4.3.1 Description of Existing Conditions 4-2

4.3.2 Description of Modeling Scenarios 4-3

4.4 MODEL RESULTS 4-7

4.4.1 Full Flow Blockage to Delta Channels 4-10

4.4.2 Partial Flow Blockage to Delta Channels 4-11

4.4.3 Flow Blockage Used in Other Projects 4-11

4.5 CONCLUSION 4-28

4.6 REFERENCES 4-36

Figures

Figure 4-1 Gate Locations in the Delta Channels 4-2

Figure 4-2 Flow Triggered Gate Operation (open/close) 4-5

Figure 4-3 Velocity Triggered Gate Operation (open/close) 4-7

Figure 4-4 Model Output Locations 4-10

Figure 4-5 Monthly Average Flow at Georgiana Slough for Flow Trigger Location in Channels 4-12

Figure 4-6 Monthly Average Flow at Head of Old River for Flow Trigger Location in Channels 4-12

Figure 4-7 Monthly Average Flow at Columbia Cut for Flow Trigger Location in Channels 4-13

Figure 4-8 Monthly Average Flow at Turner Cut for Flow Trigger Location in Channels 4-13

Figure 4-9 Monthly Average Flow at Georgiana Slough for Flow Trigger Location in Rivers 4-14

Figure 4-10 Monthly Average Flow at Head of Old River for Flow Trigger Location in Rivers 4-14

Figure 4-11 Monthly Average Flow at Columbia Cut for Flow Trigger Location in Rivers 4-15

Figure 4-12 Monthly Average Flow at Turner Cut for Flow Trigger Location in Rivers 4-15

Figure 4-13 Monthly Average EC at Clifton Court Forebay for Flow Trigger Location in Channels 4-16

Figure 4-14 Monthly Average EC at Sacramento River at Emmaton for Flow Trigger Location in Channels 4-16

Figure 4-15 Monthly Average EC at San Joaquin River at Jersey Point for Flow Trigger Location in Channels 4-17

Figure 4-16 Monthly Average EC at Old River at Tracy Road for Flow Trigger Location in Channels 4-17

Figure 4-17 Monthly Average EC at Clifton Court Forebay for Flow Trigger Location in Rivers..... 4-18
Figure 4-18 Monthly Average EC at Sacramento River at Emmaton for Flow Trigger Location in Rivers 4-18
Figure 4-19 Monthly Average EC at San Joaquin River at Jersey Point for Flow Trigger Location in Rivers 4-19
Figure 4-20 Monthly Average EC at Old River at Tracy Road for Flow Trigger Location in Rivers..... 4-19
Figure 4-21 Daily Minimum Stage at Old River at Tracy Road for Flow Trigger Location in Channels..... 4-20
Figure 4-22 Daily Minimum Stage at San Joaquin River at Brandt Bridge for Flow Trigger Location in Channels..... 4-20
Figure 4-23 Daily Minimum Stage at San Joaquin River at Prisoners Point for Flow Trigger Location in Channels..... 4-21
Figure 4-24 Daily Minimum Stage at Old River at Tracy Road for Flow Trigger Location in Rivers 4-21
Figure 4-25 Daily Minimum Stage at San Joaquin River at Brandt Bridge for Flow Trigger Location in Rivers 4-22
Figure 4-26 Daily Minimum Stage at San Joaquin River at Prisoners Point for Flow Trigger Location in Rivers 4-22
Figure 4-27 Monthly Average Flow at Georgiana Slough for Velocity Trigger Location in Rivers 4-23
Figure 4-28 Monthly Average Flow at Head of Old River for Velocity Trigger Location in Rivers..... 4-23
Figure 4-29 Monthly Average Flow at Columbia Cut for Velocity Trigger Location in Rivers 4-24
Figure 4-30 Monthly Average Flow at Turner Cut for Velocity Trigger Location in Rivers 4-24
Figure 4-31 Monthly Average EC at Clifton Court Forebay for Velocity Trigger Location in Rivers 4-25
Figure 4-32 Monthly Average EC at Sacramento River at Emmaton for Velocity Trigger Location in Rivers 4-25
Figure 4-33 Monthly average EC at San Joaquin River at Jersey Point for Velocity Trigger Location in Rivers 4-26
Figure 4-34 Monthly average EC at Old River at Tracy Road for Velocity Trigger Location in Rivers 4-26
Figure 4-35 Daily Minimum Stage at Old River at Tracy Road for Velocity Trigger Location in Rivers..... 4-27
Figure 4-36 Daily Minimum Stage at San Joaquin River at Brandt Bridge for Velocity Trigger Location in Rivers 4-27
Figure 4-37 Daily Minimum Stage at San Joaquin River at Prisoners Point for Velocity Trigger Location in Rivers 4-28
Figure 4-38 Impacts of Georgiana Slough Gate on Water Quality throughout Delta 4-29
Figure 4-39 Impacts of Head of Old River Gate on Water Quality throughout Delta..... 4-30
Figure 4-40 Impacts of Columbia Cut Gate on Water Quality throughout Delta..... 4-31
Figure 4-41 Impacts of Turner Cut Gate on Water Quality throughout Delta 4-32

Tables

Table 4-1 Modeling Scenarios of Gate Location and Operation 4-4
Table 4-2 Gate Closure Frequency..... 4-9
Table 4-3 Impacts of Modeling Scenarios on Water Quality 4-35

4 Modeling Physical Barriers (Gates) as Engineering Solutions to Satisfy National Marine Fisheries Service Biological Opinion Reasonable Prudent Alternative Action IV.1.3

4.1 Introduction

This report provides detailed modeling information on the potential impact on flow, water quality, and water level throughout the Delta of physical barriers (gates) as engineering solutions to deter fish from entering the Delta. The modeling was performed to provide information to support decision-making for engineering solutions to satisfy the National Marine Fisheries Service Biological Opinion Reasonable and Prudent Alternative (NMFS BiOp RPA) Action IV.1.3 (Action). The Action objective is to prevent emigrating salmonids from entering into the interior of the Delta and southern Delta, and to reduce exposure to the Central Valley Project (CVP) and State Water Project (SWP) export facilities. Delta Simulation Model 2 (DSM2) was used to simulate gates on the Delta channels: Georgiana Slough, Head of Old River, Turner Cut, and Columbia Cut. The modeling results have been evaluated for impact analysis of flow, water quality, and water level throughout the Delta.

4.2 The Simulation Model

DSM2 is a one-dimensional hydrodynamic and water quality model used to simulate hydrodynamics, water quality, and particle tracking in the Sacramento-San Joaquin Delta. DSM2 represents the best available planning model for Delta tidal hydraulic and salinity modeling. It is appropriate for describing the existing conditions in the Delta, as well as performing simulations for the assessment of incremental environmental impacts caused by future facilities and operations.

DSM2 consists of three modules: HYDRO, QUAL, and PTM. HYDRO simulates flow, velocities, and water level, and provides the flow input for QUAL and PTM. DSM2-HYDRO outputs are used to predict changes in flow rates, water level, and their effects on Delta channels as a result of future facilities and operations.

The DSM2-QUAL module simulates fate and transport of conservative and non-conservative water quality constituents, including salts, given a flow field simulated by DSM2-HYDRO. Outputs are used to estimate changes in salinity and their effects on Delta channels as a result of future facilities and operations.

The DSM2-PTM module, which was not used in this modeling analysis, simulates pseudo 3-D transport of neutrally buoyant particles based on the flow field simulated by DSM2-HYDRO. It simulates the fate and transport of individual particles traveling throughout the Delta. DSM2-PTM has multiple applications ranging from visualization of flow patterns to simulation of discrete organisms, such as fish eggs and larvae. Additional information on DSM2 can be found on the DWR Modeling Support Branch website: http://baydeltaoffice.water.ca.gov/modeling/deltamodeling/models/dsm2/dsm2.cfm.

4.3 Methodology

There were several scenarios investigated during this analysis, ranging from full flow blockage to partial flow blockage at four key junctions in the Delta (Figure 4-1). An additional key junction, Threemile Slough, for which prior analysis had been conducted and is discussed in this report, is not shown in Figure 4-1. The purpose of the flow blockage is to simulate a gate blocking a junction to divert emigrating salmonids from entering into the Delta channels and to keep them in the Sacramento River

or San Joaquin River for their passage to the ocean. The 16-year (water year [WY] 1976-WY 1991) DSM2 model was used to simulate these scenarios. The 16-year DSM2 model simulations have also been used for the Bay Delta Conservation Plan (BDCP) Draft EIR/EIS, South Delta Improvements Program (SDIP), Franks Tract Project, and Storage Investigations and Operations Criteria and Plan (OCAP). The DSM2 model simulation of Existing Conditions for the BDCP Draft EIR/EIS was used as a baseline. The modeled or simulated flow water quality and water level were then compared with the baseline and the incremental changes were evaluated for impacts on various Delta locations.

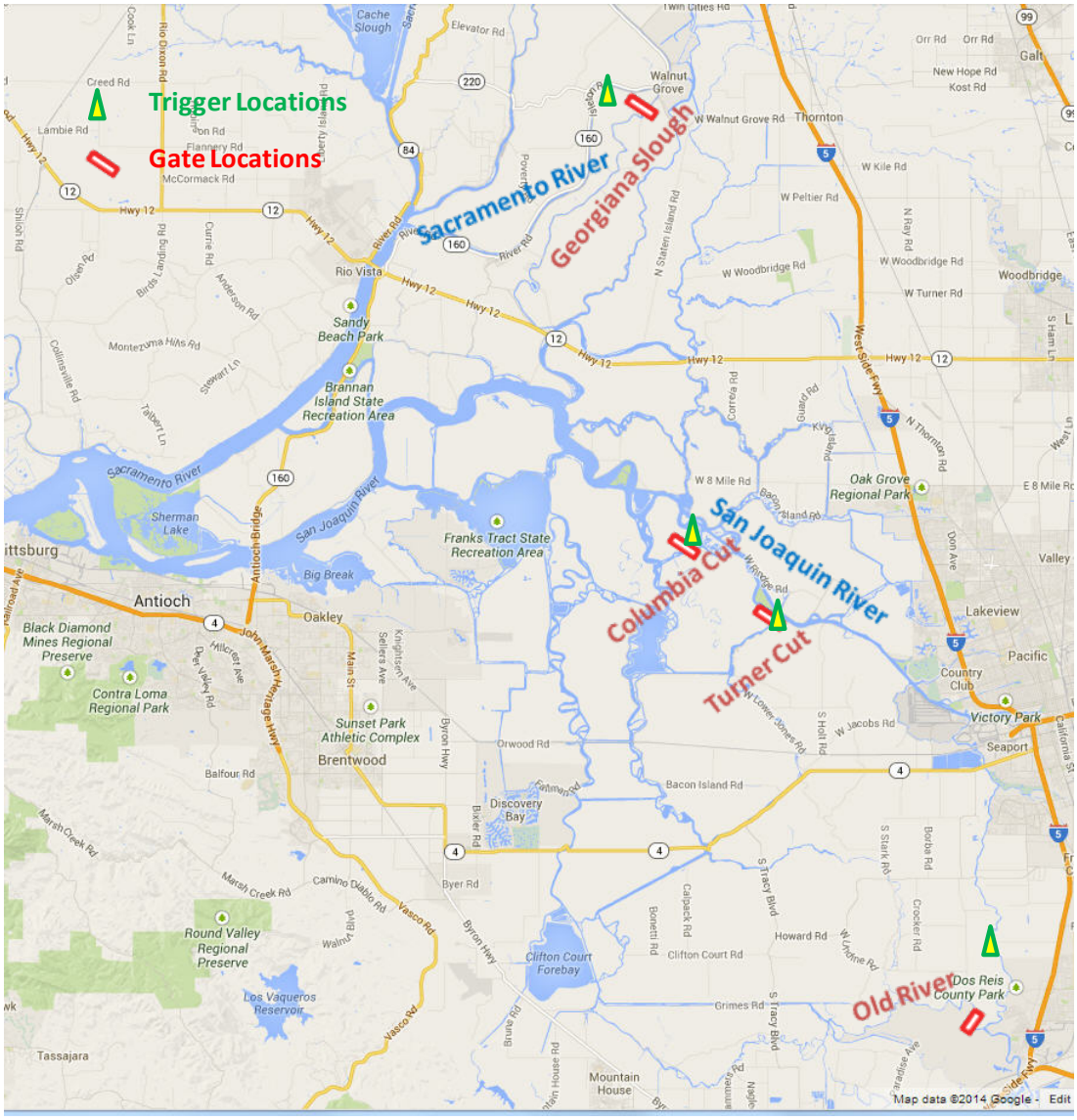

Figure 4-1 Gate Locations in the Delta Channels

4.3.1 Description of Existing Conditions

The existing conditions model simulation was developed assuming WY 2009-level of development and regulatory conditions. The existing conditions assumptions included how existing facilities and ongoing programs that existed as of February 13, 2009 (publication date of the BDCP Public EIR/EIS Notice of

Preparation and Notice of Intent) could affect or could be affected by implementation of the alternatives. The existing conditions assumptions also included assumptions related to the SWP and CVP, ongoing policies by governmental and nonprofit entities, and assumptions related to annual actions that vary every year. One exception was the NMFS BiOp on the Long-Term Central Valley Project and State Water Project Operations Criteria and Plan, released in June 2009, that was included in the development of the existing conditions simulation in the BDCP EIR/EIS (California Department of Water Resources 2013).

4.3.2 Description of Modeling Scenarios

The modeling scenarios were developed by adding a gate, or a combination of gates, to the existing conditions model simulation. The scenarios were divided into three categories: (1) full flow blockage to Delta channels, (2) partial flow blockage to Delta channels, and (3) flow blockage used in other projects. The gates in these scenarios were operated either by the flow trigger or the velocity trigger option to restrict flow to the Delta channels. The scenarios, which included Georgiana Slough or Head of Old River gate, had a gate operation trigger location either in the Delta channels containing the gates or in the river channels near the closure. The scenarios, which included the Turner Cut and Columbia Cut gates, had a trigger location only in the Delta channels. These channels are located in the Central Delta and are influenced by the tide. It was assumed that the impact from the trigger location in the rivers for these gates would be similar to that of the channels. Table 4-1 lists the categories with gate locations and operations for each of the scenarios.

Category	Location of Gate	Gate Operation Trigger	Trigger Location
Full Flow Blockage to Delta Channels	Georgiana Slough, Head of Old River, Turner Cut & Columbia Cut (Four Gates)	Closed on positive flow in channel & opened on reverse flow	Flow in Georgiana Slough, Head of Old River, Turner Cut & Columbia Cut
	Georgiana Slough	Closed on positive flow in channel & opened on reverse flow	Flow in Georgiana Slough
	Head of Old River	Closed on positive flow in channel & opened on reverse flow	Flow in Head of Old River
	Turner Cut	Closed on positive flow in channel & opened on reverse flow	Flow in Turner Cut
	Columbia Cut	Closed on positive flow in channel & opened on reverse flow	Flow in Columbia Cut

	Head of Old River, Turner Cut & Columbia Cut (Three Gates)	Closed on positive flow in channel & opened on reverse flow	Flow in Head of Old River, Turner Cut & Columbia Cut
	Georgiana Slough, Head of Old River, Turner Cut & Columbia Cut (Four Gates)	Closed on ebb & opened on flood	Flow in Sacramento River, San Joaquin River, Turner Cut & Columbia Cut
	Georgiana Slough	Closed on ebb & opened on flood	Flow in Sacramento River
	Head of Old River	Closed on ebb & opened on flood	Flow in San Joaquin River
	Head of Old River, Turner Cut & Columbia Cut (Three Gates)	Closed on ebb & opened on flood	Flow in San Joaquin River, Turner Cut & Columbia Cut
Partial Flow Blockage to Delta Channels	Georgiana Slough	Partial closed on ebb to block 50% net flow & opened on flood	Flow in Sacramento River
	Head of Old River	Partial closed on ebb to block 50% net flow & opened on flood	Flow in San Joaquin River
	Georgiana Slough	Closed on high velocity & Opened on low velocity	Velocity in Sacramento River
	Georgiana Slough	Partial closed on high velocity to block 50% net flow & opened on low velocity	Velocity in Sacramento River
	Head of Old River	Closed on high velocity & Opened on low velocity	Velocity in San Joaquin River
	Head of Old River	Partial closed on high velocity to block 50% net flow & opened on low velocity	Velocity in San Joaquin River
Flow Blockage Used in Other Projects	Threemile Slough (Franks Tract Project)	Franks Tract Project proposed operation, Seasonal operation for Fish and Water Quality	Flow in Sacramento and San Joaquin River or EC in Jersey Point

Table 4-1 Modeling Scenarios of Gate Location and Operation

4.3.2.1 Full Flow Blockage to Delta Channels

The gates were modeled to restrict flow from entering into the junctions. The gates at one site, or a combination of sites, were modeled in this category. The gates' operations were triggered by either flow in the Delta channels where the gates were placed, or flow in the rivers. The gates with a trigger location in Delta channels were closed on the positive flows in the channels and were opened on the reverse flows in the channels. The gates with a trigger location in the Sacramento or San Joaquin rivers are described below as flow trigger.

4.3.2.1.1. Flow Trigger

The gates were closed on the ebb tide when the water flowed toward the ocean from the rivers. The gates were opened on the flood tide when the water flowed from the ocean toward the rivers. The gate operation at Georgiana Slough was used to illustrate the flow trigger method. The trigger was based on the flow in the Sacramento River downstream of the gate. When the flow direction at the Sacramento River at the trigger location was toward the ocean, the Georgiana Slough gate was closed. The gate was opened during reverse flow periods. Figure 4-2 illustrates the gate closure in response to the flow trigger. The gate operation at the Head of Old River was based on the flow in the San Joaquin River downstream of the gate. The gate operation scenario was similar to the Georgiana Slough gate.

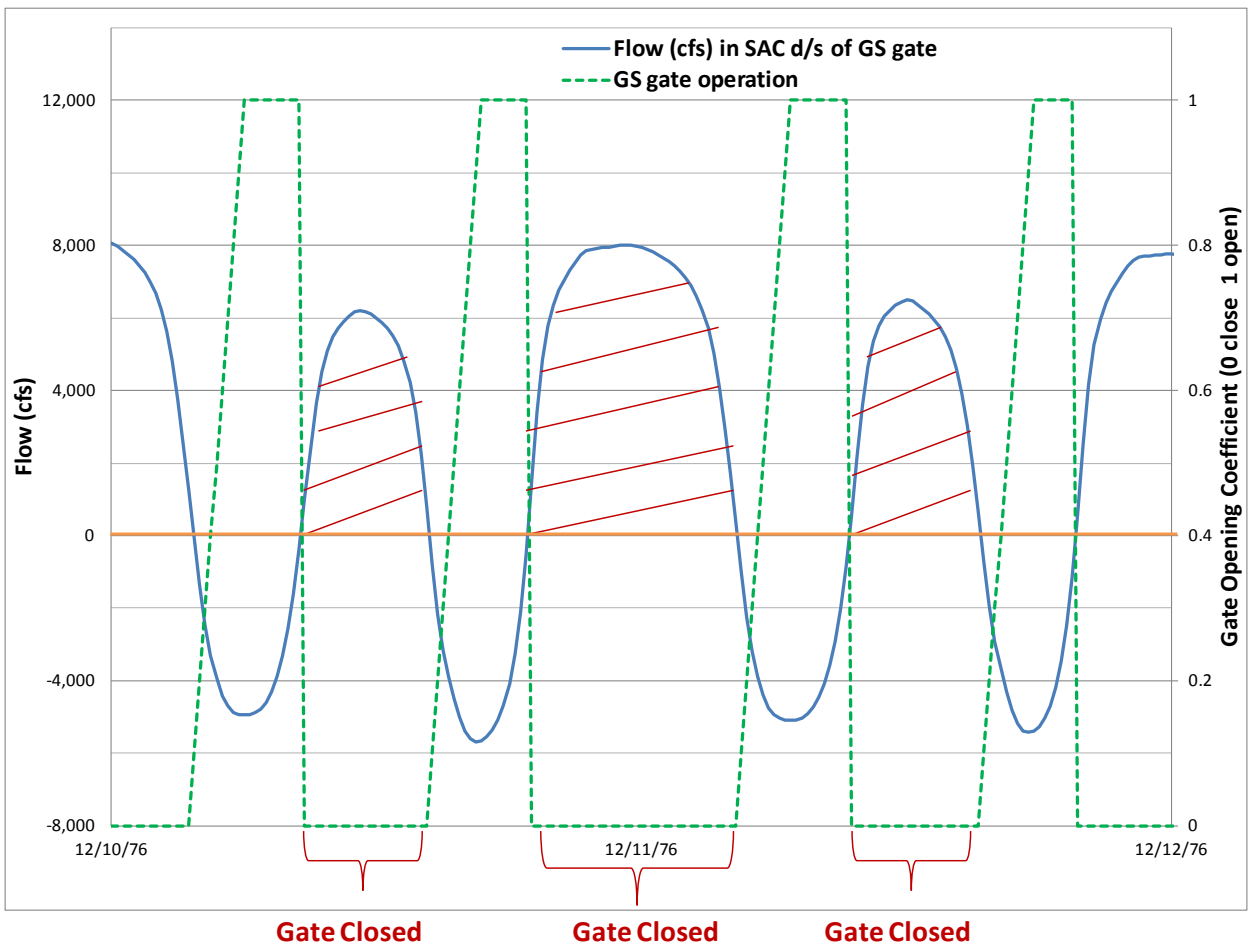

Figure 4-2 Flow Triggered Gate Operation (open/close)

4.3.2.2 Partial Flow Blockage to Delta Channels

The gates were modeled to restrict partial flow from entering into the junctions. The gates were placed in the junctions on Delta channels. In this category, flow was not fully blocked to enter into the channels from the rivers during the ebb tide. The gates' operations were triggered by either flow in the rivers, or velocity in the rivers. These triggers were described below.

4.3.2.2.1 Flow Trigger

During the ebb tide, the size of the gate was modified to attain an average flow blockage of about 50 percent during the 16-year model simulation period. The scenario was analyzed to evaluate incremental changes in water quality and water levels. The gates were closed on the ebb tide when the water flowed toward the ocean from the Sacramento or San Joaquin rivers. The gates were opened on the flood tide when the water flowed from the ocean toward the rivers. Figure 4-2 illustrates the flow trigger scenario for Georgiana Slough. The Head of Old River gate had similar operations.

4.3.2.2.2 Velocity Trigger

The gate operation was triggered by velocity in the rivers. The gate at a junction of a river and a channel operated based on velocity in the river downstream of the junction. The velocity in the Delta followed the tidal cycle and has two high and two low velocities occurring every 6 hours. When the velocity changed from high to low, the gate was closed, and when the velocity changed from low to high, the gate was opened. Figure 4-3 illustrates the gate closure in response to the velocity trigger. The gate at Georgiana Slough operated based on a velocity trigger in the Sacramento River downstream of the junction. Another scenario, which blocked about 50 percent of the flow during the gate closure period (Figure 4-3), was simulated. This modeling scenario was developed by modifying the size of the gate. The gate at the Head of Old River was operated on a similar velocity trigger formulation, but it was based on the velocity in the San Joaquin River downstream of the junction.

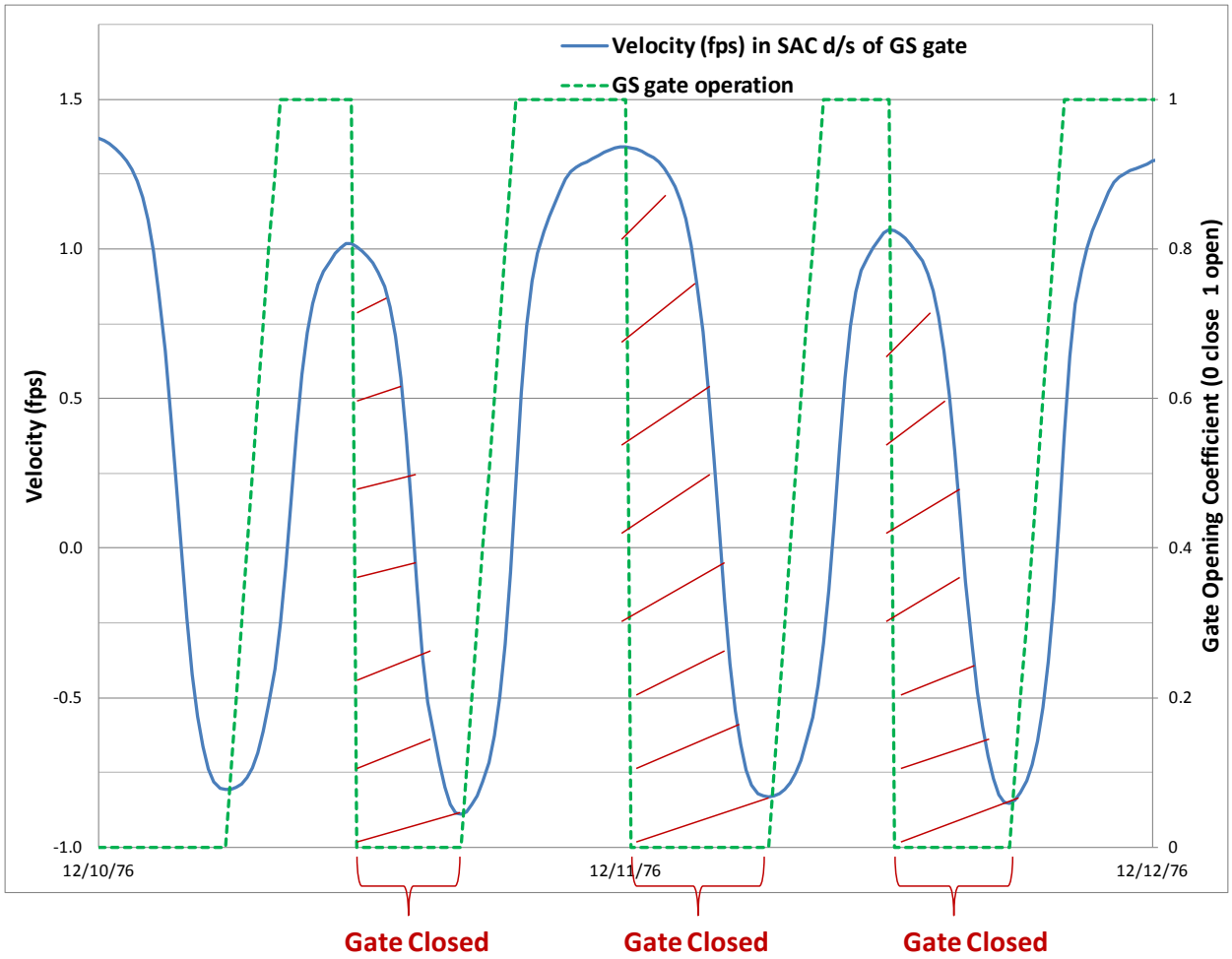

Figure 4-3 Velocity Triggered Gate Operation (open/close)

4.3.2.3 Flow Blockage used in Other Projects

As noted under section 4.3, Methodology, gate modeling analysis had already been conducted for Threemile Slough (Franks Tract Project). The Franks Tract Project objectives were different than the objective of NMFS BiOp RPA Action IV.1.3, but one of the objectives was to protect sensitive fish species and reduce seawater intrusion through modifications of flow conditions in the western Delta. The proposed Franks Tract Project includes a tidally operated gate located in the Threemile Slough. The Franks Tract DSM2 model was run again for this study analysis to simulate the proposed gate operations. The modeling results were analyzed for any impacts on the Delta.

4.4 Model Results

The DSM2 model was simulated for 16 years for existing conditions and all scenarios listed in Table 4-1. The model results were in 15-minute intervals and were processed to generate monthly average flow, monthly average EC (Electric Conductivity, used for salinity), and daily minimum water level. The percentage of time that the gates were closed throughout the simulation period is reported in Table 4-2 for all scenarios.

Category	Location of Gate	Gate Operation Trigger	Trigger Location	Percent of time gate was closed
Full Flow Blockage to Delta Channels	Georgiana Slough, Head of Old River, Turner Cut & Columbia Cut (Four Gates)	Closed on positive flows in channel & opened on reverse flows	Flow in Georgiana Slough, Head of Old River, Turner Cut & Columbia Cut	99, 99, 51 & 50
	Georgiana Slough	Closed on positive flows in channel & opened on reverse flows	Flow in Georgiana Slough	99
	Head of Old River	Closed on positive flows in channel & opened on reverse flows	Flow in Head of Old River	99
	Turner Cut	Closed on positive flows in channel & opened on reverse flows	Flow in Turner Cut	51
	Columbia Cut	Closed on positive flows in channel & opened on reverse flows	Flow in Columbia Cut	50
	Head of Old River, Turner Cut & Columbia Cut (Three Gates)	Closed on positive flows in channel & opened on reverse flows	Flow in Head of Old River, Turner Cut & Columbia Cut	99, 51 & 50
	Georgiana Slough, Head of Old River, Turner Cut & Columbia Cut (Four Gates)	Closed on ebb & opened on flood	Flow in Sacramento River, San Joaquin River, Turner Cut & Columbia Cut	80, 80, 51 & 50
	Georgiana Slough	Closed on ebb & opened on flood	Flow in Sacramento River	80
	Head of Old River	Closed on ebb & opened on flood	Flow in San Joaquin River	80
	Head of Old River, Turner Cut & Columbia Cut (Three Gates)	Closed on ebb & opened on flood	Flow in San Joaquin River, Turner Cut & Columbia Cut	80, 51 & 50

Category	Location of Gate	Gate Operation Trigger	Trigger Location	Percent of time gate was closed
Partial Flow Blockage to Delta Channels	Georgiana Slough	Partial closed on ebb to block 50% net flow & opened on flood	Flow in Sacramento River	80
	Head of Old River	Partial closed on ebb to block 50% net flow & opened on flood	Flow in San Joaquin River	80
	Georgiana Slough	Closed on high velocity & Opened on low velocity	Velocity in Sacramento River	46
	Georgiana Slough	Partial closed on high velocity to block 50% net flow & opened on low velocity	Velocity in Sacramento River	46
	Head of Old River	Closed on high velocity & Opened on low velocity	Velocity in San Joaquin River	45
	Head of Old River	Partial closed on high velocity to block 50% net flow & opened on low velocity	Velocity in San Joaquin River	45
Flow Blockage used in other Projects	Threemile Slough (Franks Tract Project)	Franks Tract Project proposed operation, Seasonal operation for Fish and Water Quality	Flow in Sacramento and San Joaquin River or EC in Jersey Point	12

Table 4-2 Gate Closure Frequency

The modeled flow for the scenarios was compared with existing conditions at downstream locations of the gates at Georgiana Slough, Head of Old River, Columbia Cut, and Turner Cut. The modeled EC was compared with EC at Sacramento River at Emmaton (Emmaton), San Joaquin River at Jersey Point (Jersey Point), Clifton Court Forebay (Clifton Court), and Old River at Tracy Road (Tracy Road). The modeled water level (stage) was compared with water levels at Old River at Tracy Road, San Joaquin River at Brandt Bridge (Brandt Bridge), and San Joaquin River at Prisoners Point (Prisoners Point) (Figure 4-4). The processed values are presented in Figures 4-5 to 4-41.

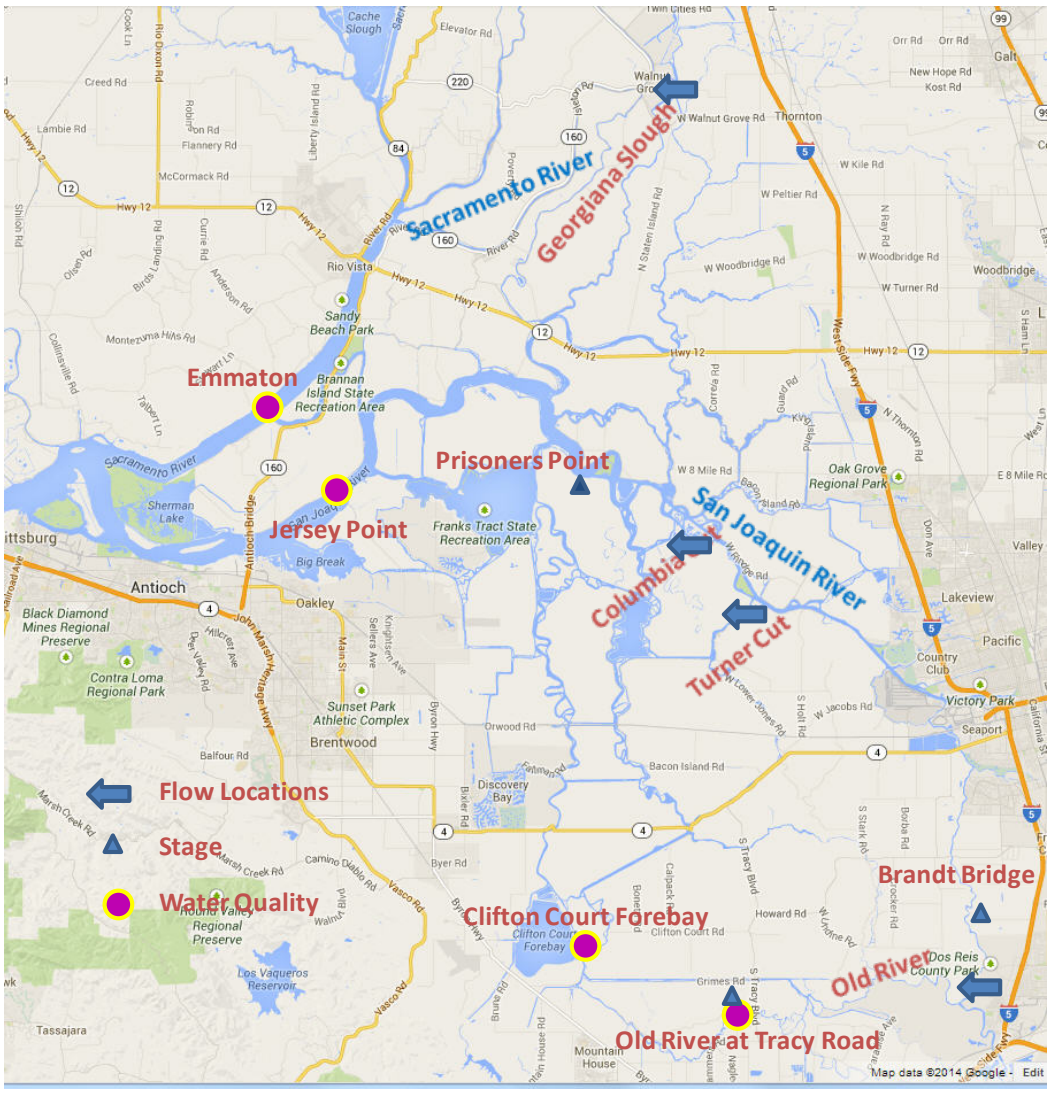

Figure 4-4 Model Output Locations

4.4.1 Full Flow Blockage to Delta Channels

The gates at Georgiana Slough and Head of Old River were closed 99 percent of the time for the flow in the Delta channels trigger scenarios. Consequently, little to no flow was going through these channels. The gates at Georgiana Slough and the Head of Old River were closed 80 percent of the time (Table 4-2) for the flow in the rivers trigger scenarios. The gates were closed less frequently than the previous scenarios, so little flow went through these channels. The gates at Columbia Cut and Turner Cut were closed or opened 50 percent of the time. Figure 4-5 to Figure 4-12 show monthly average flow in the Delta channels downstream of the gates. A positive flow direction in Columbia and Turner cuts refers to flow toward the San Joaquin River, and a negative flow direction refers to flow from the San Joaquin River into the cuts.

Figure 4-13 to Figure 4-20 show monthly average EC comparison bar plots. The Georgiana Slough gate and Four Gates scenarios (Table 4-1) blocked better quality Sacramento River flow from entering into

the interior of the Delta and southern Delta, and allowed more water to flow through the Sacramento River. This flow pattern had an impact on water quality. EC at Clifton Court and Jersey Point increased, and EC at Emmaton decreased. The Head of Old River gate and Three Gates scenarios (Table 4-1) had no impact on EC at Emmaton, Jersey Point, or Clifton Court.

The Delta Cross Channel (DCC) Gates were fully closed from February 1 through May 20 in accordance with the State Water Resources Control Board Decision 1641 (Bureau of Reclamation 2014). The DCC Gates were closed for 14 days, from May 21 through June 15. During those months, the model showed that the Head of Old River Gate and Three Gates scenarios resulted in deteriorated EC at Tracy Road, but EC improved or there were no impacts on EC for all the other months. The Four Gates scenario increased EC at Tracy Road. The Georgiana Slough gate scenario had no impact on EC at Tracy Road. The Columbia Cut gate and Turner Cut gate scenarios had no impact on EC. Consequently, no further modeling of partial flow blockage scenarios for Columbia Cut and Turner Cut gates were necessary.

Daily minimum water levels at the South Delta locations were evaluated (Figure 4-21 to Figure 4-26). The Head of Old River Gate dropped the water level by 1 foot or more during most years of the 16-year simulation period. The Head of Old River Gate restricted San Joaquin River flows from entering Old River and left more water in the San Joaquin River. As a consequence, the water level at Brandt Bridge increased by 1 foot or more 40 percent of the time. The water level at Prisoners Point, which is 45 miles downstream from the gate site, did not change. All of the other gate scenarios did not have an impact on water level in the South Delta.

4.4.2 Partial Flow Blockage to Delta Channels

For the flow trigger scenarios, with the 50 percent flow blockage on the ebb tide, more Sacramento River water went into Georgiana Slough, and more San Joaquin River water went into Old River (Figure 4-9 to Figure 4-12).

For the velocity trigger scenarios, the gates were closed 46 percent of the time in Georgiana Slough, and 45 percent of the time at Head of Old River (Table 4-2). As expected, flow was less restricted to these channels (Figure 4-27 to Figure 4-30).

EC at Clifton Court and Jersey Point increased in response to the Georgiana Slough gate operations. EC at Emmaton decreased, and there was no impact at Tracy Road. The velocity trigger scenarios had a smaller impact on EC (Figure 4-31 to Figure 4-34) than the flow trigger scenarios (Figure 4-17 to Figure 4-20).

The combined effects of the DCC Gate and the Head of Old River Gate closures deteriorated EC from February to May at Tracy Road. There were no impacts to EC at Emmaton, Jersey Point, and Clifton Court.

The Georgiana Slough gate did not have an impact on water level in the South Delta. The impacts on water level in the South Delta channels, because of the Head of Old River Gate, were similar in trends compared with the previous scenarios, but the magnitudes of changes were smaller. The velocity trigger scenarios had a smaller impact on water level (Figure 4-35 to Figure 4-37) than the flow trigger scenarios (Figure 4-24 to Figure 4-26).

4.4.3 Flow Blockage Used in Other Projects

The Franks Tract Project proposed gate at Threemile Slough was operated seasonally for water quality and fishery benefits. The gate improved water quality in Clifton Court and Jersey Point, and had no impact on water quality in Emmaton and Tracy Road. The gate had no impact on water level in the South Delta.

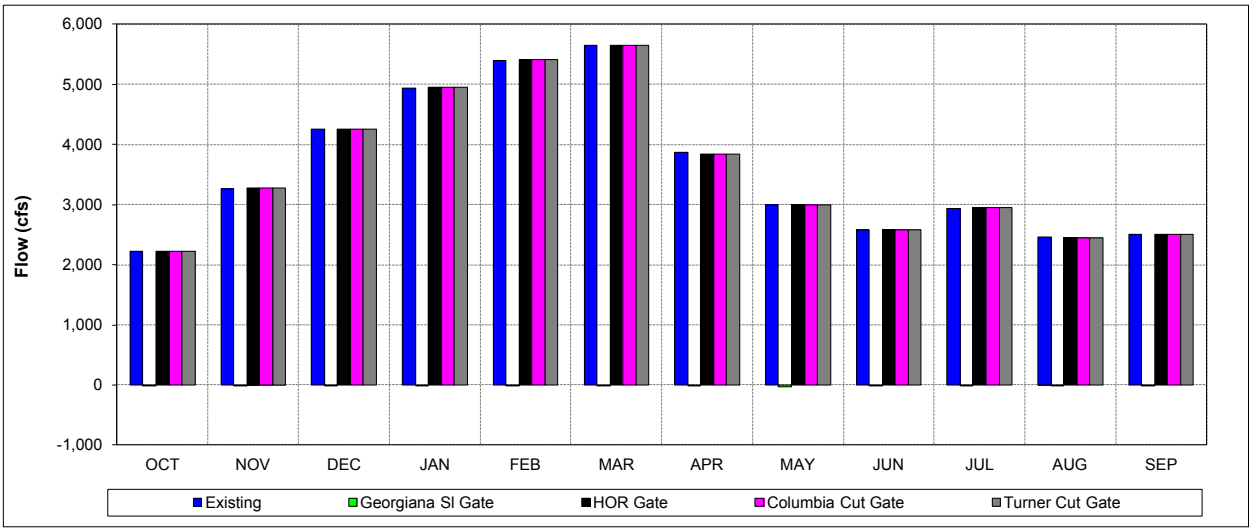

Figure 4-5 Monthly Average Flow at Georgiana Slough for Flow Trigger Location in Channels

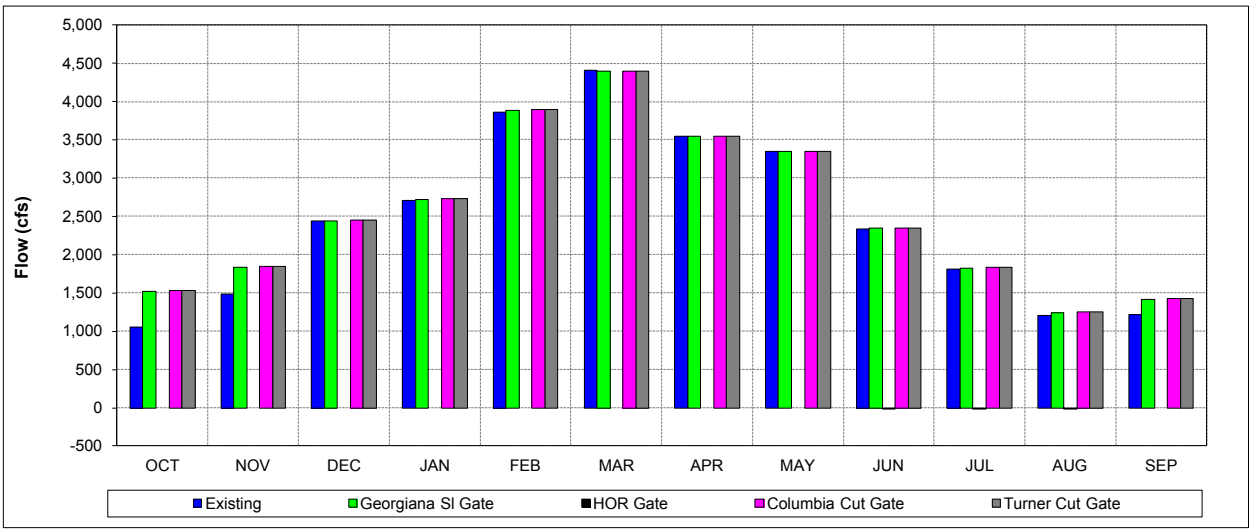

Figure 4-6 Monthly Average Flow at Head of Old River for Flow Trigger Location in Channels

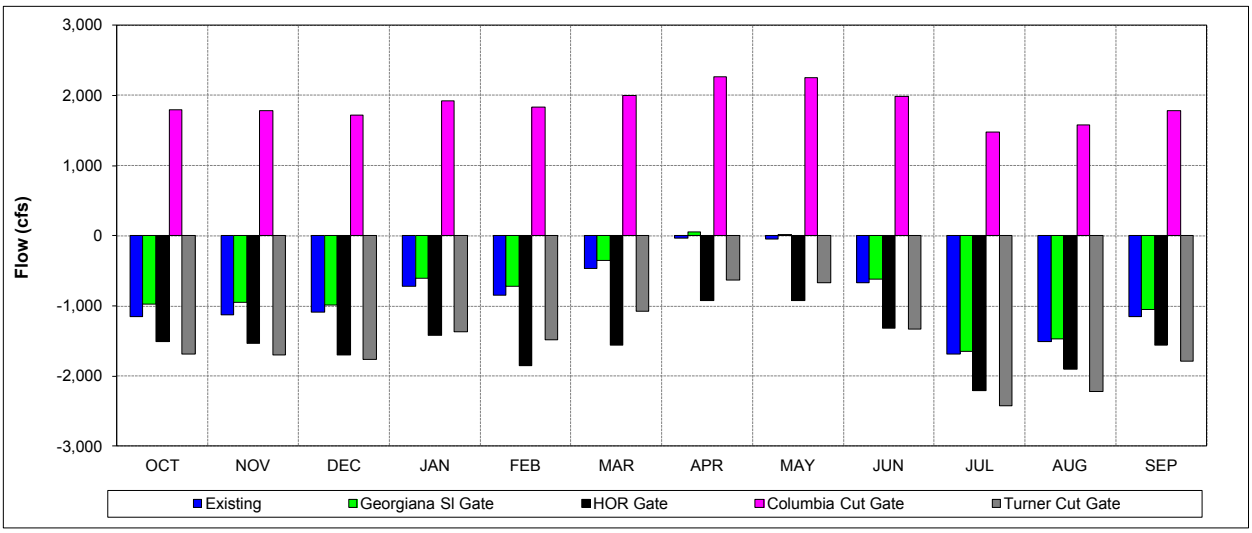

Figure 4-7 Monthly Average Flow at Columbia Cut for Flow Trigger Location in Channels

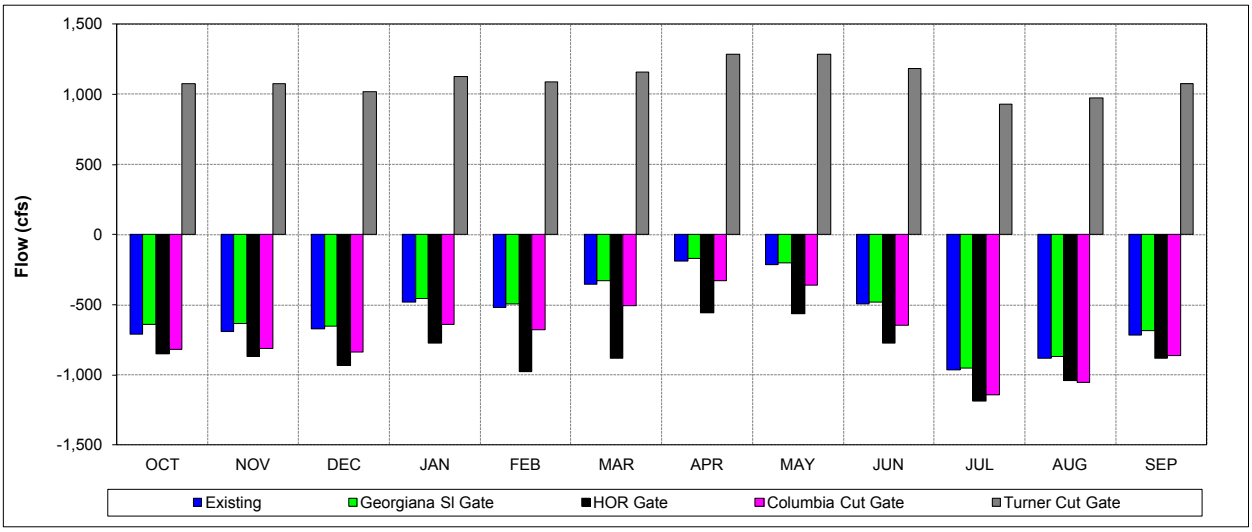

Figure 4-8 Monthly Average Flow at Turner Cut for Flow Trigger Location in Channels

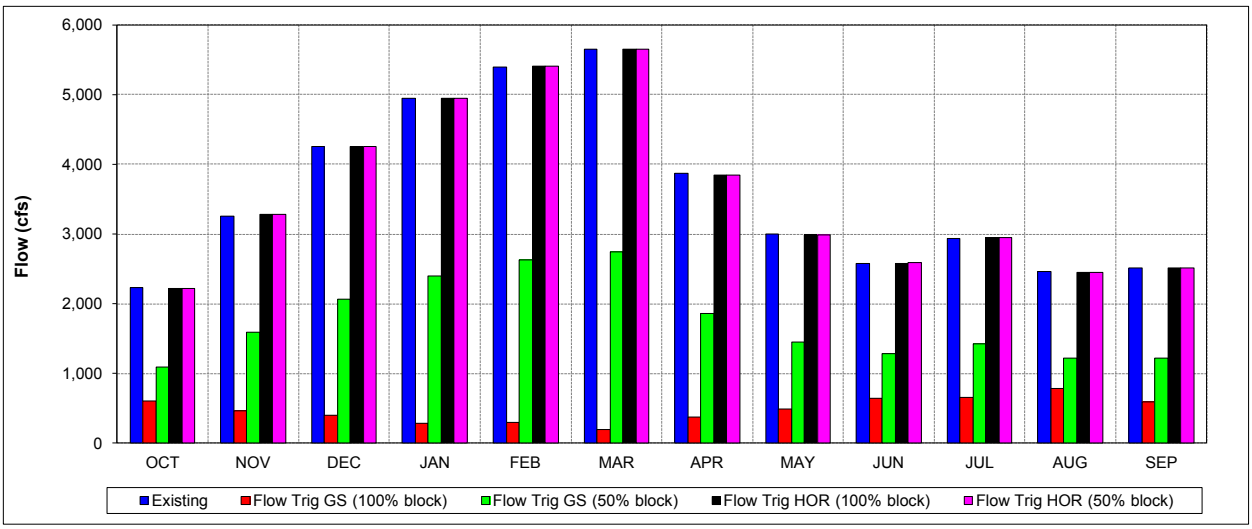

Figure 4-9 Monthly Average Flow at Georgiana Slough for Flow Trigger Location in Rivers

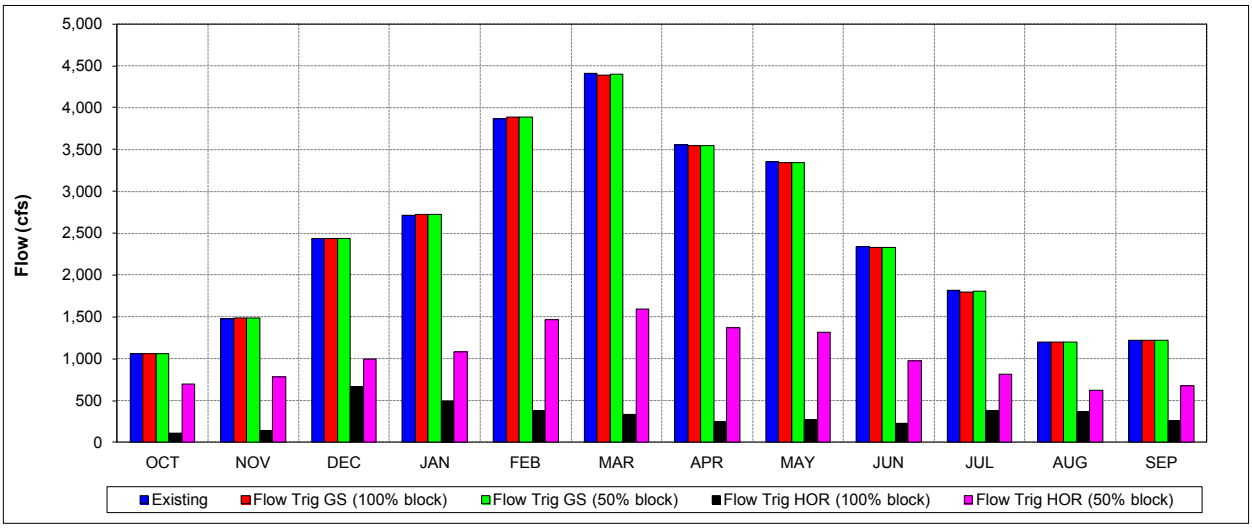

Figure 4-10 Monthly Average Flow at Head of Old River for Flow Trigger Location in Rivers

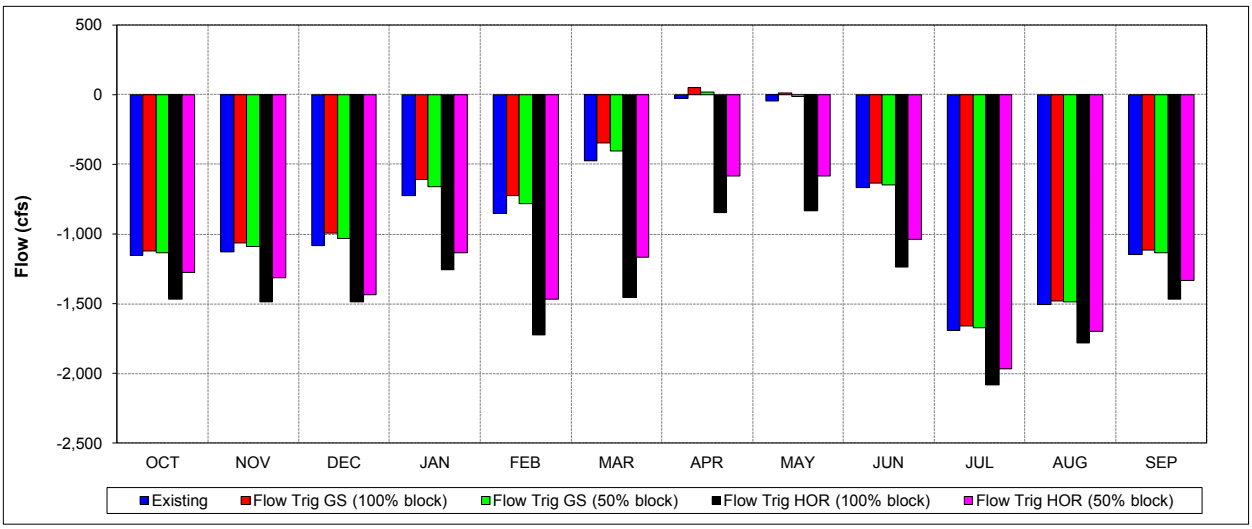

Figure 4-11 Monthly Average Flow at Columbia Cut for Flow Trigger Location in Rivers

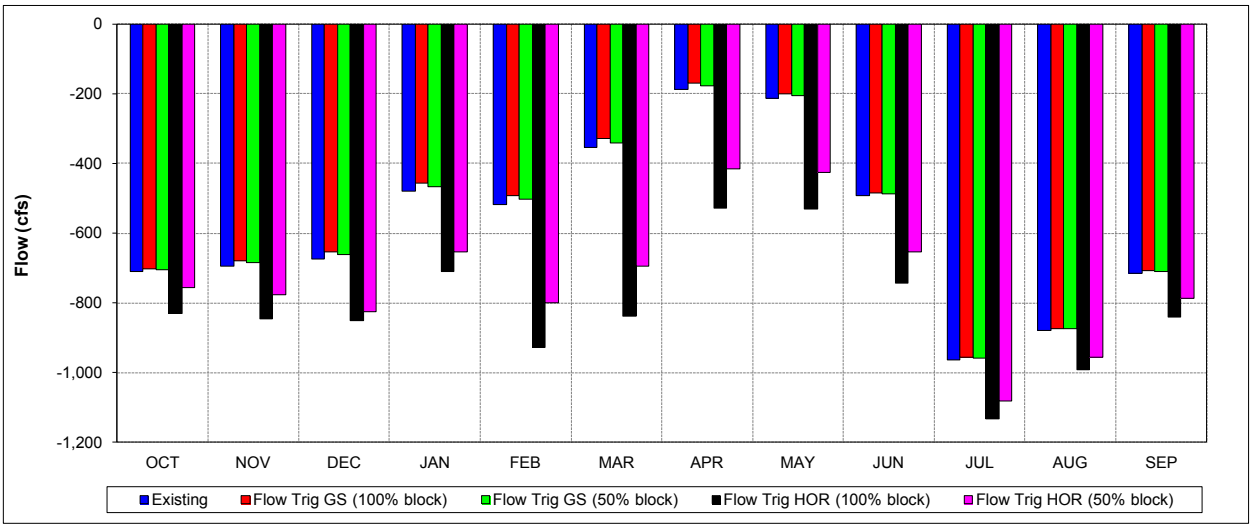

Figure 4-12 Monthly Average Flow at Turner Cut for Flow Trigger Location in Rivers

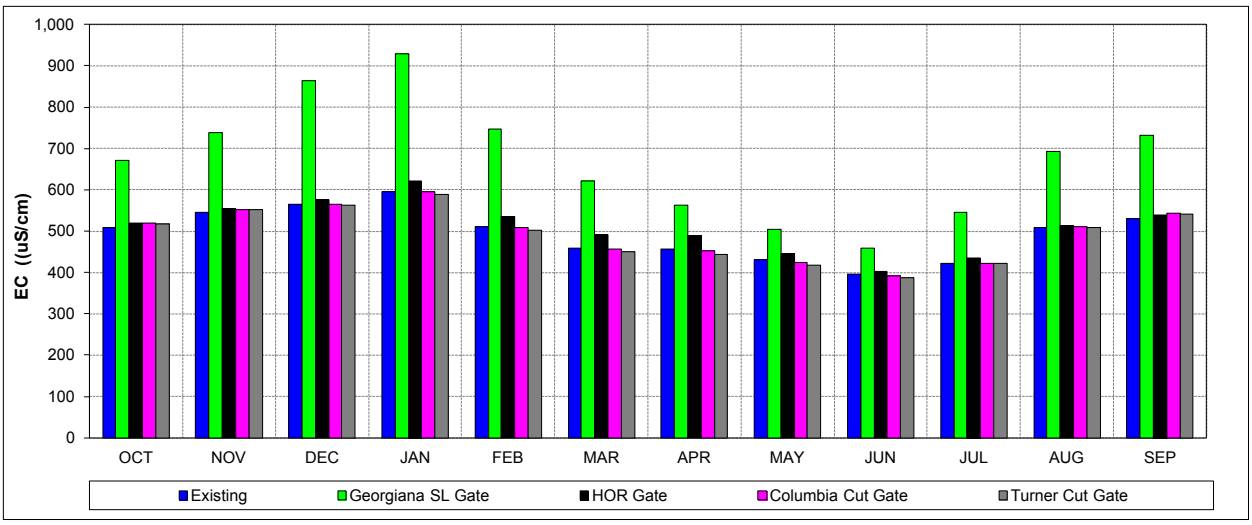

Figure 4-13 Monthly Average EC at Clifton Court Forebay for Flow Trigger Location in Channels

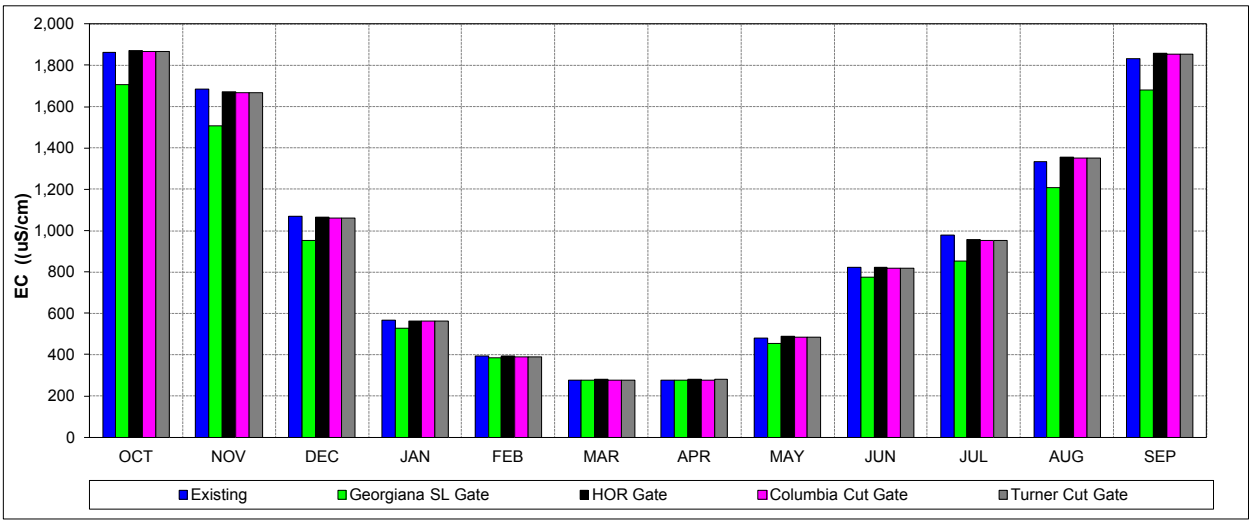

Figure 4-14 Monthly Average EC at Sacramento River at Emmaton for Flow Trigger Location in Channels

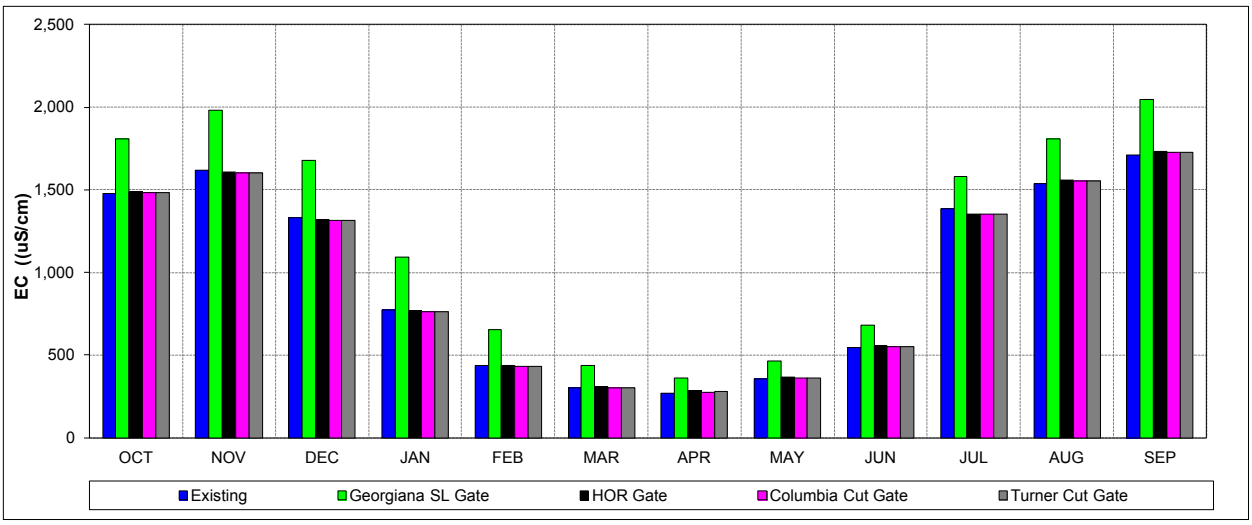

Figure 4-15 Monthly Average EC at San Joaquin River at Jersey Point for Flow Trigger Location in Channels

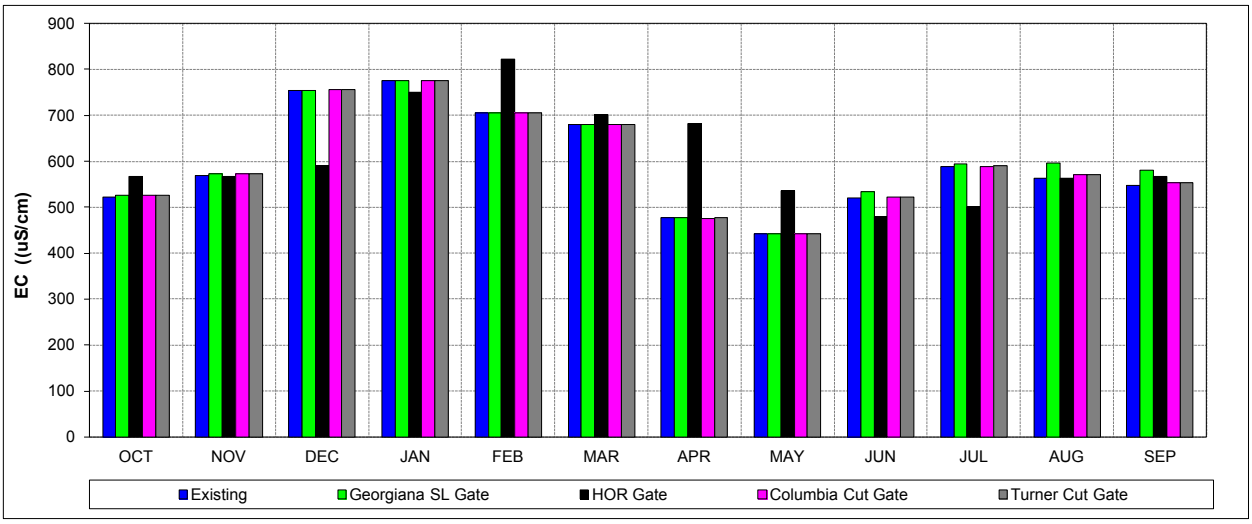

Figure 4-16 Monthly Average EC at Old River at Tracy Road for Flow Trigger Location in Channels

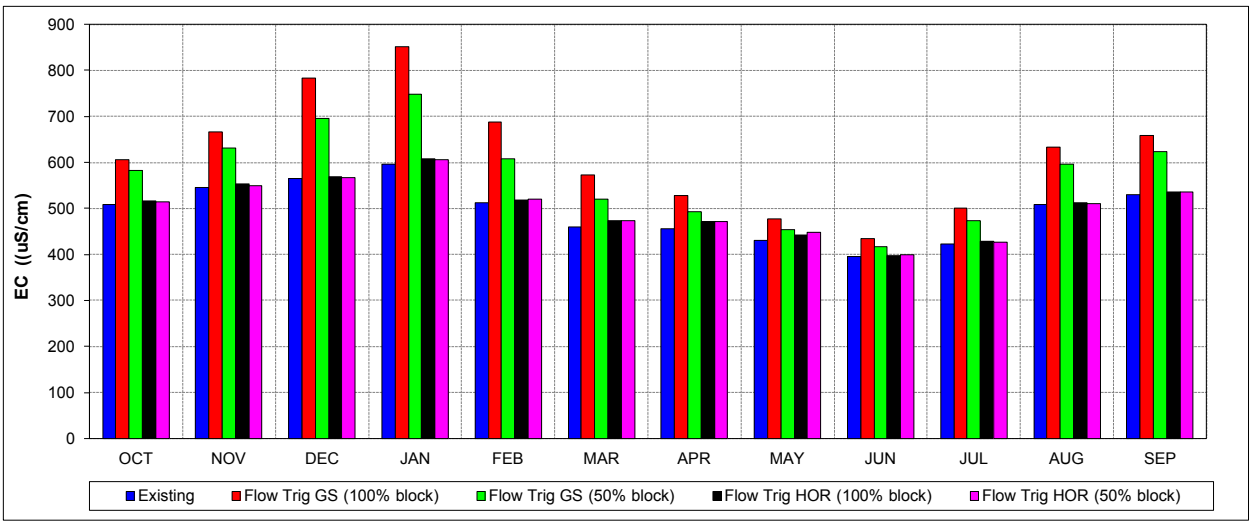

Figure 4-17 Monthly Average EC at Clifton Court Forebay for Flow Trigger Location in Rivers

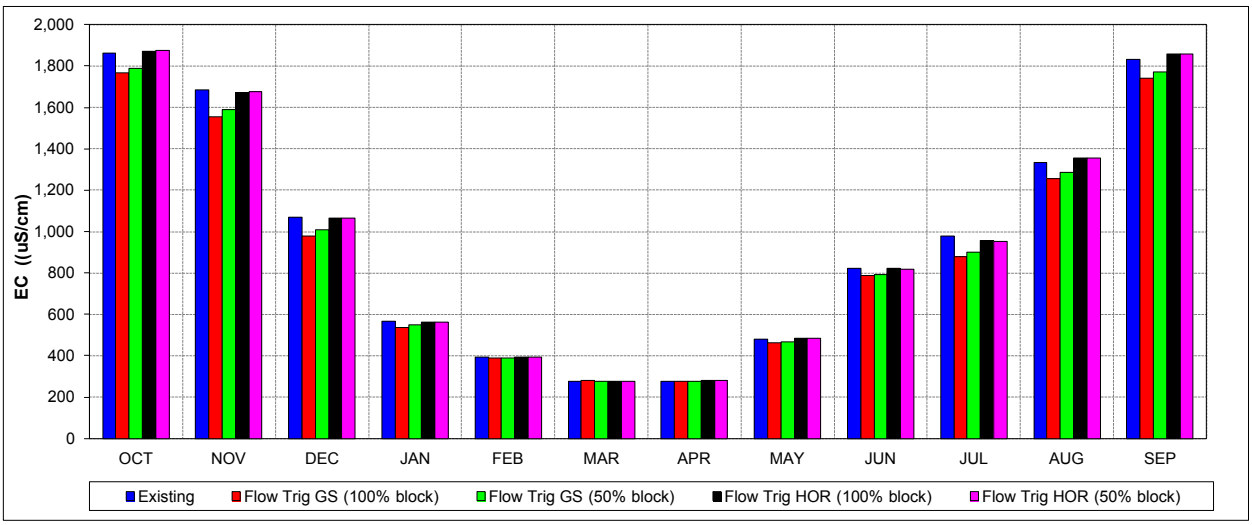

Figure 4-18 Monthly Average EC at Sacramento River at Emmaton for Flow Trigger Location in Rivers

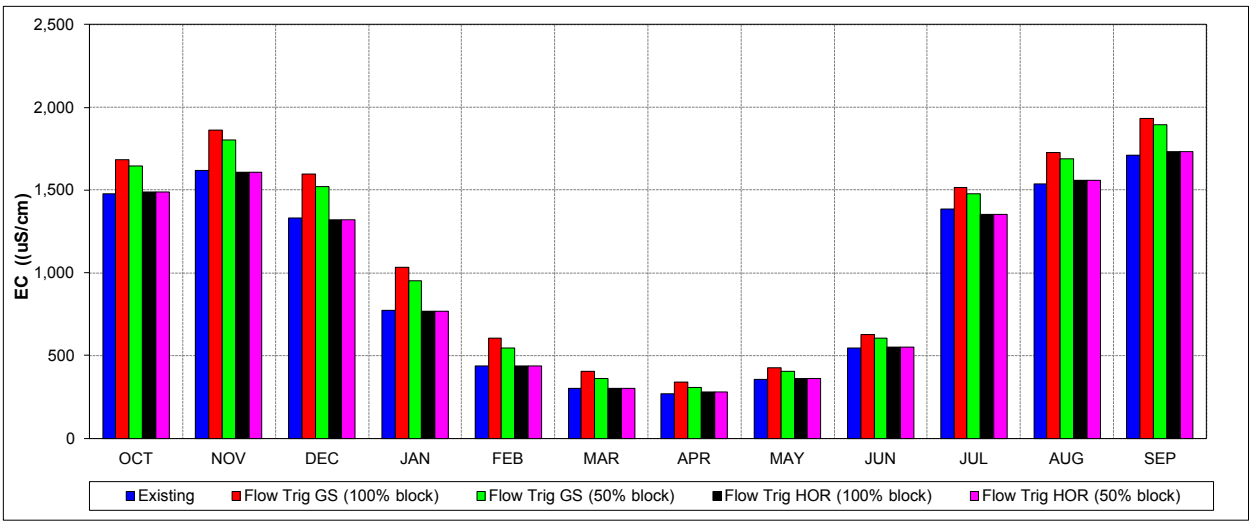

Figure 4-19 Monthly Average EC at San Joaquin River at Jersey Point for Flow Trigger Location in Rivers

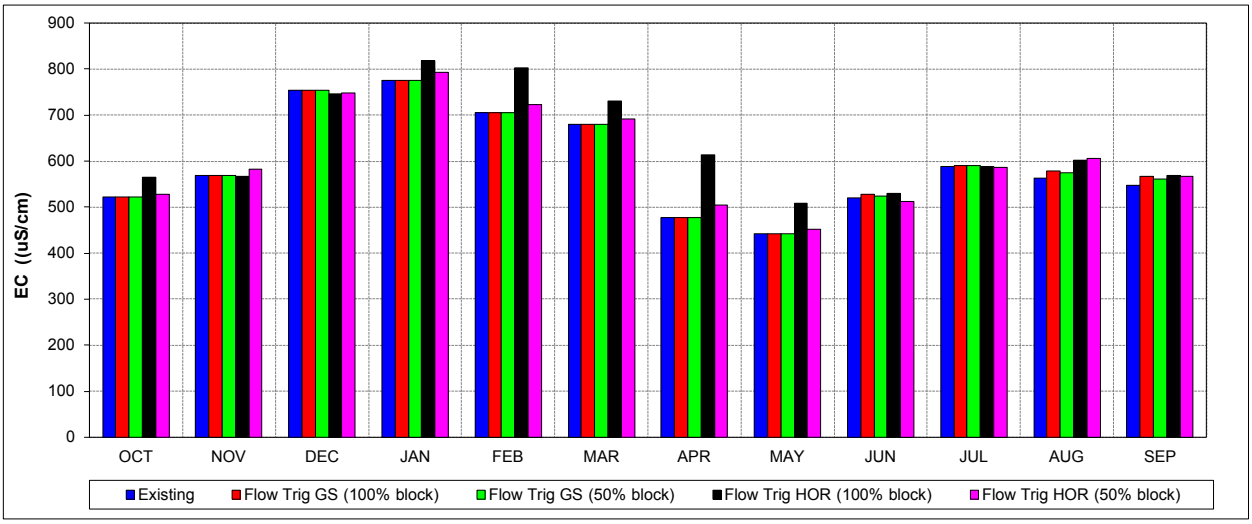

Figure 4-20 Monthly Average EC at Old River at Tracy Road for Flow Trigger Location in Rivers

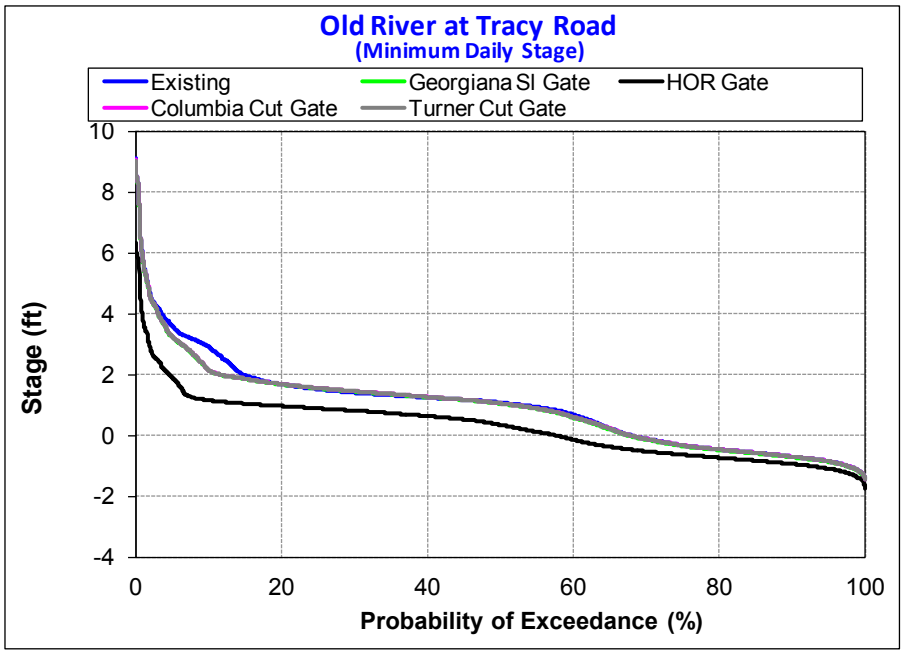

Figure 4-21 Daily Minimum Stage at Old River at Tracy Road for Flow Trigger Location in Channels

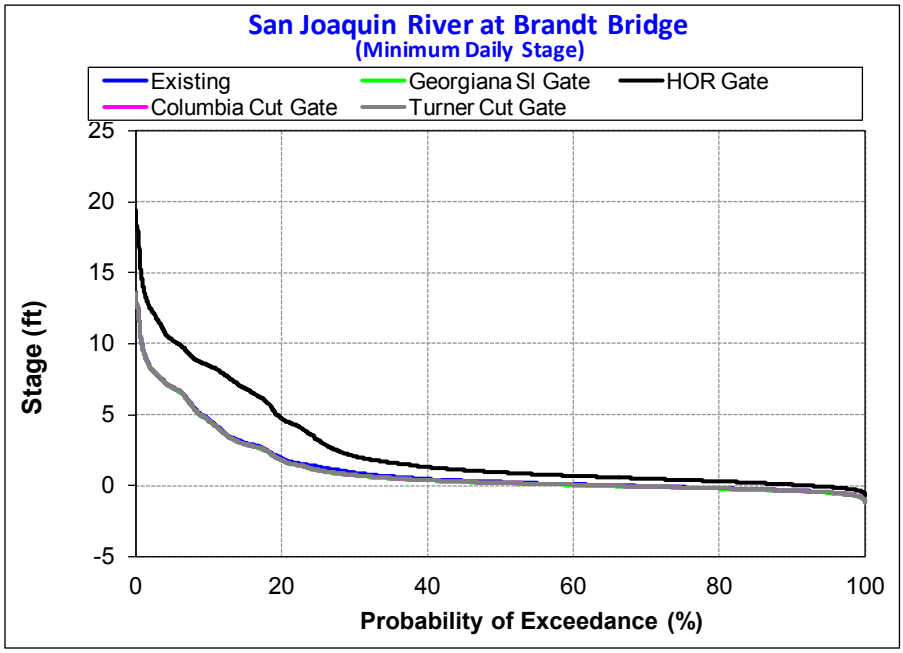

Figure 4-22 Daily Minimum Stage at San Joaquin River at Brandt Bridge for Flow Trigger Location in Channels

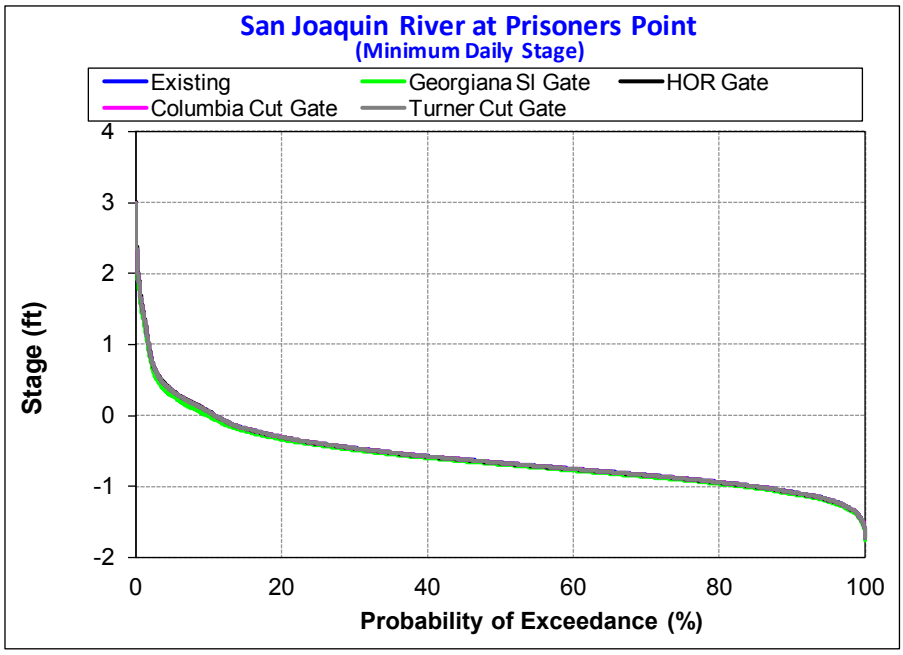

Figure 4-23 Daily Minimum Stage at San Joaquin River at Prisoners Point for Flow Trigger Location in Channels

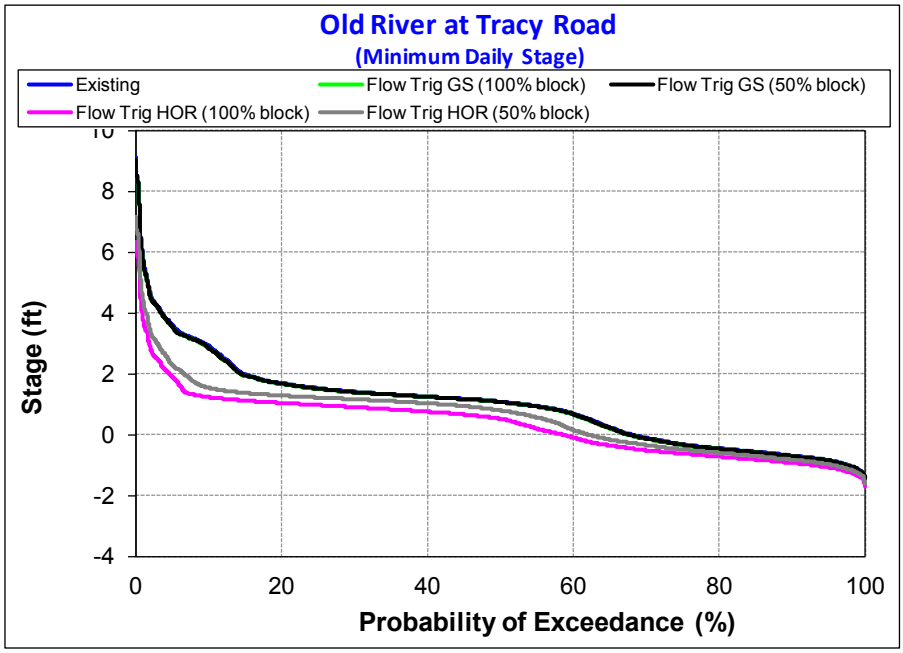

Figure 4-24 Daily Minimum Stage at Old River at Tracy Road for Flow Trigger Location in Rivers

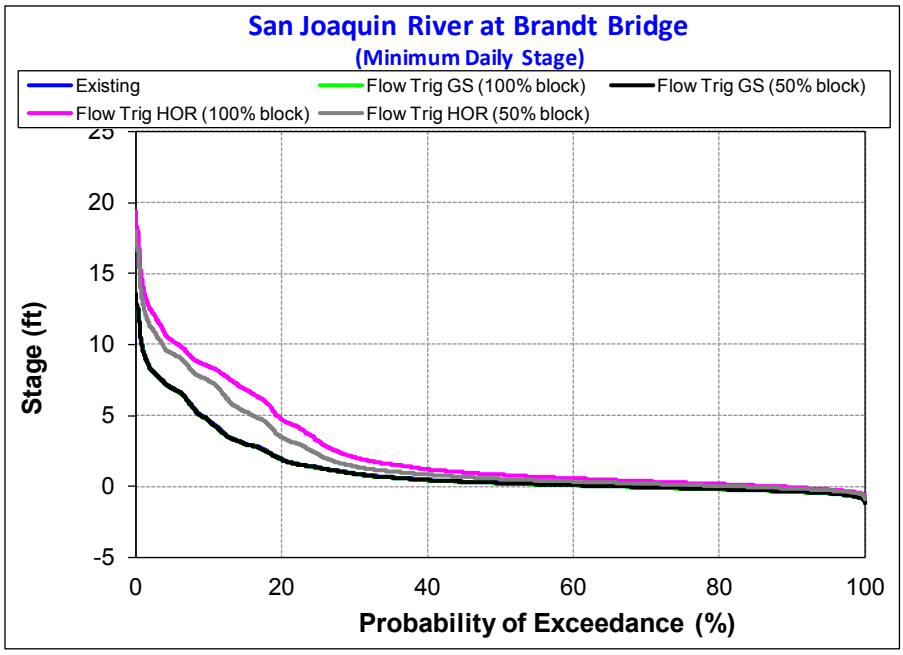

Figure 4-25 Daily Minimum Stage at San Joaquin River at Brandt Bridge for Flow Trigger Location in Rivers

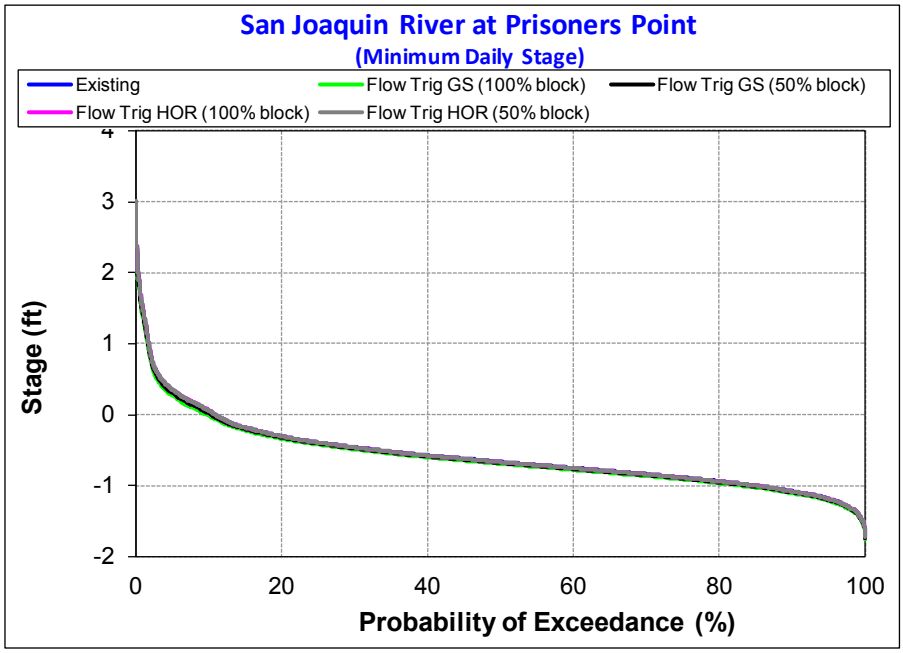

Figure 4-26 Daily Minimum Stage at San Joaquin River at Prisoners Point for Flow Trigger Location in Rivers

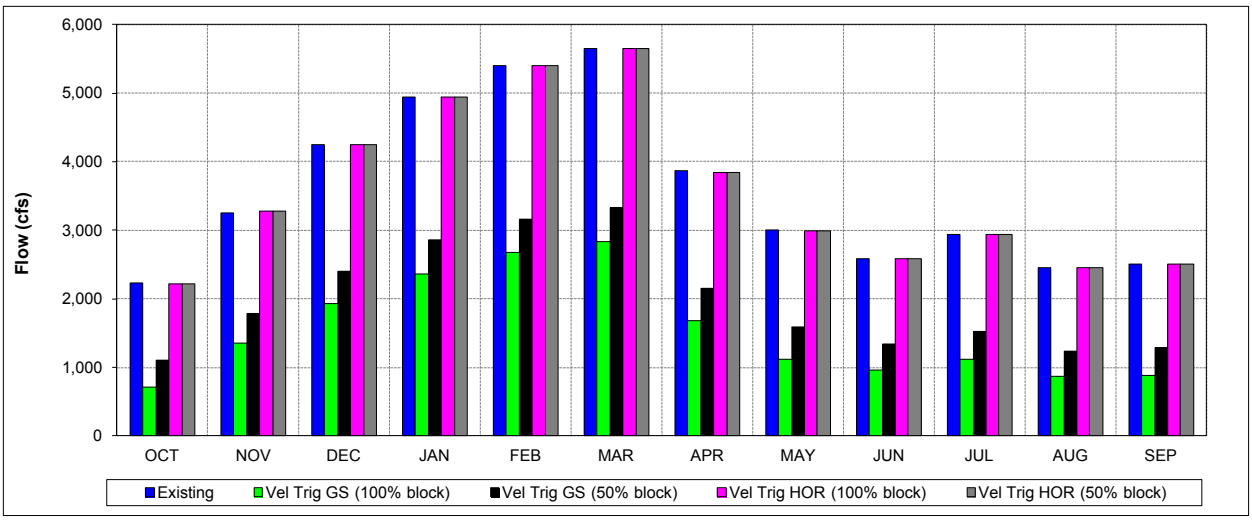

Figure 4-27 Monthly Average Flow at Georgiana Slough for Velocity Trigger Location in Rivers

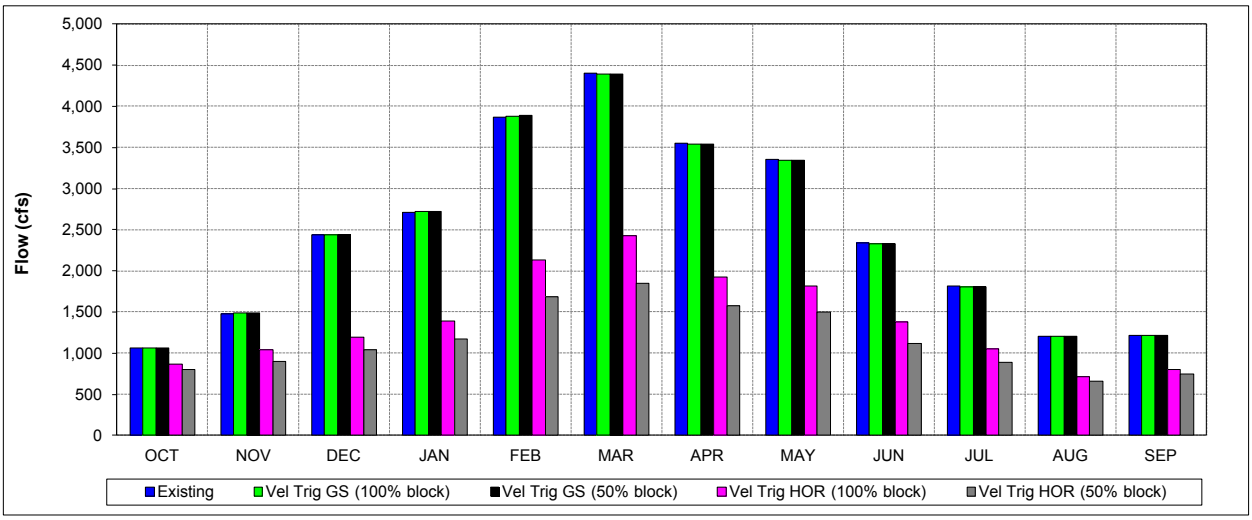

Figure 4-28 Monthly Average Flow at Head of Old River for Velocity Trigger Location in Rivers

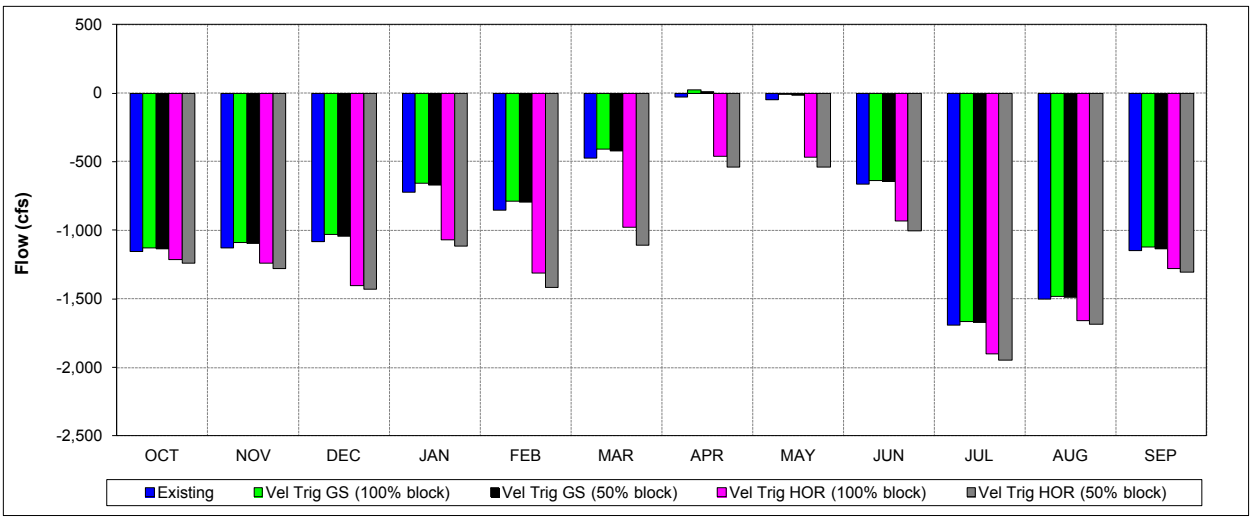

Figure 4-29 Monthly Average Flow at Columbia Cut for Velocity Trigger Location in Rivers

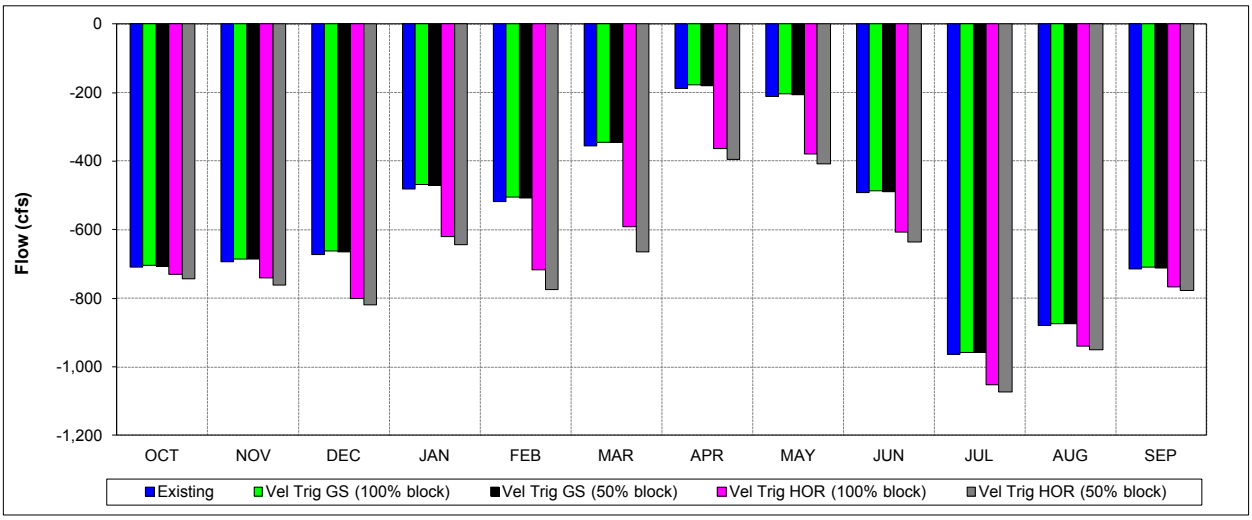

Figure 4-30 Monthly Average Flow at Turner Cut for Velocity Trigger Location in Rivers

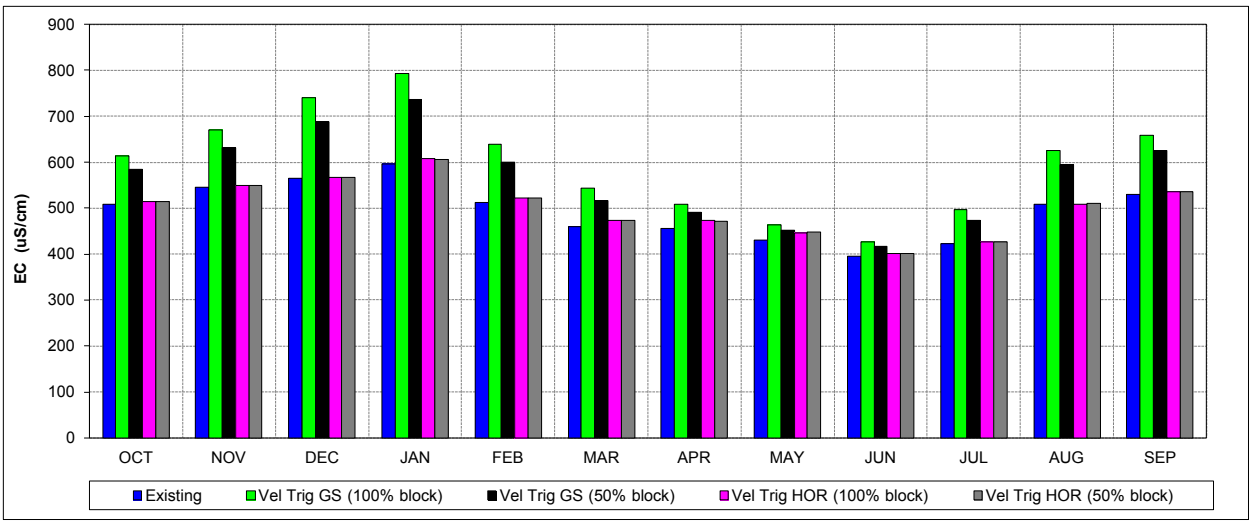

Figure 4-31 Monthly Average EC at Clifton Court Forebay for Velocity Trigger Location in Rivers

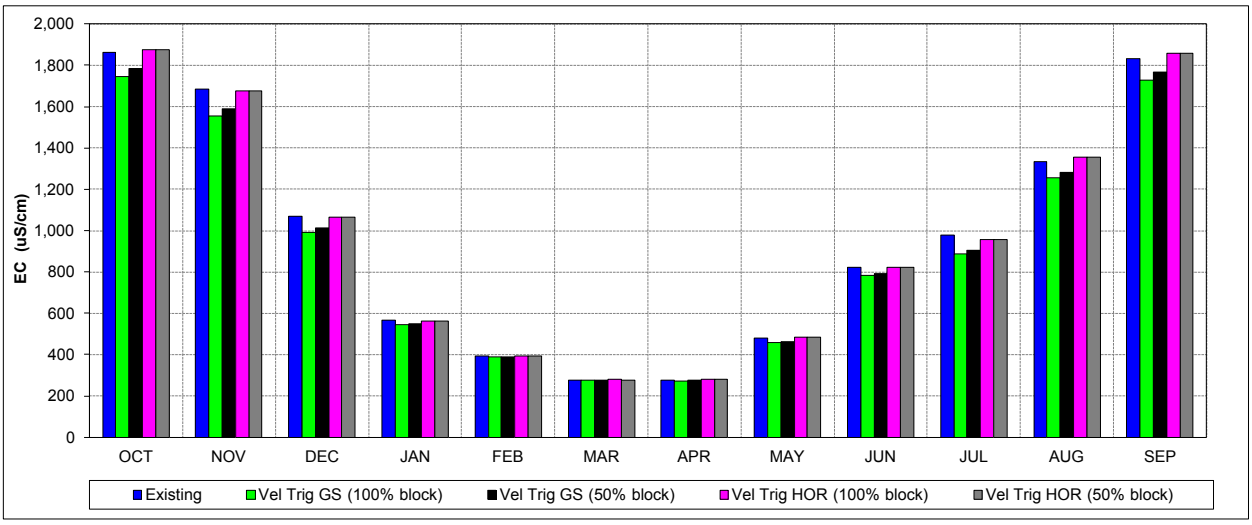

Figure 4-32 Monthly Average EC at Sacramento River at Emmaton for Velocity Trigger Location in Rivers

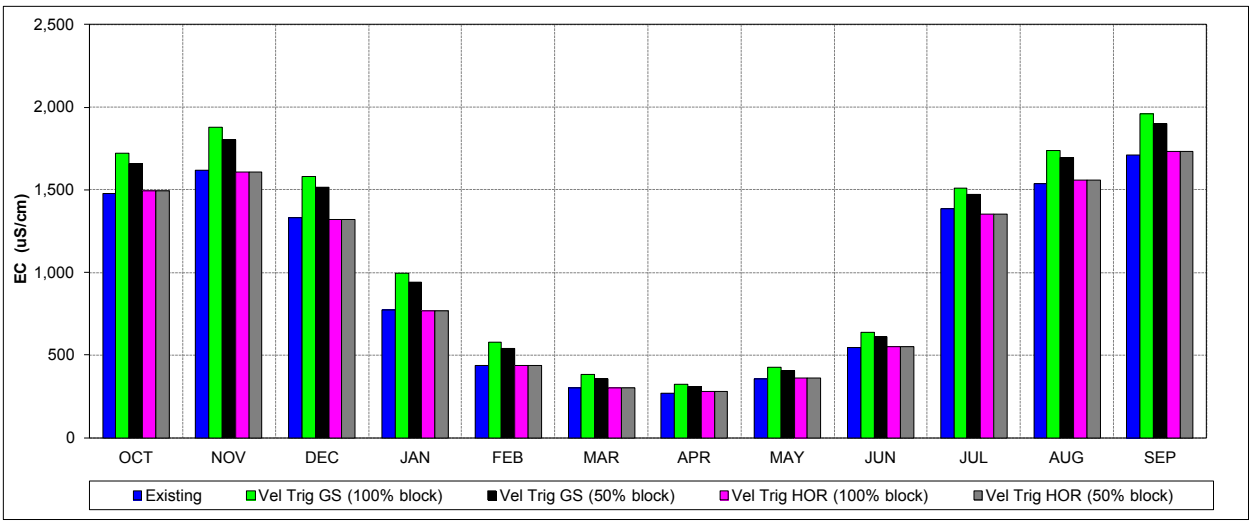

Figure 4-33 Monthly average EC at San Joaquin River at Jersey Point for Velocity Trigger Location in Rivers

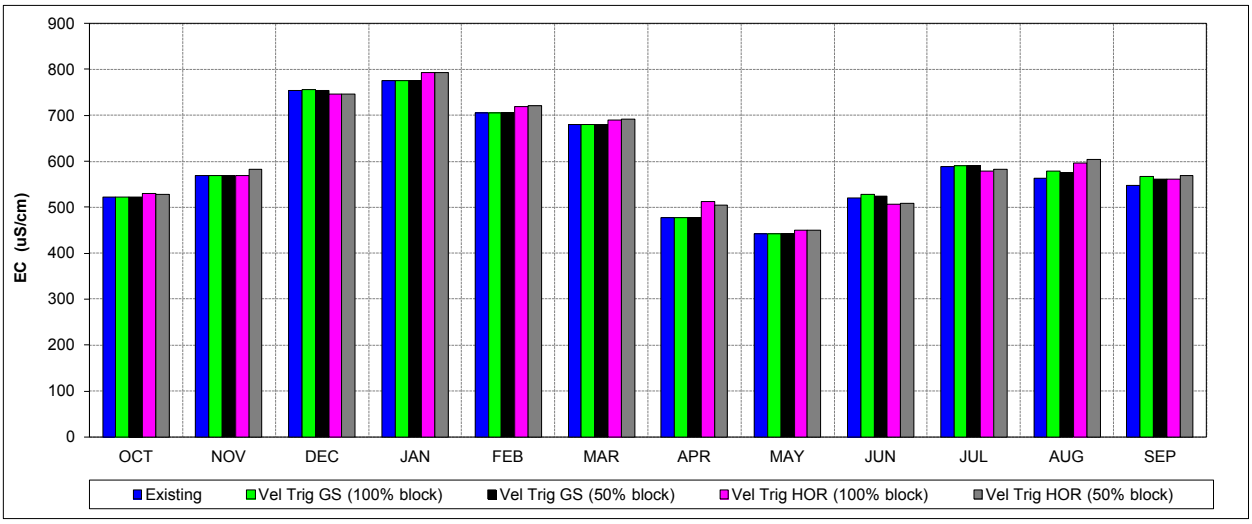

Figure 4-34 Monthly average EC at Old River at Tracy Road for Velocity Trigger Location in Rivers

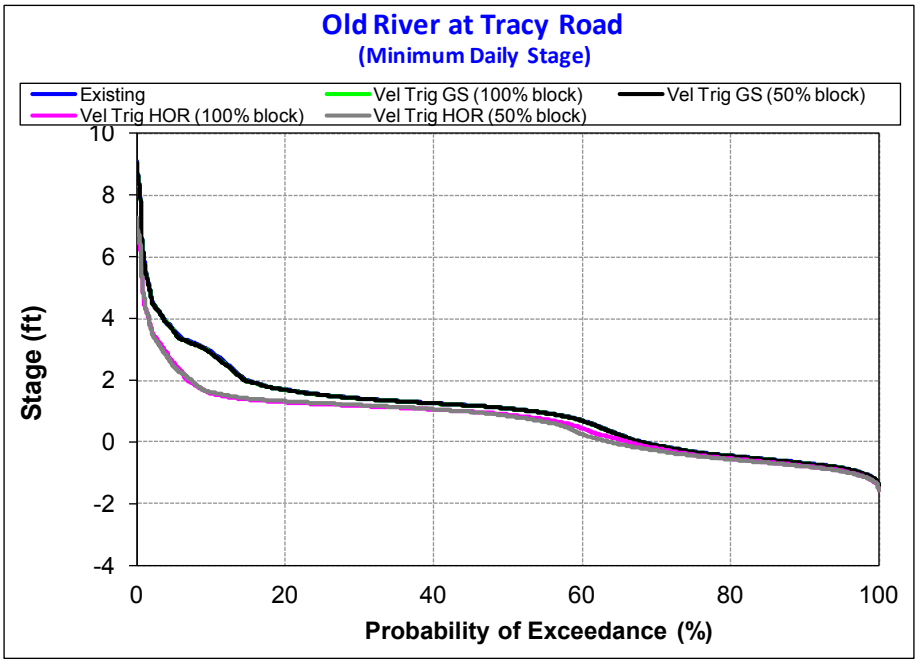

Figure 4-35 Daily Minimum Stage at Old River at Tracy Road for Velocity Trigger Location in Rivers

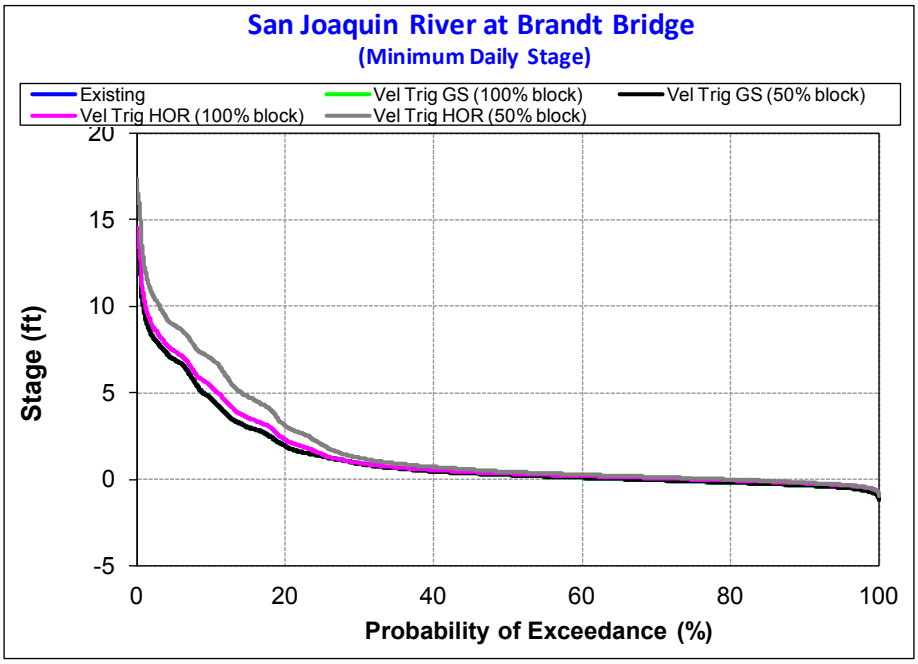

Figure 4-36 Daily Minimum Stage at San Joaquin River at Brandt Bridge for Velocity Trigger Location in Rivers

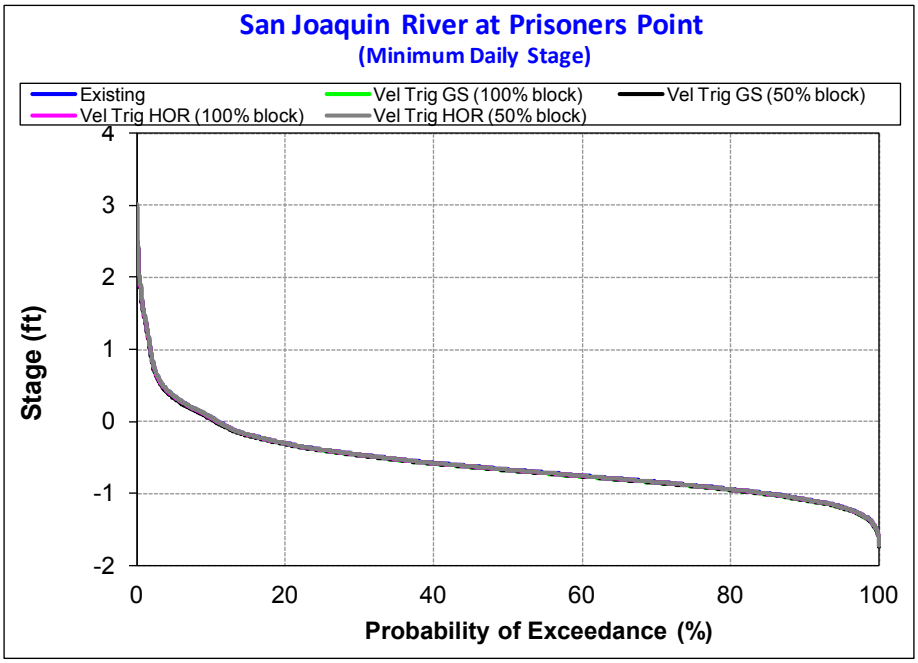

Figure 4-37 Daily Minimum Stage at San Joaquin River at Prisoners Point for Velocity Trigger Location in Rivers

4.5 Conclusion

The impacts of the Georgiana Slough, Head of Old River, Turner Cut, and Columbia Cut gates on water quality and water level varied. Figure 4-38 to Figure 4-41 represented incremental changes in water quality throughout the Delta for each of the gates. The figures also showed relative impacts among the four different gates. Table 4-3 summarizes the impacts on water quality for all scenarios.

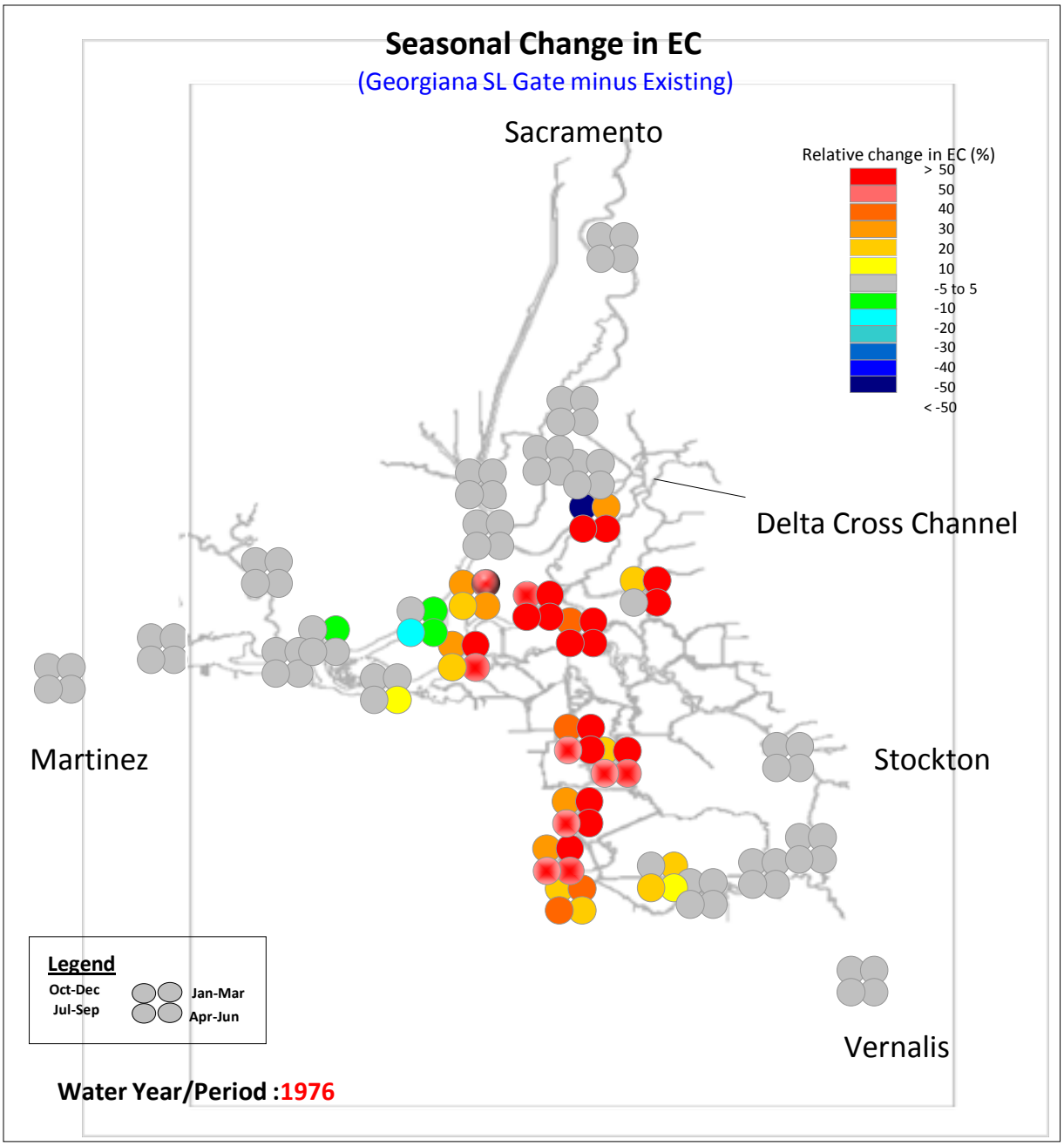

Figure 4-38 Impacts of Georgiana Slough Gate on Water Quality throughout Delta

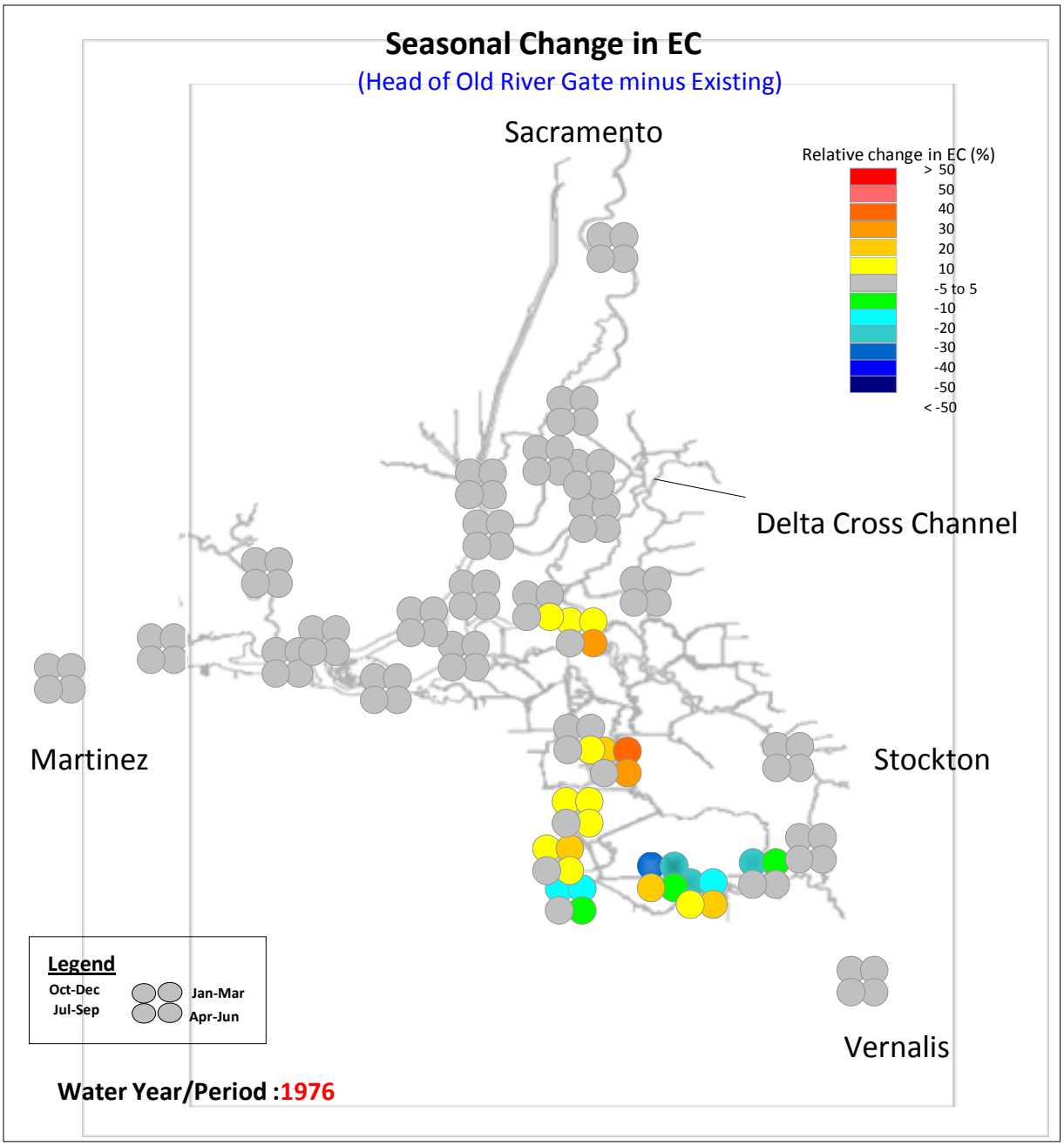

Figure 4-39 Impacts of Head of Old River Gate on Water Quality throughout Delta

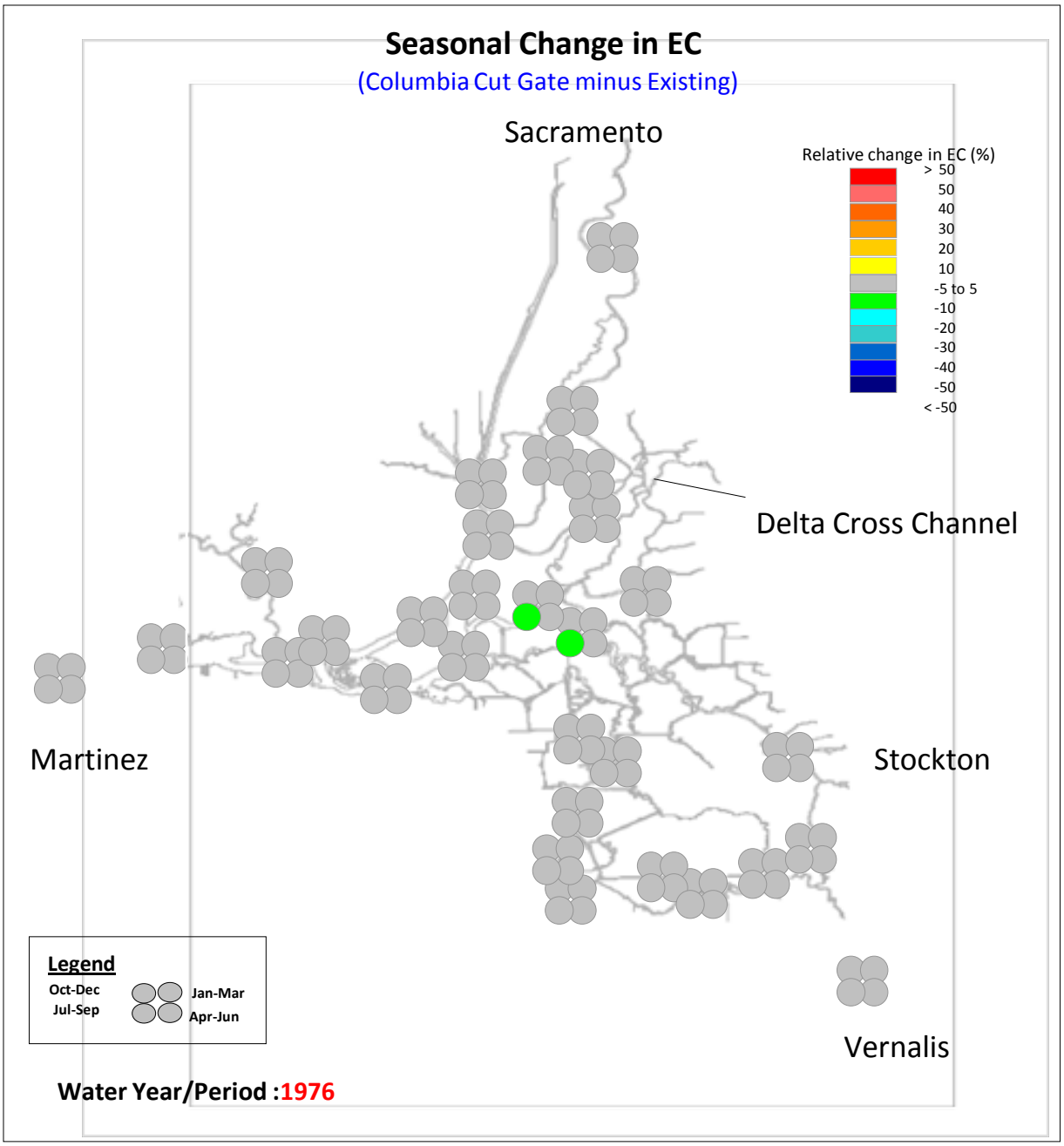

Figure 4-40 Impacts of Columbia Cut Gate on Water Quality throughout Delta

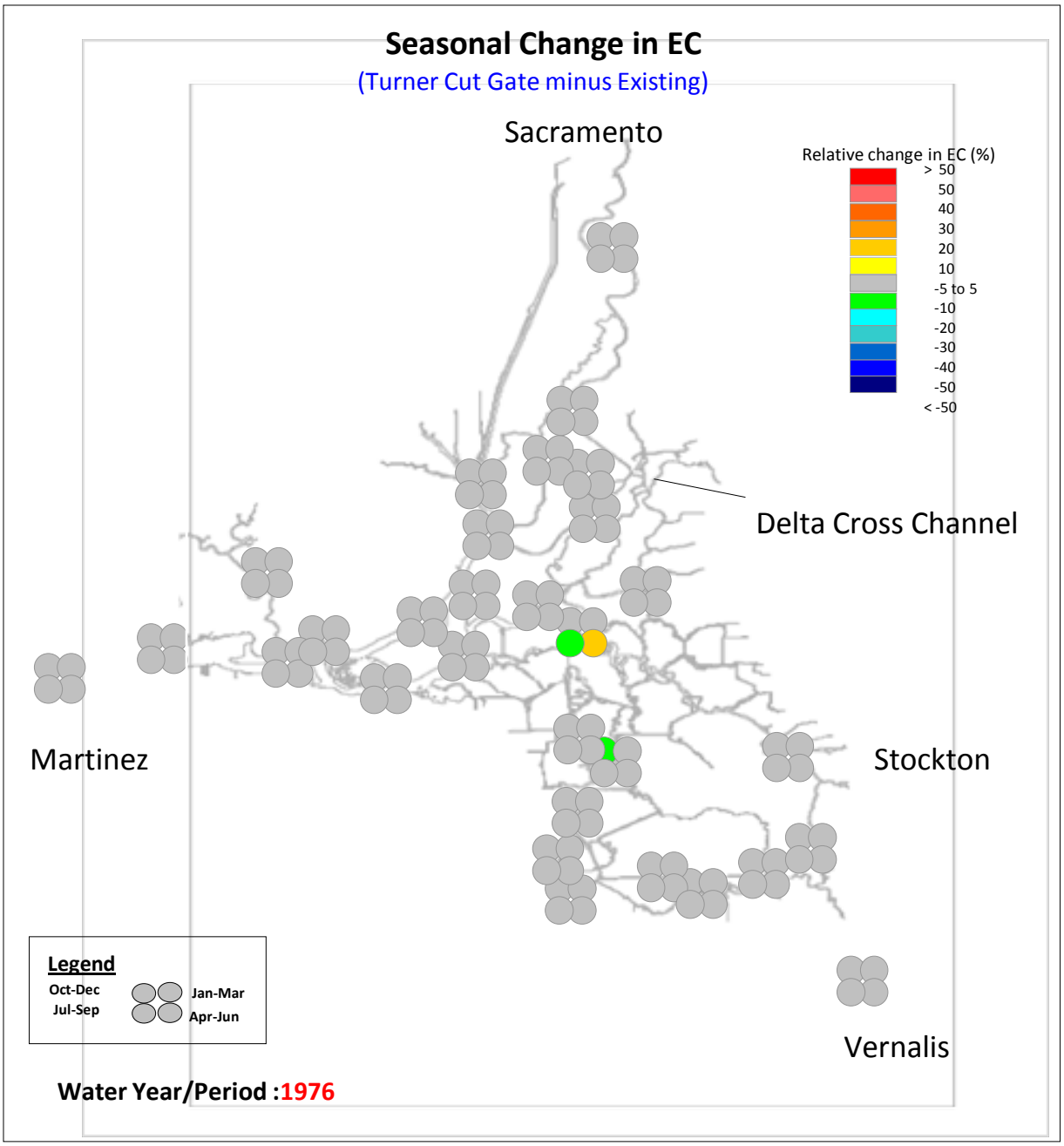

Figure 4-41 Impacts of Turner Cut Gate on Water Quality throughout Delta

			Impact on Water Quality (EC)			
Category	Location of Gate	Gate Operation Trigger	Clifton Court	Emmaton	Jersey Point	Tracy Road
Full Flow Blockage to Delta Channels	Georgiana Slough, Head of Old River, Turner Cut & Columbia Cut (Four Gates)	Closed on positive flow in channel & opened on reverse flow	Deteriorated	Improved	Deteriorated	Deteriorated*
	Georgiana Slough	Closed on positive flow in channel & opened on reverse flow	Deteriorated	Improved	Deteriorated	No/Minimal
	Head of Old River	Closed on positive flow in channel & opened on reverse flow	No/minimal	No	No	Deteriorated*
	Turner Cut	Closed on positive flow in channel & opened on reverse flow	No	No	No	No
	Columbia Cut	Closed on positive flow in channel & opened on reverse flow	No	No	No	No
	Head of Old River, Turner Cut & Columbia Cut (Three Gates)	Closed on positive flow in channel & opened on reverse flow	No/minimal	No	No	Deteriorated*

			Impact on Water Quality (EC)			
Category	Location of Gate	Gate Operation Trigger	Clifton Court	Emmaton	Jersey Point	Tracy Road
	Georgiana Slough, Head of Old River, Turner Cut & Columbia Cut (Four Gates)	Closed on ebb & opened on flood	Deteriorated	Improved	Deteriorated	Deteriorated*
	Georgiana Slough	Closed on ebb & opened on flood	Deteriorated	Improved	Deteriorated	No/Minimal
	Head of Old River	Closed on ebb & opened on flood	No	No	No	Deteriorated*
	Head of Old River, Turner Cut & Columbia Cut (Three Gates)	Closed on ebb & opened on flood	No/Minimal	No	No	Deteriorated*
Partial Flow Blockage to Delta Channels	Georgiana Slough	Partial closed on ebb to block 50% net flow & opened on flood	Deteriorated	Improved	Deteriorated	No/Minimal
	Head of Old River	Partial closed on ebb to block 50% net flow & opened on flood	No	No	No	Minimal*
	Georgiana Slough	Closed on high velocity & Opened on low velocity	Deteriorated	Improved	Deteriorated	No/Minimal

			Impact on Water Quality (EC)			
Category	Location of Gate	Gate Operation Trigger	Clifton Court	Emmaton	Jersey Point	Tracy Road
	Georgiana Slough	Partial closed on high velocity to block 50% net flow & opened on low velocity	Deteriorated	Improved	Deteriorated	No/Minimal
	Head of Old River	Closed on high velocity & Opened on low velocity	No	No	No	Minimal*
	Head of Old River	Partial closed on high velocity to block 50% net flow & opened on low velocity	No	No	No	Minimal*
Flow Blockage used in other Projects	Threemile Slough (Franks Tract Project)	Franks Tract Project proposed operation, Seasonal operation for Fish and Water Quality	Improved	No	Improved	No

*EC deteriorated at Tracy Road when both DCC and Head of Old River gates were closed.

Table 4-3 Impacts of Modeling Scenarios on Water Quality

The modeling analysis conclusions are:

- The impacts on water quality and water level decreased as gate closure time decreased.
- The Georgiana Slough Gate deteriorated water quality in the Central and South Delta, as well as in the SWP and CVP export facilities.
- The Georgiana Slough Gate improved water quality at Emmaton.

- The Head of Old River Gate deteriorated water quality locally, and caused lower water level in the South Delta.
- The Columbia and Turner Cut Gates had no impact on water quality or water level.

4.6 References

California Department of Water Resources. 2013. *Draft Environmental Impact Report/Environmental Impact Statement Bay Delta Conservation Plan* Appendix 3D. "Defining Existing Conditions, No Action Alternative, No Project Alternative, and Cumulative Impact Conditions." Sacramento (CA): California Department of Water Resources. November. 112 pp.

Bureau of Reclamation. "Delta Cross Channel Gates." Sacramento (CA): Bureau of Reclamation Central Valley Operations Office [website]. Viewed online at:.http://www.usbr.gov/mp/cvo/vungvari/xcgtxt.html . Accessed: September 18, 2014.

Methodology for Flow and Salinity Estimates in the Sacramento-San Joaquin Delta and Suisun Marsh

36th Annual Progress Report
June 2016

Chapter 5
Visualizing DSM2 Simulation Results with ArcMap

Authors: Siqing Liu, Bob Suits, Hari Rajbhandar
Delta Modeling Section
Bay-Delta Office
California Department of Water Resources

Contents

5 Visualizing DSM2 Simulation Results with ArcMap 5-1
5.1 INTRODUCTION 5-1
5.1.1 Python 5-1
5.1.2 ArcGIS 5-1
5.1.3 DSM2 Output 5-1
5.1.4 NetCDF 5-2
5.2 STEPS TO CREATE ANIMATION IN ARCMAP 5-2
5.3 EXAMPLES 5-9
5.4 CONCLUSIONS 5-10
5.5 REFERENCES 5-10

Figures

Figure 5-1 A Table Stored in Geodatabase with Flow Results Retrieved from a DSM2 HDF5 File 5-2
Figure 5-2 A NetCDF File Opened with HDFView 5-3
Figure 5-3 Processes for Storing DSM2 Simulation Results to a NetCDF File 5-4
Figure 5-4 Time Series Data is Appended to the Attribute Table of a Layer with Geographic Information by Using the Join Operation 5-5
Figure 5-5 Data Stored in a NetCDF File is Loaded to ArcMap as a Raster Layer Through Multidimension Tools 5-6
Figure 5-6 Enable Time on a Layer 5-7
Figure 5-7 Configure Visual Display 5-8
Figure 5-8 Time Slider 5-8
Figure 5-9 Stage Profile for Two Scenarios (with/without barriers) 5-9
Figure 5-10 EC in the Delta with X2 Shown in Black 5-10

5 Visualizing DSM2 Simulation Results with ArcMap

5.1 Introduction

The Delta Simulation Model 2 (DSM2) has been widely used for three types of Delta simulations: historical conditions, near- and long-term forecasting, and planning studies. DSM2 simulations have been applied for various purposes. Some examples include forecasting water quality in the Delta and the California Aqueduct system, generating hydrologic information for a permit application, and providing support for litigation. Since DSM2 simulation results can be presented to members of the public coming from various backgrounds, it is vital to present simulation results tailored to meet the needs of different audiences. In the past, the visualization of DSM2 EC (Electrical Conductivity) results was readily accepted. Even so, it takes many steps to prepare an animation, and the process relies on a program called Tecplot, which was fairly uneconomical to purchase, especially considering that Tecplot has been rarely used by other staff in the Bay-Delta Office.

In this chapter, we will present several ways to visualize DSM2 simulation results with ArcMap, a product of Environmental Systems Research Institute (ESRI). A programming language, Python, is used to convert DSM2 output to ArcGIS geodatabase or NetCDF files.

5.1.1 Python

Python is a widely used, general purpose, high-level programming language. As an open source and freely distributed language, Python has an extensive standard library that provides tools suited for many tasks. It is great for use as a scripting language to connect existing components together. Python was introduced to the ArcGIS community at version 9.0. Since then, it has been accepted as the scripting language of choice for ArcGIS users and its use has continued to grow. At ArcGIS Desktop 10, Python scripting is tightly integrated into ArcMap and ArcCatalog, allowing users to create and automate geographic information system (GIS) workflows quickly and easily. Python scripts can be executed outside of ArcMap's Python console to perform geographic data analysis, data conversion, data management, and map automation. In the Bay-Delta Office, a large number of site packages or modules were developed to post-process DSM2 simulation results.

5.1.2 ArcGIS

ArcGIS is a GIS developed by ESRI for working with maps and geographic information. ArcMap is the main component of ESRI's ArcGIS suite of geospatial processing programs. It is used primarily to view, edit, create, and analyze geospatial data. Animation tools are available in ArcMap since ArcGIS 9.2 was released. A Python site package, ArcPy that comes with ArcGIS 10, enables the integration of ArcGIS tools and functionality in Python.

5.1.3 DSM2 Output

DSM2 supports two types of output format, which are the U.S. Army Corps of Engineers' Hydrologic Engineering Center Data Storage System (HEC-DSS) and Hierarchical Data Format (HDF). Both were originally developed at the National Center for Supercomputing Applications. DSM2 uses HEC-DSS files to store simulation results at specified locations and time intervals, and HDF5 files to store simulation results for all DSM2 upstream and downstream channels. Before DSM2 8.1, only hydro simulation results could be stored in HDF5 files. Now both Hydro and QUAL simulation results, such as EC, EC fingerprinting and volumetric fingerprinting can also be stored in HDF5 files. Accordingly, animations can be created for all DSM2 simulation results.

5.1.4 NetCDF

NetCDF is an array-based data structure for storing multidimensional data. It is interoperable with HDF5, and so a common program can be used to view both HDF5 and NetCDF data. ArcGIS version 9.2 introduces support for working with NetCDF files. With the Multidimension Tools toolbox, a user can create raster layers, feature layers, and table views from NetCDF data in ArcMap, or convert feature, raster, and table data to NetCDF. At any given time, only one slice of multidimensional data is visible.

5.2 Steps to Create Animation in ArcMAP

It takes several steps to create animations to visualize DSM2 simulation results.

Step 1: Data Conversion

DSM2 simulation results cannot be directly imported to ArcMap for visualization. As a result, Python scripts were written to store DSM2 simulation results in ArcGIS geodatabase in the form of a data table with at least three fields: channel number, date/time, and value (Figure 5-1). Python scripts were also written to convert DSM2 simulation results to raster and store in a NetCDF file (Figure 5-2).

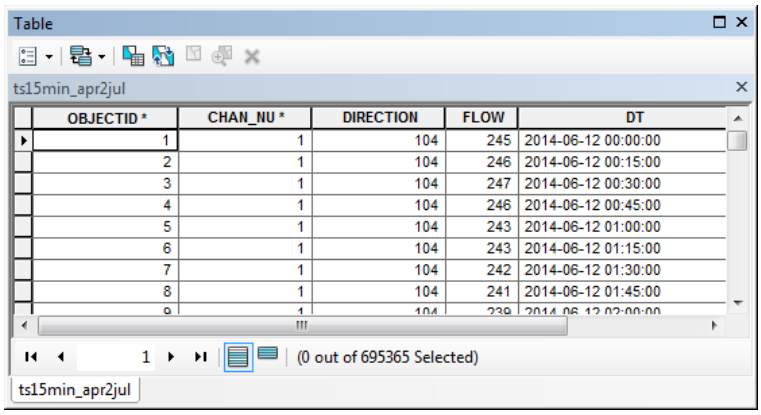

OBJECTID *	CHAN_NU *	DIRECTION	FLOW	DT
1	1	104	245	2014-06-12 00:00:00
2	1	104	246	2014-06-12 00:15:00
3	1	104	247	2014-06-12 00:30:00
4	1	104	246	2014-06-12 00:45:00
5	1	104	243	2014-06-12 01:00:00
6	1	104	243	2014-06-12 01:15:00
7	1	104	242	2014-06-12 01:30:00
8	1	104	241	2014-06-12 01:45:00
9	1	104	239	2014-06-12 02:00:00

Figure 5-1 A Table Stored in Geodatabase with Flow Results Retrieved from a DSM2 HDF5 File

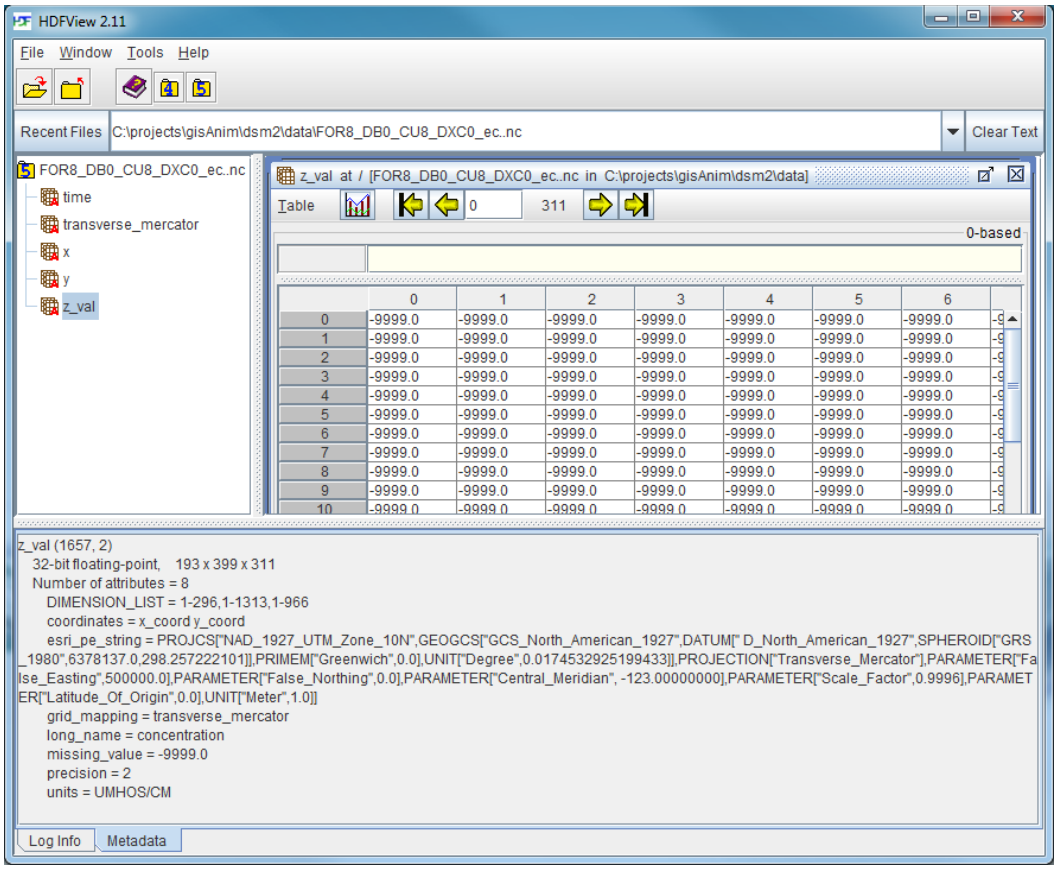

Figure 5-2 A NetCDF File Opened with HDFView

To store DSM2 simulation results in ArcGIS geodatabase, the Python scripts first call functions in Vtools developed by the Bay-Delta Office to read DSM2 simulation results from HEC-DSS files, or call the site package h5py to read DSM2 simulation results from HDF5 files. Then, the Python scripts save time series data in an Excel csv file. Finally, the Python scripts call the function TableToGeodatabase_conversion in site package ArcPy to store the table from the Excel csv file in a geodatabase that can be used in the next step.

To store DSM2 simulation results in NetCDF files, a Python script uses h5py to read DSM2 simulation results from a HDF5 file. Each time the script reads data for all channels, but only for a one-time step. Then, the Python script saves data in an Excel csv file, creates an ArcGIS shape file from the Excel csv file, converts the shape file to a raster file, exports the raster file to an ASCII file, and stores ASCII data in a NetCDF file. The steps are repeated until all the simulation results during the period specified by a user are processed. Figure 5-3 shows the flowchart for post-processing DSM2 simulation results stored in a HDF5 file and stored in a NetCDF file, which can be used in the next step.

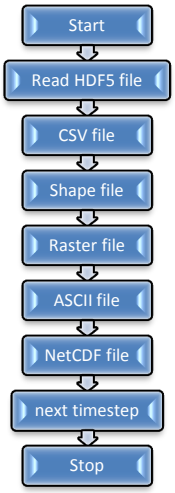

Figure 5-3 Processes for Storing DSM2 Simulation Results to a NetCDF File

Step 2: Add Data to ArcMap

A table with stored DSM2 results in a geodatabase does not have spatial information. Once it is added to ArcMap, it can be joined with a geographic layer by using a join key. From ArcMap, right click the table, from the content menu, choose “joins and relates” -> “join…”, a window with join information will pop up. Figure 5-4 is such a window which shows the table (ts15min_apr2jul) in a geodatabase that is joined to a DSM2 channel layer using the common field for Channel Number. After the Join operation is finished, the geographic layer contains time series from another table.

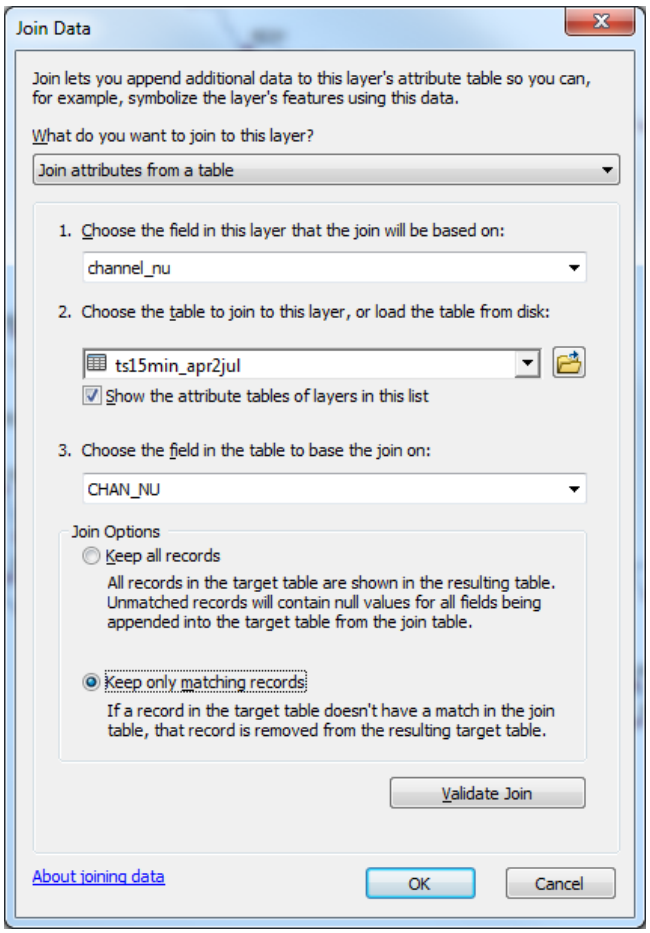

Figure 5-4 Time Series Data is Appended to the Attribute Table of a Layer with Geographic Information by Using the Join Operation

Multidimensional data stored in a NetCDF file can be loaded as a raster layer through the Multidimension Tools in ArcMap Toolbox as shown on the left side of Figure 5-5. The NetCDF file contains geographic information, such as coordinates and spatial reference, so it does not need to get this information from another geographic layer.

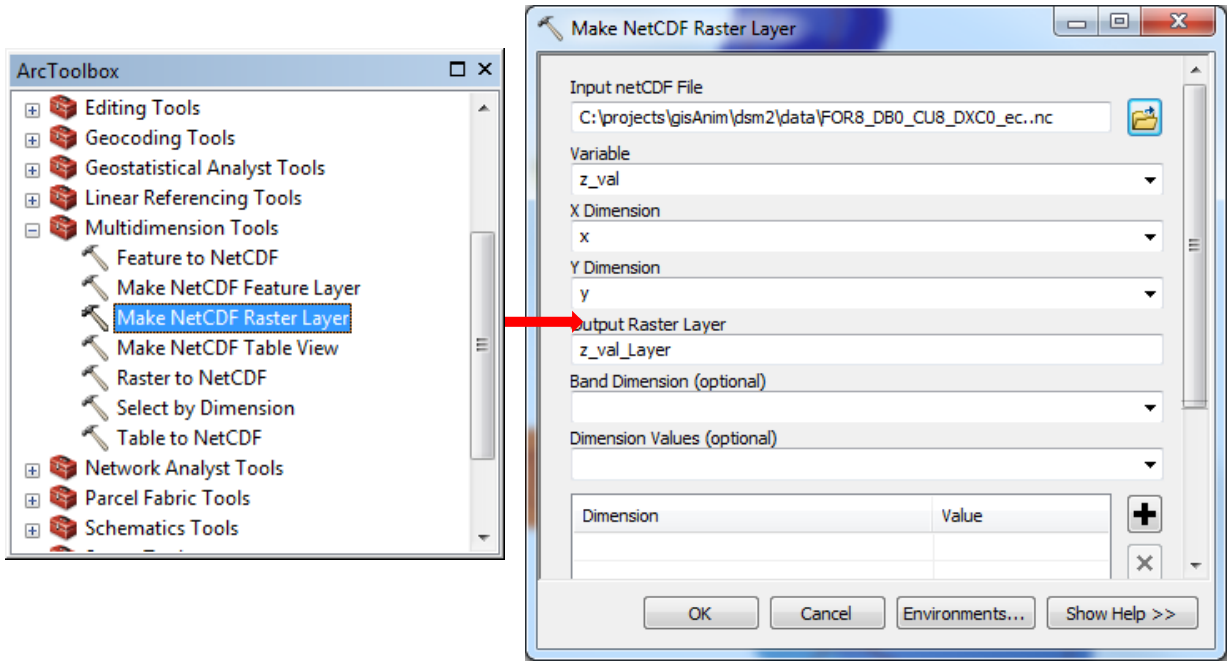

Figure 5-5 Data Stored in a NetCDF File is Loaded to ArcMap as a Raster Layer through Multidimension Tools

Step 3: Enable Time on a Layer

Once the table is joined to a layer or is loaded as a raster layer, access the layer properties by right-clicking the layer name in the Table of Contents pane. Navigate to the Time tab and check the box labeled as "Enable time on this layer". ArcMap needs to know which table field contains time information, as well as the format. If the Join operation was successful, the fields that represent the data joined to the geographic layer are visible from the table of the geographic layer. If the Join operation was not successful, then check files created by Python scripts to ensure they are correctly created. In this example, the Time Field is labeled DT. Also, specify the date/time format (Figure 5-6). Available time formats are listed on the drop-down list shown in Figure 5-6.

If a geographic layer gets its data from a data table through the Join operation, which is a way we recommend, then it is also necessary to enable time on the data table as well. To do this, right-click the data table in the Table of Contents pane. Follow the same steps listed to enable time on the geographic layer.

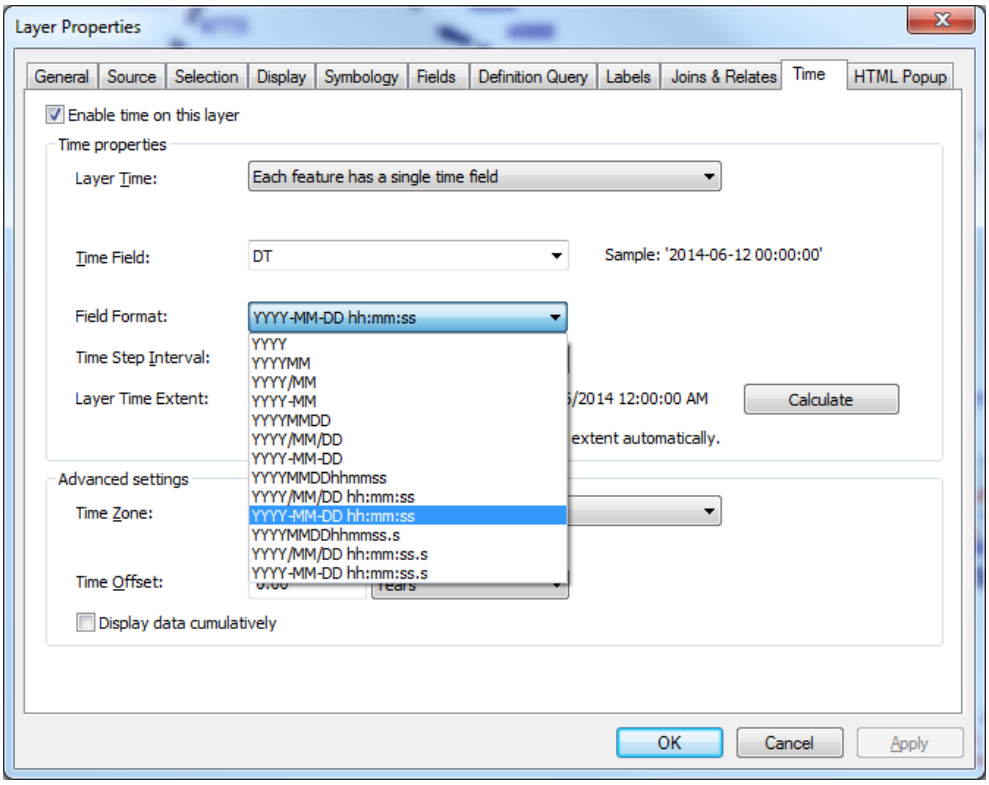

Figure 5-6 Enable Time on a Layer

Step 4: Configure Visual Display

In this step, it is necessary to specify what will be shown on the map. For a feature class layer, enter the Layer Properties window by right-clicking the layer name in the Table of Contents pane. Navigate to the Symbology tab and click on it. The options for Symbology are displayed in Figure 5-7. In this example, table field Flow is chosen to show on this map as either red or blue arrows that represent negative or positive flow. On the right side near the bottom of the window is the “Advance” pushbutton with a pull-down menu. From there, choose the “rotation” option and set the direction of flow to the direction of a channel, which is a field in the geographic layer. The size of an arrow can be specified to represent the magnitude of flow by choosing the “size” option and assigning the size of an arrow to be a function of flow (in this example, the function is 3*log(abs(flow rate))). Also, the Layer Properties window has an option to show flow numbers from the Labels tab.

A raster layer can show data for the whole domain at each time step so the spatial change of EC, flow, velocity and other DSM2 outputs can be animated. For a raster layer, follow similar steps to specify how to visualize data. From the Layer Properties window, navigate to the Symbology to choose Color Ramp and Range, navigate to the NetCDF to select variable to be animated, and the x and y dimensions, and navigate to the Time tab to check ‘Enable time on this layer” , specify time dimension, and field format for Date/Time.

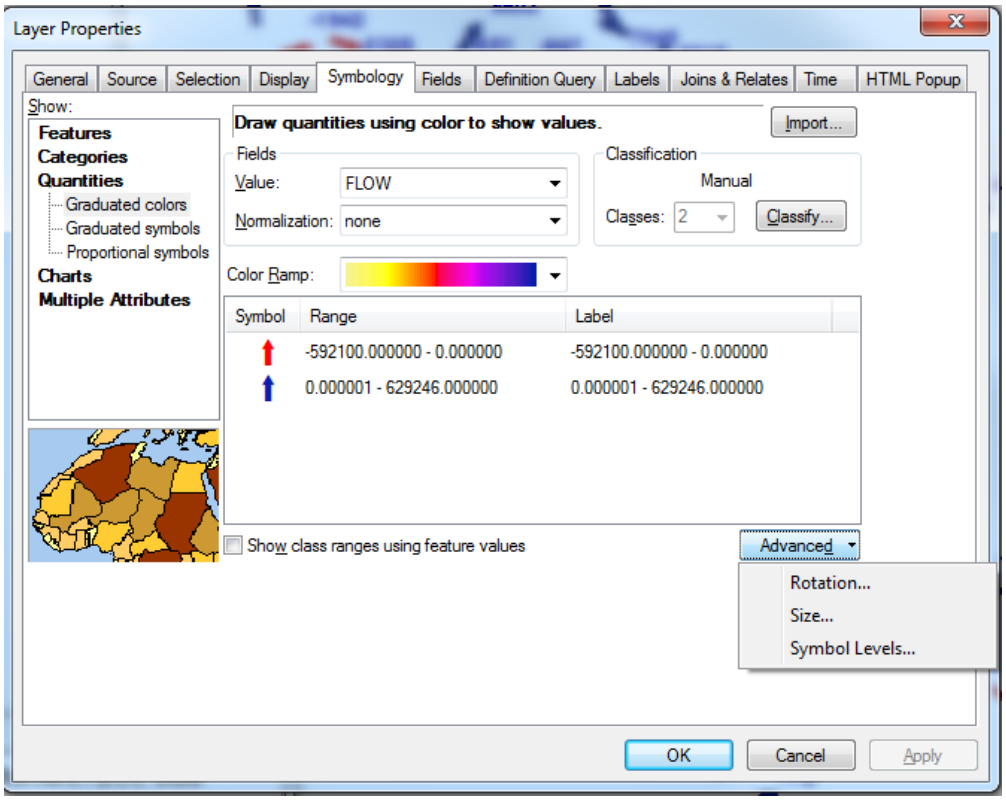

Figure 5-7 Configure Visual Display

Step 5: Start Visualization

Now that ArcGIS understands the data structure, start time visualization. From the Tools toolbar, which contains the most commonly used tools, open the Time Slider window (Figure 5-8). The slider spans the time range of the data, identifies what point in this range is currently displayed on the map, and allows for access to a variety of playback and recording options. To access these options, click the Options button (the middle button of the three buttons on the top left of the window shown in Figure 5-8).

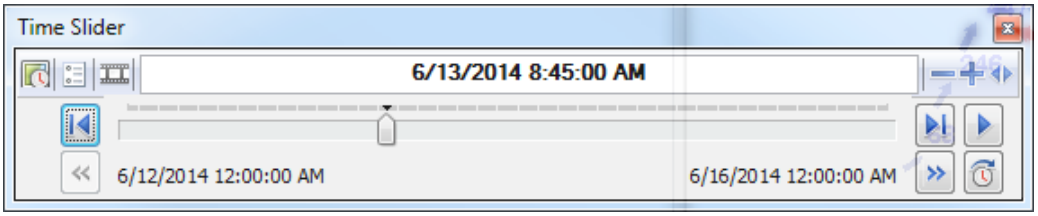

Figure 5-8 Time Slider

This is a Play button. By clicking on it, the data from the first time point to the last will be played.

This is the Forward button with data point moving forward in one-step increments. The buttons with an arrow pointing from right to left and a vertical line is the Reverse button.

This button exports the display to video. This is the final step.

Step 6: Export to Video

Once the map is satisfactory, export the map to video or to sequential images. Click the Export to Video button on the Time Slider window. Videos can be exported as AVI files or other formats, while sequential images are exported to a folder either as bitmaps or JPEGs. The first attempt may not produce the desired results, but trying different options (video resolution, fame rate, enable off-screen recording, and etc.) should produce a satisfactory product.

5.3 Examples

Any DSM2 simulation results can be visualized with ArcMap. Templates have been developed to visualize flow, stage, velocity, EC, EC fingerprint, and volumetric fingerprint. Animations can be created from either a feature class layer or a raster layer. Figure 5-9 is an example of visualizing stage data through a feature layer. Two sets of bars stand side by side. The bar on the left side is a stage profile for the scenario without drought barriers. The bar on the right side is a stage profile for the scenario with drought barriers. The two stars indicate the two proposed drought barrier locations. Figure 5-10 is an example of visualizing data contained in both a feature layer and a raster layer. EC values are shown as rasters for the entire Delta. X2 location (the location where the salinity of the water near the bottom is 2 parts per thousand) is marked as black. Inflow and outflow/exports are shown in text.

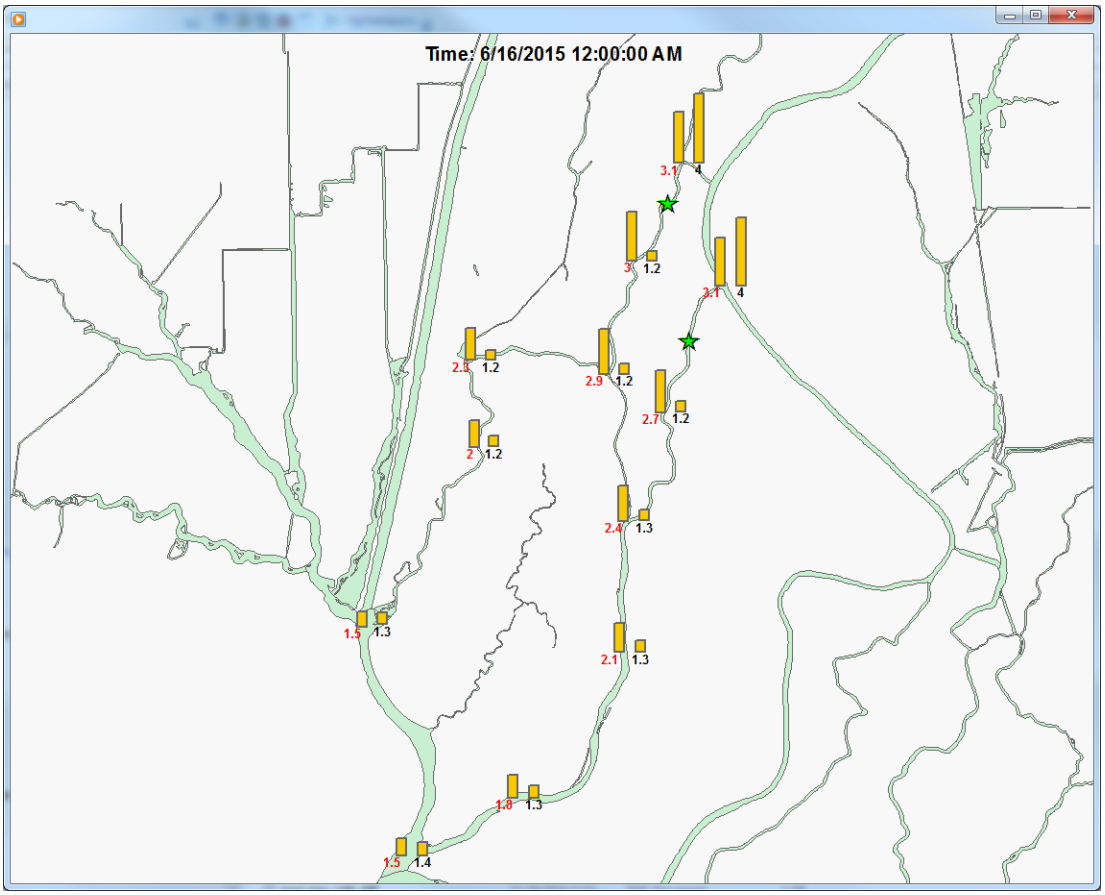

Figure 5-9 Stage Profile for Two Scenarios (with/without barriers)

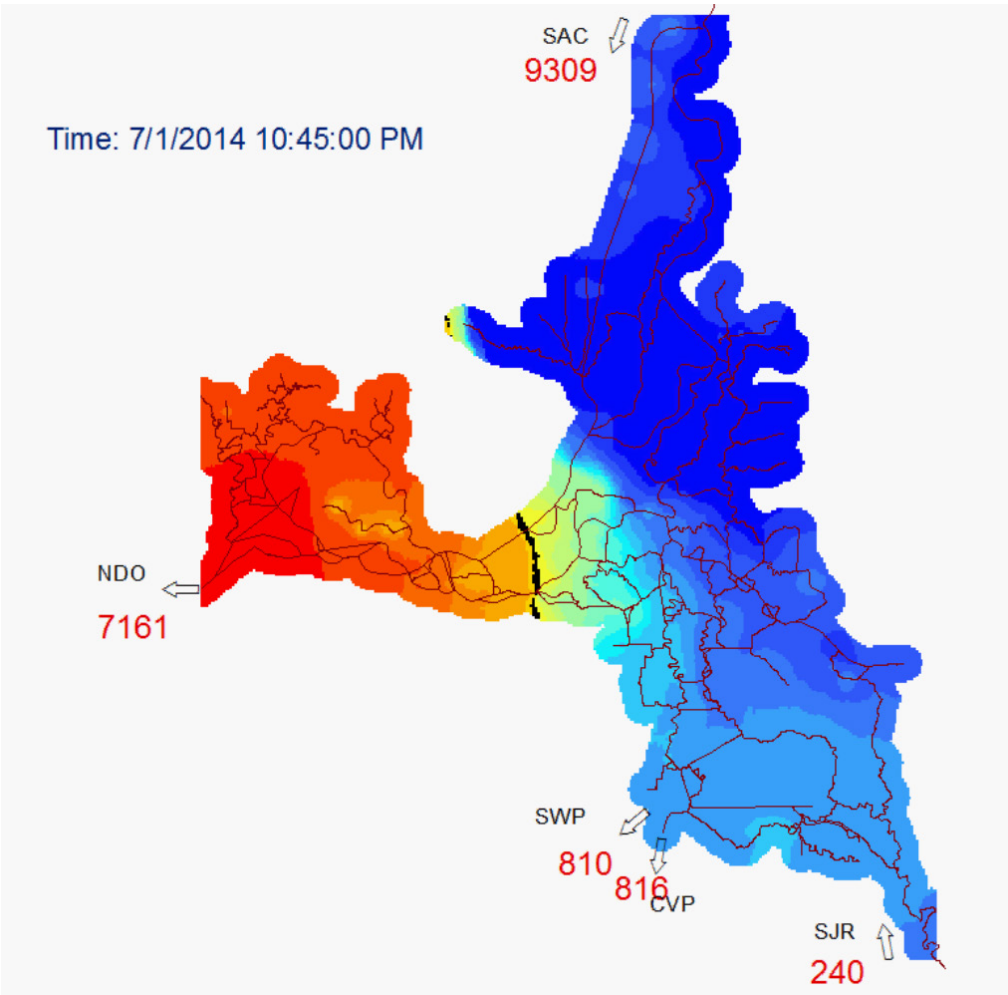

Figure 5-10 EC in the Delta with X2 Shown in Black

5.4 Conclusions

Visualization tools can help in understanding Delta hydrodynamics, and the tools also make it easier to verify model results and compare different scenarios. In this chapter, we pointed out the programs/tools that were used to create animations for visualizing DSM2 simulation results with ArcMap. We listed the key steps to create an animation from scratch, and provided two animation examples; one for a feature layer and another one mainly for a raster layer. With ArcMap, we may place several animations together without much extra work. A user can also show static information along with dynamic information to enhance visualization effects. With the help of Python scripts, it is much easier to create animations for visualizing DSM2 simulation results with ArcMap.

5.5 References

Bajwa H, Willison J. 2009. ArcGIS 9 Animation in ArcMap. Environmental Systems Research Institute. Redlands (CA): Tutorial. Viewed online at: http://webhelp.esri.com/arcgisdesktop/9.3/pdf/Animation_in_ArcMap_Tutorial.pdf.

Denniston R. 2011. *Time Series Visualizations in ArcGIS – An Introduction*. Data and Visualization Services. Duke University Libraries. Durham (NC): Viewed online at: http://blogs.library.duke.edu/data/2011/07/18/time-series-visualizations-in-arcgis-an-introduction/.

Martin D. 2014. Visualizing hydrologic data and simulation results with Python and ArcGIS. 2014 California Water and Environmental Modeling Forum (CWEMF) Annual Meeting. Folsom(CA):.

Methodology for Flow and Salinity Estimates in the Sacramento-San Joaquin Delta and Suisun Marsh

36th Annual Progress Report
June 2015

Chapter 6
Calculation of Clifton Court Forebay Inflow and Re-rating the Forebay Gates

Authors: Eli Ateljevich, Ming-yen Tu, Kate Le
Delta Modeling Section
Bay-Delta Office
California Department of Water Resources

Contents

6 Rating Clifton Court 6-1
6.1 SUMMARY 6-1
6.2 CLIFTON COURT FOREBAY 6-1
6.3 PROJECT DATA 6-3
6.4 PRIOR GATE RATINGS 6-4
6.5 DYNAMIC RESPONSE TO RADIAL GATES 6-5
6.6 THE NEW RATING 6-6
6.7 SYNTHESIZING HEIGHTS 6-8
6.8 VALIDATION THROUGH FLOW BALANCE 6-9
6.9 DSM2 EXPERIMENTS WITH FULL AND LIMITED DATA 6-16
6.10 OLD VERSUS NEW RATING 6-16
6.11 DATA GRANULARITY 6-19
6.12 BANKS DATA GRANULARITY 6-21
6.13 GATE TIMING: SCHEDULED PRIORITY 3 VERSUS HISTORICAL 6-21
6.14 CONCLUSION 6-22
6.15 REFERENCES 6-23

Figures

Figure 6-1 Location and Aerial View of Clifton Court Gates (adapted from Wilde 2006) 6-1
Figure 6-2 Priority 3 Gate Schedule (adapted from Wilde 2006) 6-2
Figure 6-3 Average Clifton Court Radial Gate Height over Three Recent Years 6-3
Figure 6-4 Comparison of Daily Gate Flow Calculations from DAYFLOW (SLP is Gate Inflow) with Daily Averages of Flows Reported Based on the Hills Equation 6-5
Figure 6-5 Components of Flow Balance Used to Calibrate the Gate Rating 6-9
Figure 6-6 Water Levels (top), SWP Exports (middle) and Gate Heights (bottom) at Clifton Court in Winter 2004-2005 6-10
Figure 6-7 Water Levels (top), SWP Exports (middle) and Gate Heights (bottom) at Clifton Court in 2008 6-11
Figure 6-8 2004-5 Forebay Water Level Fluctuations and Gate Flows from the New Rating Compared with Field Data Utilizing Instantaneous Gate Height and Pumping Data and the Simple Mass Balance Model 6-12
Figure 6-9 Rating Validation in 2008 Under Low Flows and "Sipping" Gate Operations, Including Clifton Court Water Levels (top), Daily Flows (middle), and Gate Heights (bottom) 6-13
Figure 6-10 Close-up of Intratidal Water Level Fluctuations in the 2008 Mass Balance Experiment 6-14

Figure 6-11 Forebay Water Level Fluctuations and Gate Flows from the DSM2 Gate Rating and Simple Mass Balance Model 6-15

Figure 6-12 Fitted Versus Observed Values for the ADCP Data 6-16

Figure 6-13 Water Level and Flow Results for DSM2 Experiment with Old (R1) and New (R2) Rating 6-17

Figure 6-14 Clifton Court Electrical Conductivity (EC) under Old and New Ratings with Instantaneous Gate and Pumping Data 6-18

Figure 6-15 Old River at Tracy Bridge Water Levels Under Old and New Ratings with Instantaneous Gate and Pumping Data 6-18

Figure 6-16 Clifton Court Water Elevations with Different Quality and Granularity of Gate Height Data..... 6-19

Figure 6-17 Clifton Court EC with Different Quality and Granularity of Gate Height Data 6-20

Figure 6-18 Old River at Tracy Bridge Water Elevations with Different Quality and Granularity of Gate Height Data 6-20

Figure 6-19 Clifton Court Water Levels with New Rating, Instantaneous Gate Heights and Two Granularities of Banks Pumping Data, Instantaneous (full) and Daily 6-21

Figure 6-20 Comparison of Scheduled Timing and Actual Historical Gate Timing using DSM2 with the Prior Rating and Gates Treated as Always Open/Closed 6-22

Tables

Table 6-1 Parameter Fits for Coefficients and Comments from Drought Modeling 6-8

6 Rating Clifton Court

6.1 Summary

With the help of staff at California Department of Water Resources (DWR) Operations and Maintenance (O&M), Delta Field Division (DFD), and North Central Region Office (NCRO), the Delta Modeling Section has developed a new rating for the Clifton Court radial gates — a formula for estimating flow into the forebay based on gate heights and water levels inside and outside the gates. The new rating is suitable for operational and modeling purposes.

Clifton Court Forebay (CCFB) is included explicitly in our models, DSM2 and SCHISM. In addition to presenting the new rating, we describe DSM2 modeling experiments that show the role the gates play in the local balance and where modeling error tends to manifest. Although our main results are obtained with detailed gate data and pumping data, we also address situations, such as planning scenarios, where detailed time series of gate heights and exports are not available.

The main potential impact of the work presented here is on water levels in the forebay, where the Clifton Court gate characterization and modeling practices have an enormous impact on results. There are more minor impacts as well on exterior water levels in the South Delta, on high tide, on water quality, and residence time in the forebay.

6.2 Clifton Court Forebay

The intake structure to Clifton Court is comprised of five 20’ x 20’ radial gates along Old River. Figure 6-1 shows the location and configuration of the gates. These gates are operated over the tidal cycle to reduce approach velocities, prevent scour in adjacent channels, and minimize water-level fluctuation in the South Delta. When a large head differential exists between the outside and the inside of the gates, instantaneous flows into the forebay can reach 15,000-20,000 cubic feet per second (cfs).

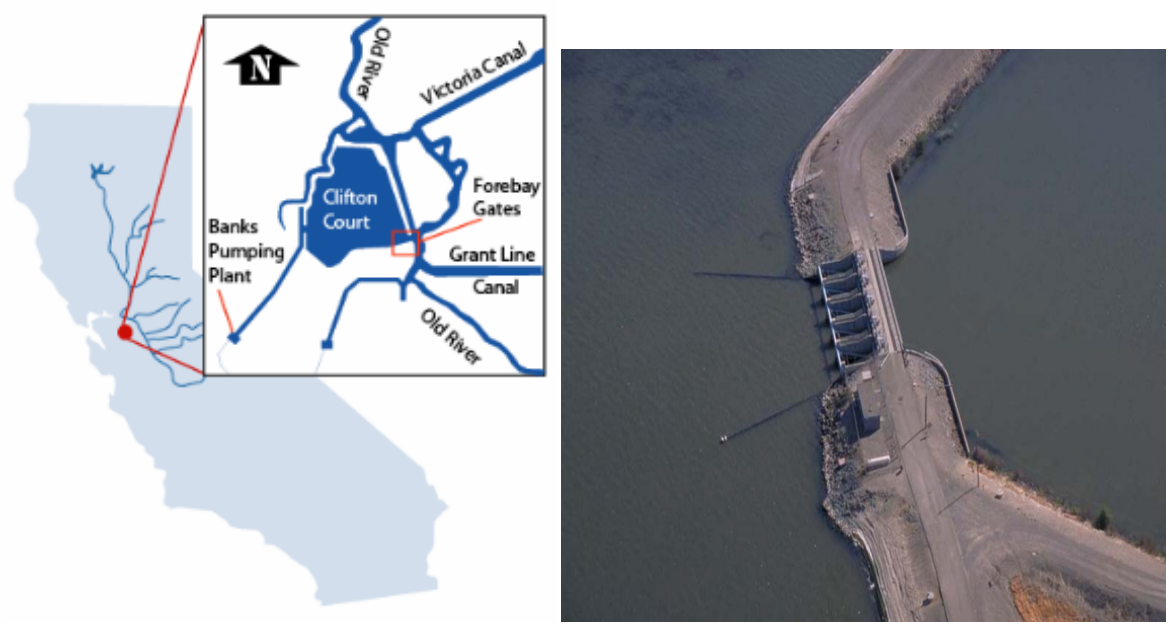

Figure 6-1 Location and Aerial View of Clifton Court Gates (adapted from Wilde 2006)

Generally, operators open all five gates in tandem, but a gate(s) may be independently operated strategically or during maintenance. The daily opening and closing of gates depends on the scheduled State Water Project (SWP) export allotment, timing, amplitude of the local tides, and storage availability in the forebay. Gate operations are constrained by water level concerns in the South Delta for local agricultural irrigators. The criteria for the gate operation are defined in the O&M Standing Operating Order PC 200.7-A (California Department of Water Resources 1989) with respect to agreements with the South Delta Water Agency. The most common operation of the CCFB intake gates is what is commonly termed Priority 3: "Intake gates open 1 hour after the low-low tide, close 2 hours after the high-low tide, reopen 1 hour before the high-high tide, and close 2 hours before the low-low tide." This is shown in Figure 6-2. Some ambiguities in this schedule occur during crossover neap tides when tidal energy is low and the pattern of high and low tides does not follow its usual patterns. These issues are resolved by O&M using conservative scheduling. An important aspect of the Priority schedule is that this is the *potentially* open period. In practice, the gates are closed immediately after the day's allotment is fulfilled, a point that is not included in planning scenarios.

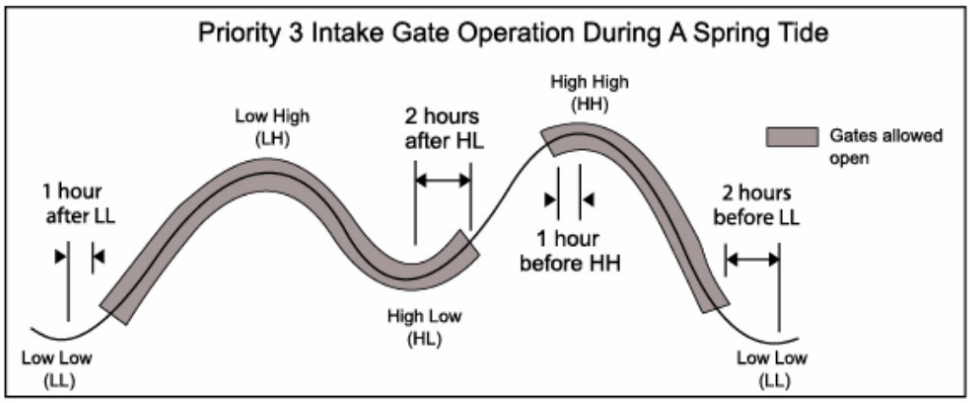

Figure 6-2 Priority 3 Gate Schedule (adapted from Wilde 2006)

In addition to issues of timing, there are two main operational strategies associated with how high the gates are lifted during each open period. For part of the year, Clifton Court gates are operated in a mostly fully open (~15 ft.) or closed fashion and are closed once the day's allotment has been satisfied. Since 2009, operators have followed a *sipping* strategy for part of the year to reduce velocity under the hypothesis that this will increase fish survival. Under the sipping regime, the gates are open to a smaller height for a longer period. Figure 6-3 shows the average Clifton Court radial gate height from April 2009 to April 2012 and illustrates the difference and seasonality Sipping requires greater effort and uncertainty. According to operators, it is still unclear whether this will become a permanent strategy.

Rather than being driven by the tidal calendar, the Harvey O. Banks pumping plant (Banks) follows a 24-hour daily schedule driven by diurnal variation in electricity prices. In addition, recently some emphasis has been placed on consistency in order to reduce stress on equipment. During periods when exports are relatively high, conveyance and cavitation considerations dictate that water levels in the forebay do not get too low. An elevation of -2 ft. sea level (datum assumed to be National Geodetic Vertical Datum of 1929 [NGVD]) is the level used as a cavitation warning. At the same time, the challenge of taking in the daily allotment of water through the gates during low energy tides favors low water levels, and the forebay is allowed to be drawn down more during weak neap periods for this reason. In the absence of these special considerations, one rule of thumb employed

by operators is to try to bring water levels to-0.5 ft. mean sea level every day at midnight and lower during weak neap periods.

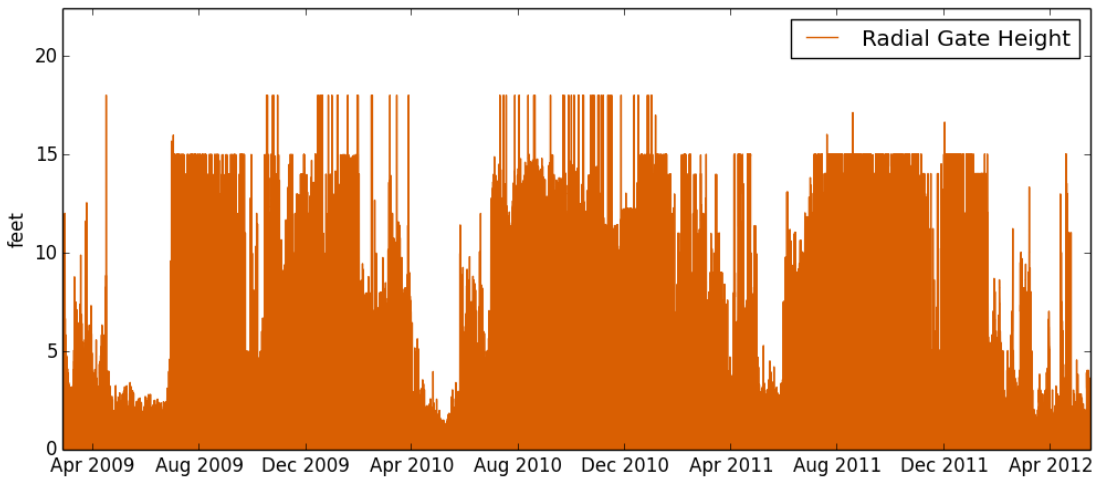

Figure 6-3 Average Clifton Court Radial Gate Height over Three Recent Years

6.3 Project Data

To develop a rating, upstream and downstream water levels are required. Upstream stage is taken from the NCRO station 95340, Old River, at Clifton Court Ferry, which is the reference used by operators for the exterior water levels. Interior water levels are observed at a station just south of the gates wing walls, and are fairly well isolated from the dynamics of the gate and far from drawdown near the pumps. Interior water levels are not distributed in real time.

For fitting the new rating, we used flow data from several boat-mounted (downward-looking) Acoustic Doppler Current Profiler (ADCP) campaigns at the intake channel just outside the forebay. Four collections were made by NCRO in 2004-2005, two in 2012, and one by Cathy Ruhl of the U.S. Geological Survey in 2008. While our data set has more variety than any of its predecessors, the ADCP datasets span mostly periods of small-medium gate heights. We sought to get data from more large gate openings, but in late 2012 the winter sipping season was declared two days before our proposed outing, and in late 2013, one of the gates fell off its hinges the week before our second attempt. Because of these mishaps, in part, one of our validation periods, using a flow balance, emphasizes a 2004-2005 period with large openings.

Several other datasets are sometimes described in association with the Clifton Court gates. The first is the daily value available from the DAYFLOW program and on the California Data Exchange Center (CDEC) as the Clifton Court station identified as CLC. This gate flow is inferred from a daily mass balance that includes Banks flow, Byron-Bethany Irrigation District (BBID) exports, and changes in volume in the forebay. The second is an hourly or instantaneous flow stored in DWR operational databases at hourly or finer intervals at least as far back as 2004. This second “flow” is really a computation based on the Hills Equation, a rating known to be very inaccurate. The gates have never been fitted with a continuous flow monitoring device, although a pilot effort was made in

2004 to establish an ADCP flow station just upstream of the gates in the intake of this channel. This year, plans for that station have been revived, and observations may begin as early as this fall.

Hourly or more frequently timed records of gate heights exist in scattered form over several DWR databases, most recently in the DWR Control Systems Branch Information Server (Wonderware). We collated the data across sources for the period covered by this project, which goes back to December 2004. There are also large gaps in the record. Often the calculated gate flow, as well as upstream and downstream water levels, were recorded even when the gate height was not. In these cases, the Hills Equations can be inverted to reverse engineer, although imperfectly, a gate height from water levels and flow. In addition to these gate height records, historical opening and closing times at the CCFB gates have been included in the DSM2 historical input datasets for many years. Only the timing is included in this dataset, but it is by far the most lengthy and widely disseminated record of gate openings.

As with gate flow, Harvey O Banks flow and BBID exports (CDEC stations identified as HRO and BBI) are widely distributed in daily averaged form. Instantaneous data is not directly recorded. The Banks pumps are equipped with flow instruments, but they are rarely functional. Instead, DFD calculates pumping volumes using the capacity of each pumping unit and the start/stop times of the units. The calculation is subject to some transient error at startup, variations caused by upstream and downstream conditions, and assumptions concerning the design and age of the impellors. We encountered three sets of pumping ratings used by different groups in DWR, though the difference among them was only a few percentages. It is this calculation, summarized as a daily total using a spreadsheet, that is reported on CDEC as station HRO. Although the method seems like it implies the creation and integration of a fine time-scale-flow-time series, that actually is not the case — operators are primarily concerned with volumes, and a time series of flows is not produced.

DWR does, on the other hand, create an approximate instantaneous time series of Banks flows on a monthly basis using stored start/stop times as part of the service rate report, which is delivered to contractors. It is mostly from this effort that we learned how to calculate Banks pumping on a fine time scale, although we used the pump ratings for each unit given to us by DFD, which are slightly different. We are able to compute a flow that matches the daily averaged CDEC calculation fairly accurately for periods after 2004. In principle, a detailed time series of exports could be constructed going farther back, but this would require significant researching of archived records using the Operations and Control Office MAPPER software or even paper records.

6.4 Prior Gate Ratings

One of the original operational ratings for the Clifton Court gates was devised by Edward Hills in 1988, based on a few dozen observations with hand-held velocity meters with gate heights in the common range of the day, 12-15 ft. There were no examples of the much lower gate heights (3-10 ft.) that are common nowadays. An optimistic skill assessment of the Hills Equation was published by Le (2004), but this validation was based on a misunderstanding concerning quantities stored in DWR databases and essentially just compared two versions of the same calculation. We have found to the contrary that the Hills rating performs poorly even in its design range, with sustained errors of thousands of cubic feet per second (or 30-40 percent) common over a wide range of flows. Figure 6-4 shows a comparison of daily averaged Hills Equation flow with daily DAYFLOW estimates based on daily flow balances, which are thought to be fairly accurate. Significant overestimation

and underestimation are evident. Importantly, as far as we know, **DWR does not rely on flows from the Hills Equation for any critical operational or regulatory purpose**.

The second gate rating that was of interest to us is the one in DSM2. DSM2 used a submerged gate equation to model the forebay gates. The traditional DSM2 gate coefficient has some minor difficulty reproducing Clifton Court water levels when used with realistic gate heights. But the potential performance is hampered by overly simple modeling assumptions made concerning gate heights. For instance, in historical modeling, gates are presumed to be fully closed or open. We will demonstrate it is not possible to model water levels accurately during the sipping season under this constraint.

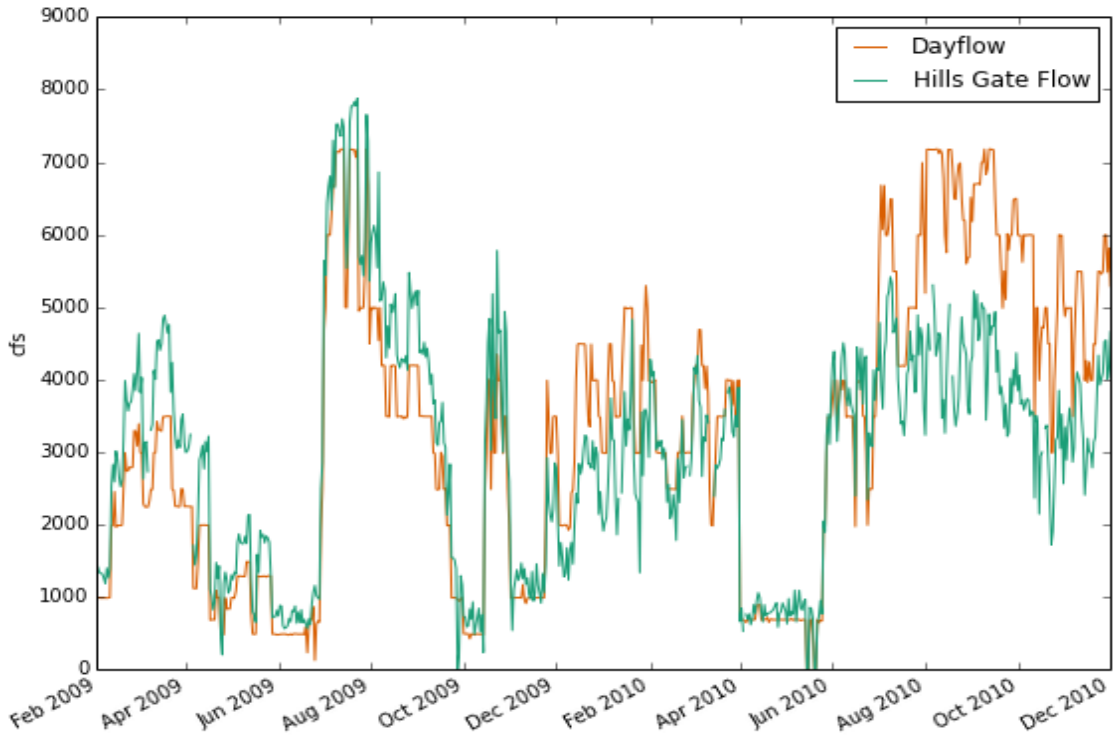

Figure 6-4 Comparison of Daily Gate Flow Calculations from DAYFLOW (SLP is Gate Inflow) with Daily Averages of Flows Reported Based on the Hills Equation

6.5 Dynamic Response to Radial Gates

The sensitivity of a model to gate ratings depends on the use to which the rating is put. A rating can be used offline to produce an estimate of flow boundary conditions. This is particularly likely to be the case for a model that includes just the Delta or just Clifton Court. Alternatively, the gate can be embedded within the model and used to dynamically couple the two sides of the gate as it is in SCHISM and DSM2.

MacWilliams and Gross (2013) studied residence time in Clifton Court using the UnTRIM model. Their study was an isolated model of the forebay using gate flows based on the Hills Equations and historical gate heights and water elevations to force the boundary. Encountering the inaccuracy of the Hills formula described in this chapter, they proposed a two-step procedure to estimate gate flows, using the Hills Equation, for disaggregation of the daily pattern of flows and daily historical CDEC values to re-scale the flows to the correct daily total volume. In principle, their technique can be used to transfer flows between the Delta and forebay, and we tried this during the calibration of the 3D model SCHISM. For us,

it turned out to be a high quality but brittle solution for long-term simulations of the coupled system. A small (e.g., 2-5 cfs) systematic discrepancy between Banks pumping and the gate flow will fill the forebay during just a few months.

When the Clifton Court gate is embedded in a model that allows water levels to respond dynamically, approximation error manifests more in the interior water level of the forebay than in the flow. Although Figure 6-1 implies persistent errors of thousands of cubic feet per second, a surplus or deficit this size is unsustainable, because it would overtop or drain the forebay within a few days. In a dynamic model, forebay water levels respond and provide the negative feedback needed to maintain stability. For instance, if inflow through the gates is overestimated, water levels go up in Clifton Court and act through the gate rating to reduce the influx. Long-term flows in such a model can be accurate and robust, matching exports. Even short-term variations in flows and water levels can be surprisingly good depending on how gate heights are approximated. Even so, water levels within the forebay drift unrealistically. We will demonstrate this phenomenon below when we consider DSM2 modeling results.

6.6 The New Rating

In selecting a formula for the gate, we considered a variety of parameterizations of varying complexity, ranging from the submerged gate equation used in DSM2 to the energy-momentum method of Clemmens (2004) and Wahl and Clemmens (2005).

The impetus for considering the energy-momentum method was the possibility that Clifton Court operates in the “partially submerged” regime. This is a region of flow that is hard to characterize with the typical (energy-only) equations due to complex tail water control from inside the reservoir. Acting on reviewer comments, MacWilliams and Gross (2013) suggested one reason for the failure of the Hills Equations under modern flows, where both sides of the gate are deeply submerged, is that they were calibrated with data almost solely in the partially submerged regime, which was common in 1988, and that is why the calibration does not extrapolate well to submerged flow, which was common in 2008. We have some doubts concerning this explanation. First, the foibles of the Hills rating extend across a wide range of flows, including ones similar to those under which it was calibrated. Second, conditions in Clifton Court are rarely partially submerged based on the usual criteria. The U.S. Army Corps of Engineers (Hydrologic Engineering Centers River Analysis System [HEC-RAS]) criterion for partial submergence is a ratio of downstream tail water to upstream head of 0.67-0.80. This ratio is rarely, if ever, satisfied at the CCFB. The sill is deep and both sides of the gate are too constrained by sea level and cavitation constraints for the depths to become very different from one another. We have surveyed several years of data, and it seems the ratio is often in the 0.85-0.95 range, which is typical of fully submerged conditions. We do not consider this matter resolved; certainly, anyone experimenting with a hypothetical scenario involving lower-than-historical water levels in the CCFB would need to reconsider the comments in Wahl and Clemmens (2005) concerning submergence.

Eventually we settled on a modified form of the submerged gate equation [1].

$$Q = nCA\sqrt{(2g)(z_{up} - z_{down})} \quad [1]$$

Where

Q is the gate flow,

n is the number of gates operating (with non-zero heights),

C is the dimensionless state-dependent gate coefficient described below,

g is gravity,

z_{up} is the stage upstream of the forebay (assessed by DFD at Clifton Court Ferry),

z_{down} is stage inside the forebay,

z_{sill} is the bottom elevation where the flow pours over, and

A is the average area of the gates in operation, based on width W, and limited from above either by the free surface or by the average height G of gates that are open, $A = \min(G, z_{up} - z_{sill})$.

As expressed above, this formulation has the same form as in DSM2. Inspired by a parameterization in Wahl (2013), we made the gate coefficient linearly dependent on the ratio of gate height to upstream depth from the sill located at -15.5 ft. NGVD (-13.2 ft. North American Vertical Datum of 1988 [NAVD])[2], [3].

$$C = d + sR \quad [2]$$

$$R = \min\left(\frac{G}{z_{up} - z_{sill}}, 1.0\right) \quad [3]$$

Where d and s are parameters.

We used linear least squares to fit the coefficient conditional on the data, excluding a small number of observations taken when the gates were in the process of lifting or closing rapidly. The standard error of the fit is 400 cfs, although the residuals seem to scale as a fraction at about 5 percent of gate flow magnitude so that higher flows have higher residuals. Since 5 percent would represent acceptable accuracy for the ADCP flows, overall the fit is roughly on par with the accuracy of the measurements used to derive it. The reported coefficient of determination, R^2, of all our fits is well over 0.95. We do not wish to publish a specific value in light of the serial correlation of the residuals and a small amount of sample dependence of the statistic.

The original formula suggested in Wahl (2004) involved a quadratic rather than a linear formula, and we had hoped including a quadratic term might improve the handling of a wide range of gate heights. We tested this hypothesis using leave-out-5 cross-validation. Even though the quadratic coefficient makes

the rating look better in most fits, cross-validation rejects the extra coefficient. The coefficients given in Table 6-1 are appropriate under a wide range of conditions.

Coefficient	Value	Comment
d	0.67	Range 0.67-0.75
s	0.67	Range 0.6 – 0.8

Table 6-1 Parameter Fits for Coefficients and Comments from Drought Modeling

Our rating does not assign individual coefficients to the five Clifton Court Gates. We felt the gates have not been operated independently in enough configurations to infer the individual character of a gate from historical data. Also, this per-gate effect would be easily conflated with that of relative location within the row of gates. For instance, Gate #2 might be on the outside of the set of open gates one day when Gate #1 is closed for maintenance, but then Gate #2 would be on the inside the next day when Gate #1 comes back online. If specific gate coefficients are assigned in the future, we hope they will be properly tested against the null hypothesis that the individual gates should be treated the same.

6.7 Synthesizing Heights

The new rating requires more access to data and more preparation. At the very least, Clifton Court gate heights are needed at fairly short time intervals, and subtidal water level variation at the outside of Clifton Court will affect results (i.e., astronomical forecasts may not represent difficult minima). Large errors in forebay water levels are introduced in planning studies when modelers assume that the gates are fully open (Priority 3), at the times when they are designated to be open.

Some approximations are possible, though. For historical periods, when explicit gate heights or Banks pumping data are not available, we have had some luck converting target gate flows to gate heights using the following method.

1. Obtain daily gate flow from DAYFLOW (SWP) or CDEC (CLC) or the planning scenario and distribute this volume evenly over the period the gate is open, which is part of the DSM2 standard inputs and usually comprises a subset of the Priority 3 period.
2. Determine a gate height, G, for all five gates by inverting this simplified rating based on gate heights only.

$$Q = aG + bG^2,$$

where $a = 1100\ \mathrm{ft}^2/\mathrm{s}$ and $\mathrm{b} = -16.8\ \mathrm{ft/s}$.

We will demonstrate the effectiveness of this synthetic gate height in section 6.8 below. So far, this formula is more accurate for historical modeling than for planning because it assumes we know the flow at the gate and how this flow is different from the daily exports. This difference is driven by strategies that are difficult to mimic for planning.

In the first half of 2015, exports were low and a new gate operation became common – operating a single gate briefly, Priority 1, (Le 2004) and at a significant height. The above formula predicts a gate height that is too small under these conditions. Imposing a minimum opening of 1-2 feet is sufficient to

stabilize the water balance. Correcting for a change in period and a single gate is expected to be more accurate, but we have not tested this assumption.

6.8 Validation through Flow Balance

Although we performed our calibration against ADCP observations, we also wanted to validate the fit using a mass balance around Clifton Court. Figure 6-5 shows the domain of our conceptual model. Exterior water levels, gate heights, and exports (SWP plus BBID) were based on observations. Interior water level is the state variable we integrated and compared with observed values. We ignored wind and evaporation.

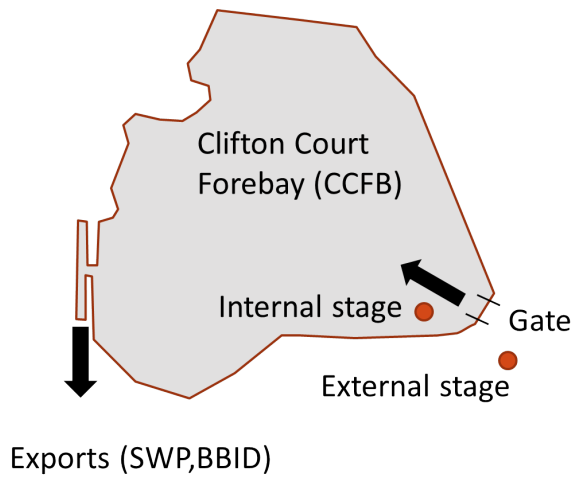

Figure 6-5 Components of Flow Balance Used to Calibrate the Gate Rating

To capture a more comprehensive set of gate operations, two periods were used for validation using this model. The first was winter 2004-2005, a period in which the gates were often fully open. The second was March-December 2008, a period where sipping was more common. Water levels and flows are shown for the 2004-2005 and 2008 periods in Figure 6-6 and Figure 6-7, respectively. Results of the water balance validation are shown in Figure 6-8 and Figure 6-9 with a shorter length zoomed view of the 2008 case in Figure 6-10. Figure 6-11 shows the forebay water level fluctuations and gate flows from the DSM2 gate rating and simple mass balance model for 2004-2005. Figure 6-12, a scatter plot, also shows the flow results from the new rating as compared to the ADCP observed data. The new rating performs well in both periods, capturing most of the trend and short-term variation in water levels. The fit is slightly high in 2008, and we noticed that this was again true when doing drought modeling in 2014 with SCHISM. This may be due to the rating, a physical factor such as evaporation, or different relative error in Banks flows at low volumes.

For the sake of comparison without the complication of model error, we also applied the DSM2 gate rating to the 2004-2005 hydrology, but using our simple mass balance model as the context rather than DSM2. The main difference is that upstream stage is pegged to historical observations without the model error from DSM2, which in this area is typically a small exaggeration of tidal range. Water levels are consistently biased downward by 1 ft. or more for large gate heights in order to coax more water through the gate (the coefficient is lower than the new fit). Other aspects of the fit, including flow through the gate, are acceptable. This result is in keeping with modeling results we will show in the next section on DSM2 experiments.

Although the ADCP fit and flow-balance based validation were two distinct exercises, the two agreed well.

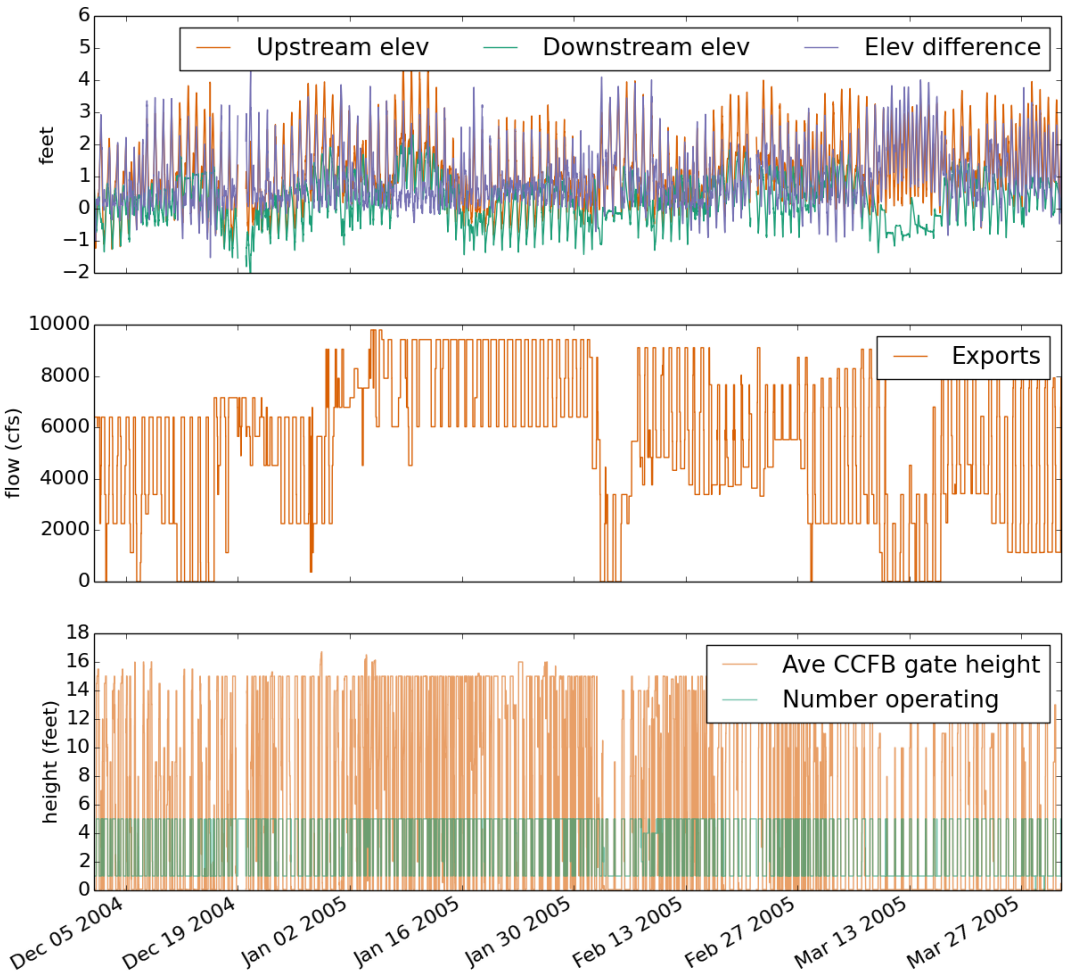

Figure 6-6 Water Levels (top), SWP Exports (middle) and Gate Heights (bottom) at Clifton Court in Winter 2004-2005

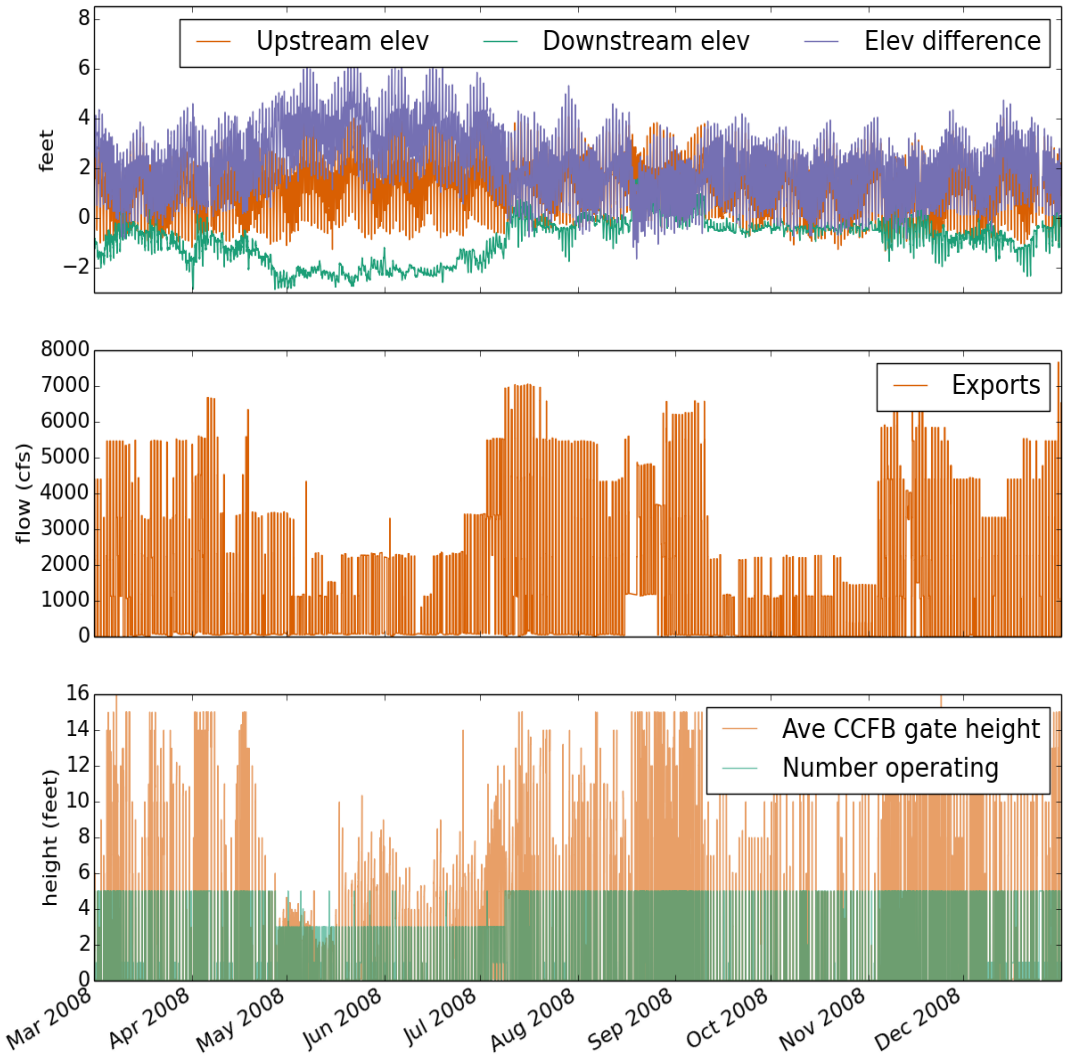

Figure 6-7 Water Levels (top), SWP Exports (middle) and Gate Heights (bottom) at Clifton Court in 2008

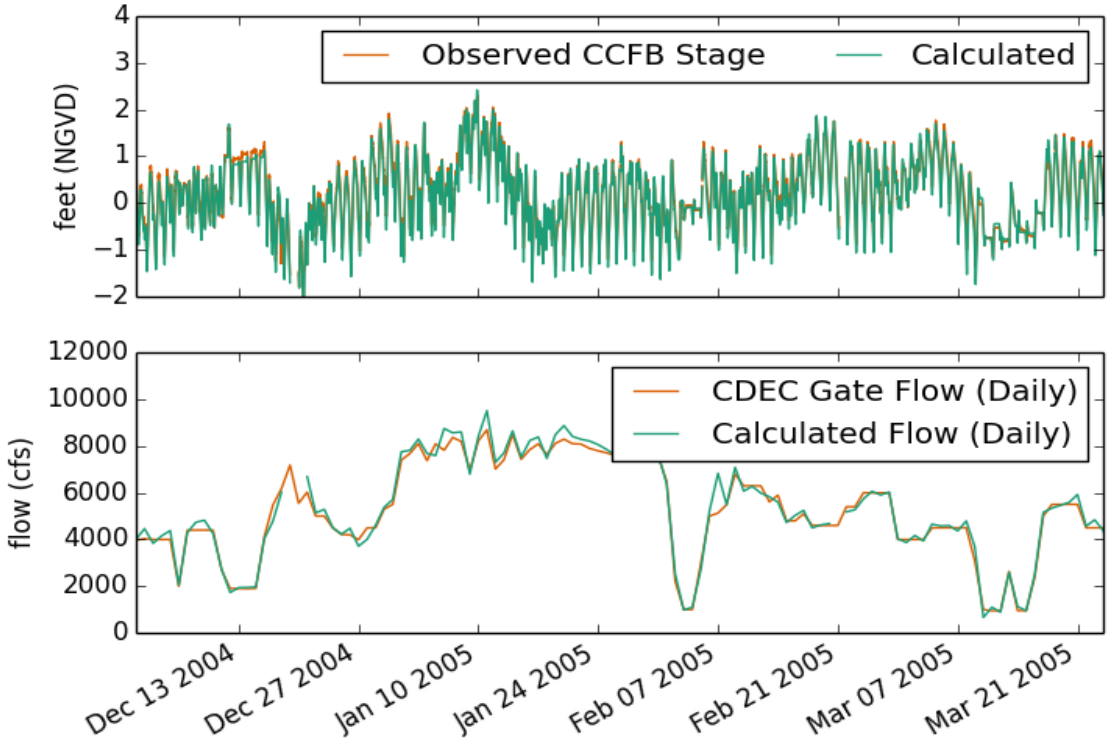

Figure 6-8 2004-5 Forebay Water Level Fluctuations and Gate Flows from the New Rating Compared with Field Data Utilizing Instantaneous Gate Height and Pumping Data and the Simple Mass Balance Model

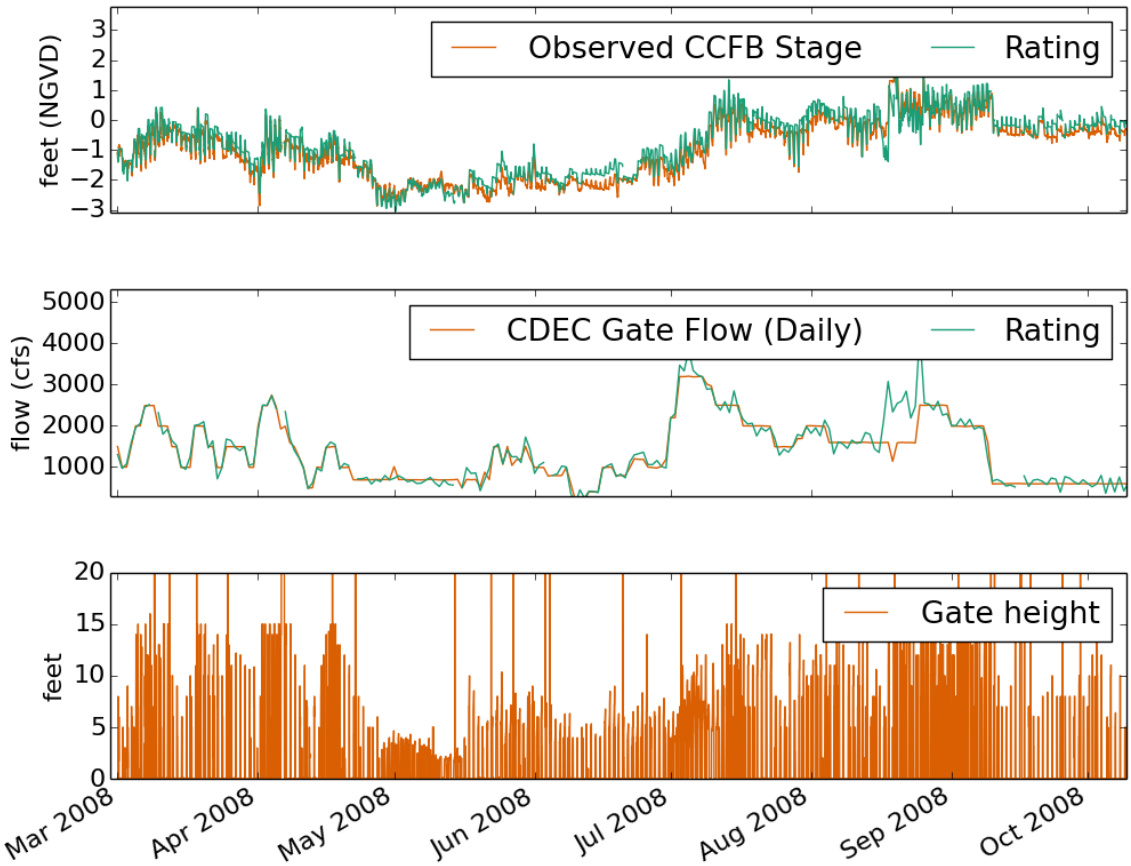

Figure 6-9 Rating Validation in 2008 Under Low Flows and "Sipping" Gate Operations, Including Clifton Court Water Levels (top), Daily Flows (middle), and Gate Heights (bottom)

Note:The slight positive bias indicates that the coefficient is slightly too high for these flows.

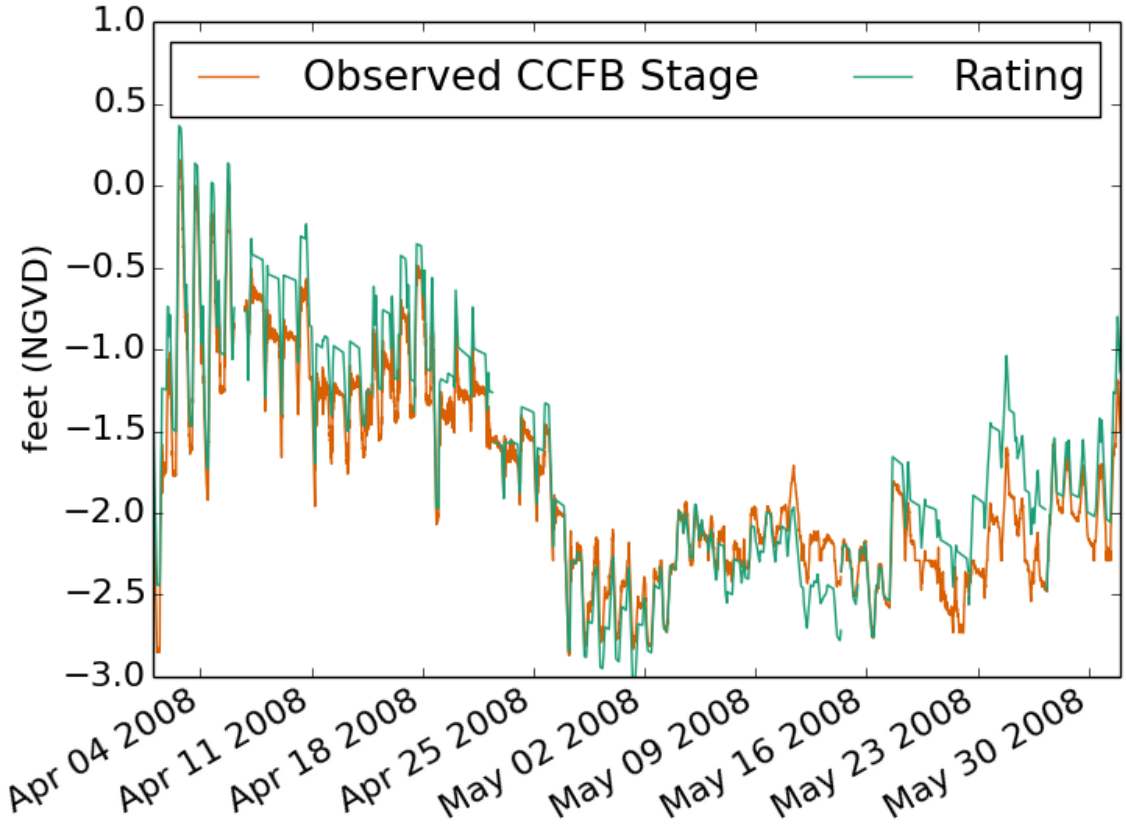

Figure 6-10 Close-up of Intratidal Water Level Fluctuations in the 2008 Mass Balance Experiment

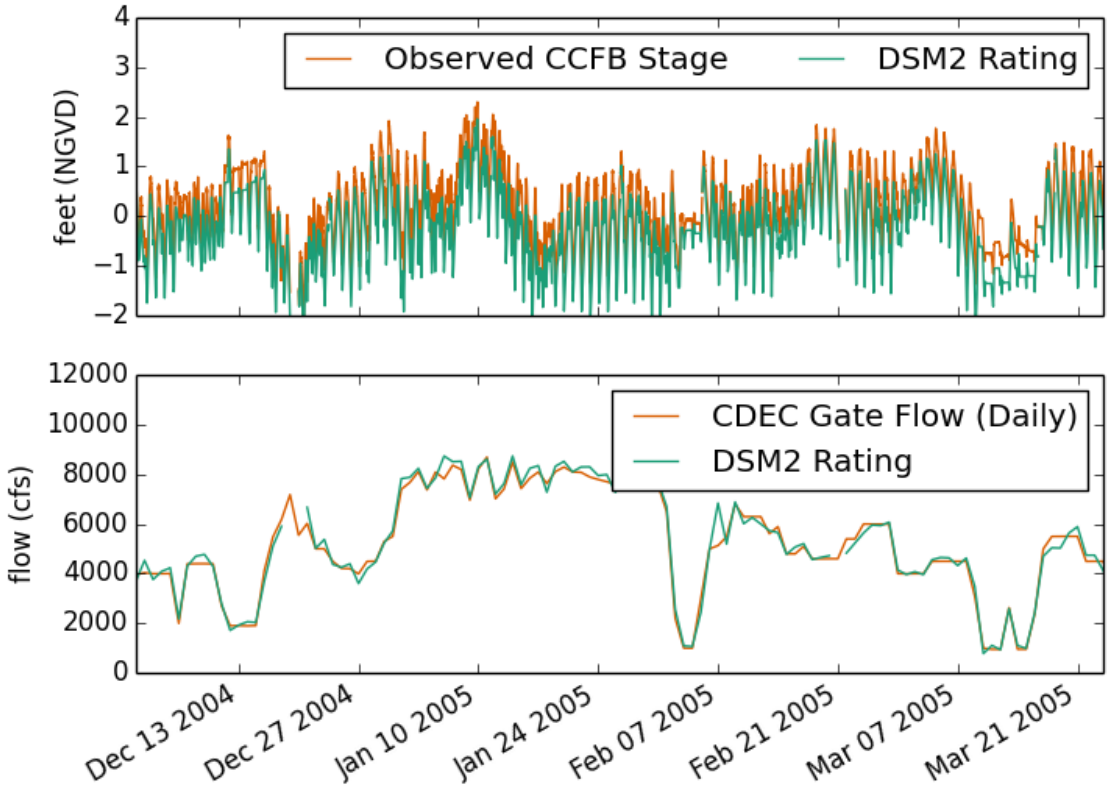

Figure 6-11 Forebay Water Level Fluctuations and Gate Flows from the DSM2 Gate Rating and Simple Mass Balance Model

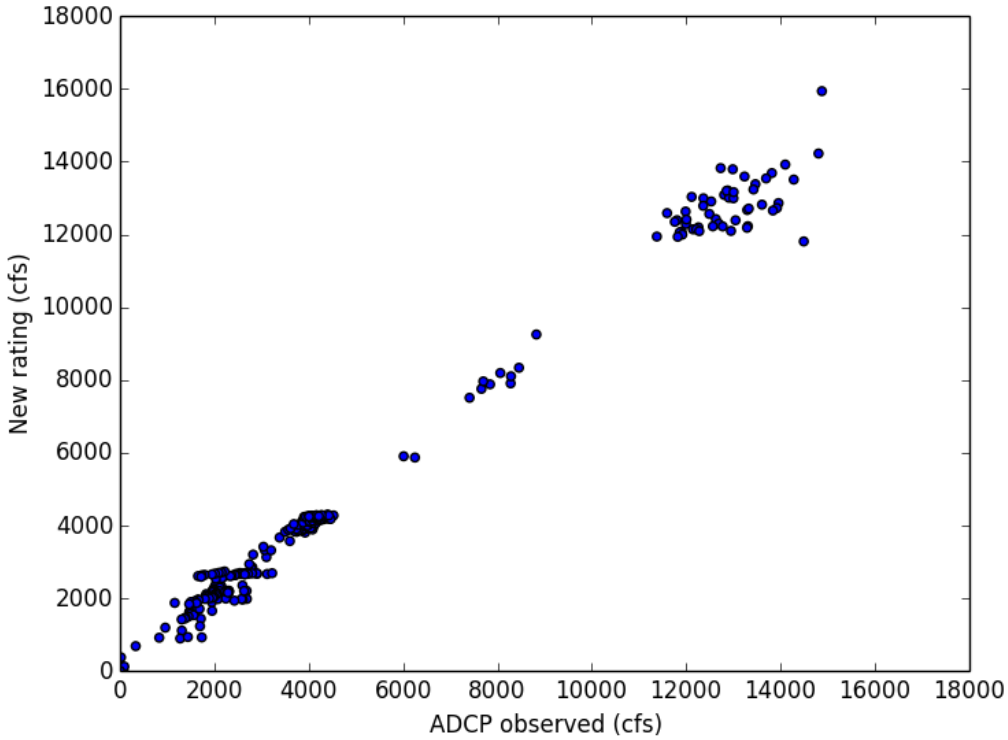

Figure 6-12 Fitted Versus Observed Values for the ADCP Data

6.9 DSM2 Experiments with Full and Limited Data

The gate rating presented here is sufficiently accurate and appears to be robust when tested in isolation. Typical errors in flow for the rating are 5-10 percent, and any tendency for Clifton Court water levels to wander appears to be self-correcting.

This section adds the additional complication of a model. We show how the gate formulation interacts with the DSM2 model. Since the costs of preparation are not insignificant, we sought also to confirm how important this might be on dynamics throughout the South Delta, and to see how important fine time scale data is to the modeling of the region.

6.10 Old versus New Rating

Our main experiment is intended to isolate the performance of the new rating while holding data granularity the same. The cases all use instantaneous Banks pumping and gate height data. The two cases are:

R1: DSM2 original rating.

R2: New rating.

Figure 6-13 shows the water level and flow results for both ratings, with interior water levels compared with observations. During May, the old rating has a clear bias, and we note that it is in a different direction than Figure 6-9, which is common during sipping operations. Figure 6-14 shows the corresponding water quality results. Although residence time is probably affected significantly by the change in water levels, the effect on concentration is negligible. The same is true for Old River stage at

Tracy Road Bridge (Figure 6-15). Clearly, Clifton Court water levels are the only DSM2 variable affected by the change.

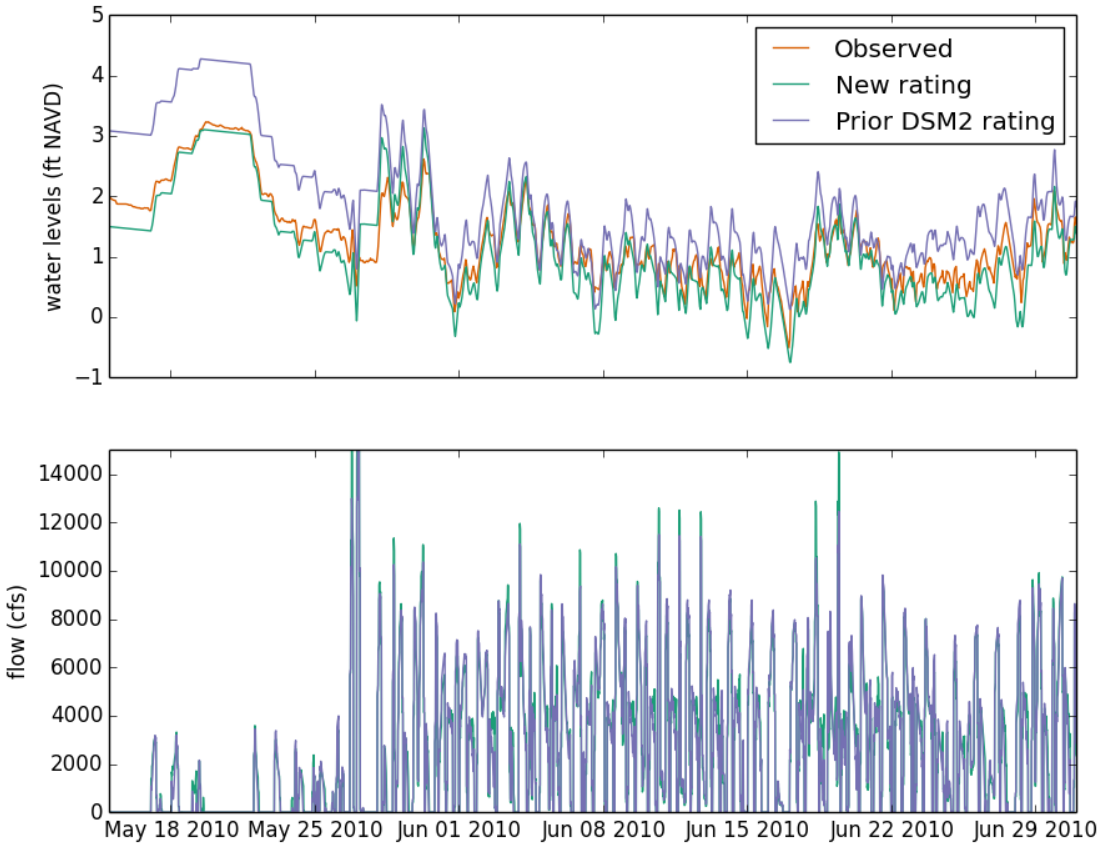

Figure 6-13 Water Level and Flow Results for DSM2 Experiment with Old (R1) and New (R2) Rating

Figure 6-14 Clifton Court Electrical Conductivity (EC) under Old and New Ratings with Instantaneous Gate and Pumping Data

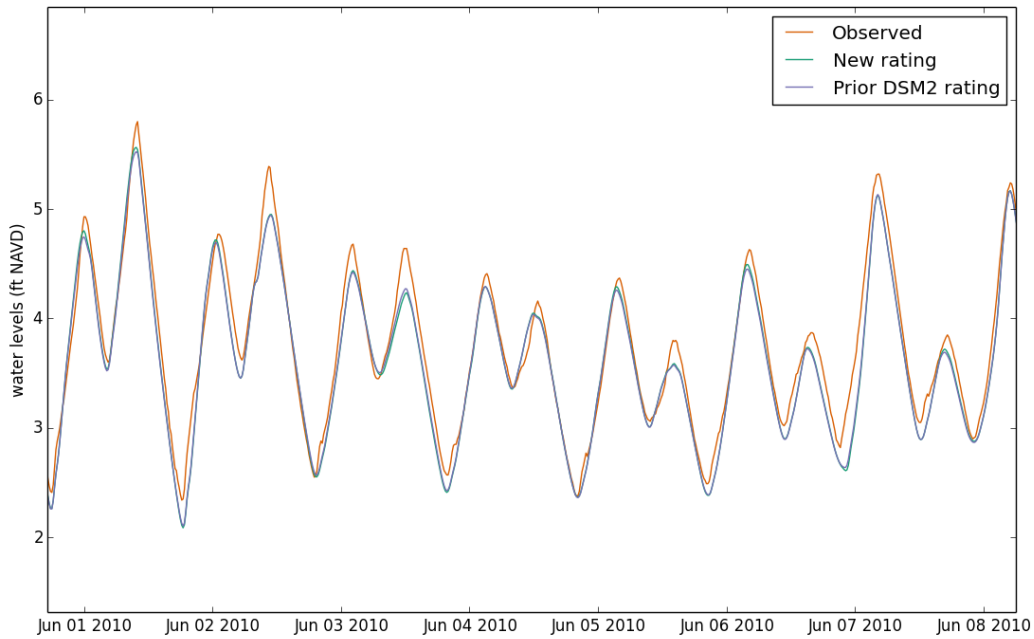

Figure 6-15 Old River at Tracy Bridge Water Levels Under Old and New Ratings with Instantaneous Gate and Pumping Data

6.11 Data Granularity

Our second group of experiments isolates the effect of holding data granularity constant while holding the new rating fixed. Variations we attempted are as follows.

C1 (Planning Priority 3): Gates are assumed to be fully open or closed over full possible Priority 3 period.

C2 (DSM2 historical): Gates are assumed to be fully open or closed. Timing is historical and instantaneous.

C3: Gate heights are synthesized from daily gate allotment (section 6.7, "Synthesizing Heights").

C4: Instantaneous gate heights (10 minutes or less, except during filled gaps).

Results are shown in Figures 6-16, 6-17, and 6-18. The most striking water level results are in Figure 6-16 and show that the water levels for the Priority 3 case (C1) are very high and unfortunately represent the practice in planning DSM2 runs. The 2 ft. errors shown in the figure are not exceptional. In the next section we will show errors as significant as 5 feet. The higher interior water levels occur because of the feedback mechanism we noted before; the reservoir fills up to compensate for the exaggerated high gate heights. Flows are somewhat disorganized and incorrectly timed, though on average, of course, they match exports.

Figure 6-17 shows Electrical Conductivity (EC) for the different quality and granularity of gate height data. EC results are similar except in June 2009 and April 2010. Figure 6-18 shows the water level impacts of the gate height data on a location upstream at Old River and Tracy Road Bridge.

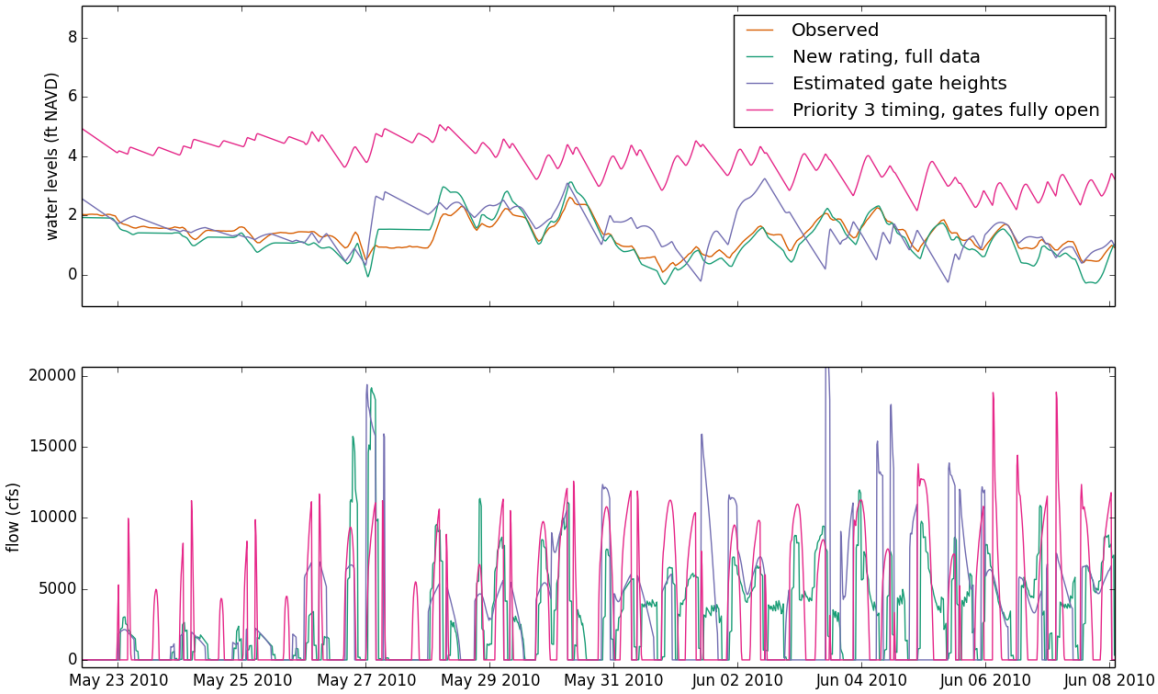

Figure 6-16 Clifton Court Water Elevations with Different Quality and Granularity of Gate Height Data

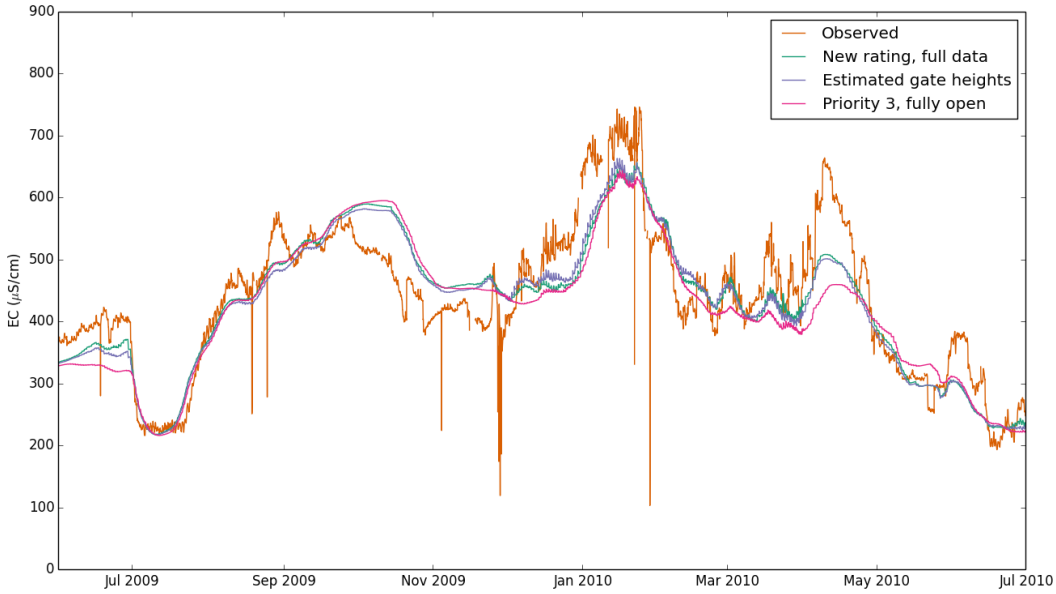

Figure 6-17 Clifton Court EC with Different Quality and Granularity of Gate Height Data

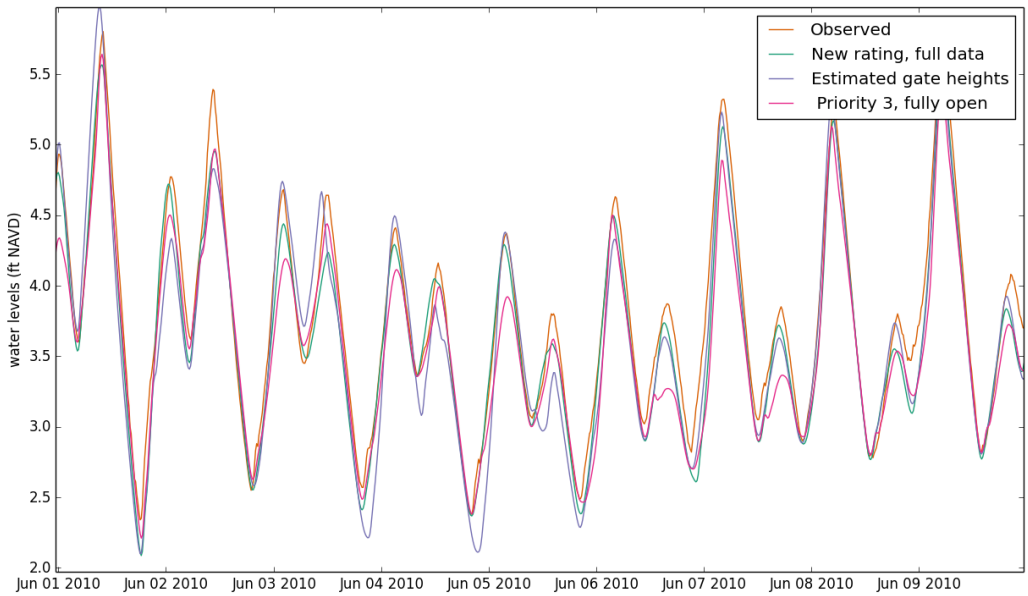

Figure 6-18 Old River at Tracy Bridge Water Elevations with Different Quality and Granularity of Gate Height Data

6.12 Banks Data Granularity

We tested the granularity of Banks (SWP) pumping data using the new rating and instantaneous gate heights:

B1: Banks pumping data is available instantaneously.

B2: Daily Banks pumping data.

Results for these two cases are shown in Figure 6-19. Our impression looking over years of data is that, in general, detailed Banks pumping information is only sporadically helpful in modeling with DSM2. This is a fortunate result in that detailed Banks pumping data is very inconvenient to acquire compared with other measurements. For detailed circulation near the pumps with SCHISM or another 3D model, such as UnTRIM, pumping would be required in more detail, of course.

6.13 Gate Timing: Scheduled Priority 3 versus Historical

In a planning run, gates are often held open for the entire Priority 3 period, whereas in the field, gates are closed as soon as the day's allotment is achieved. Using the original DSM2 rating and fully open gates, we looked at what difference this makes in water levels. The result is shown in Figure 6-20. Both answers are erratic, with maximum errors of water surface up to 5 feet. This is true of all the cases with the gates raised fully open. The historical timing does not seem to be beneficial. The result with historical timing seems to be almost exactly the same most of the time with huge unrealistic swings. One reason the historical timing might not be helpful is that it is supposed to represent fulfillment of the day's allotment. When the gate is fully open, that fulfillment is probably achieved much earlier than in the field and so the historical timing no longer satisfies this interpretation.

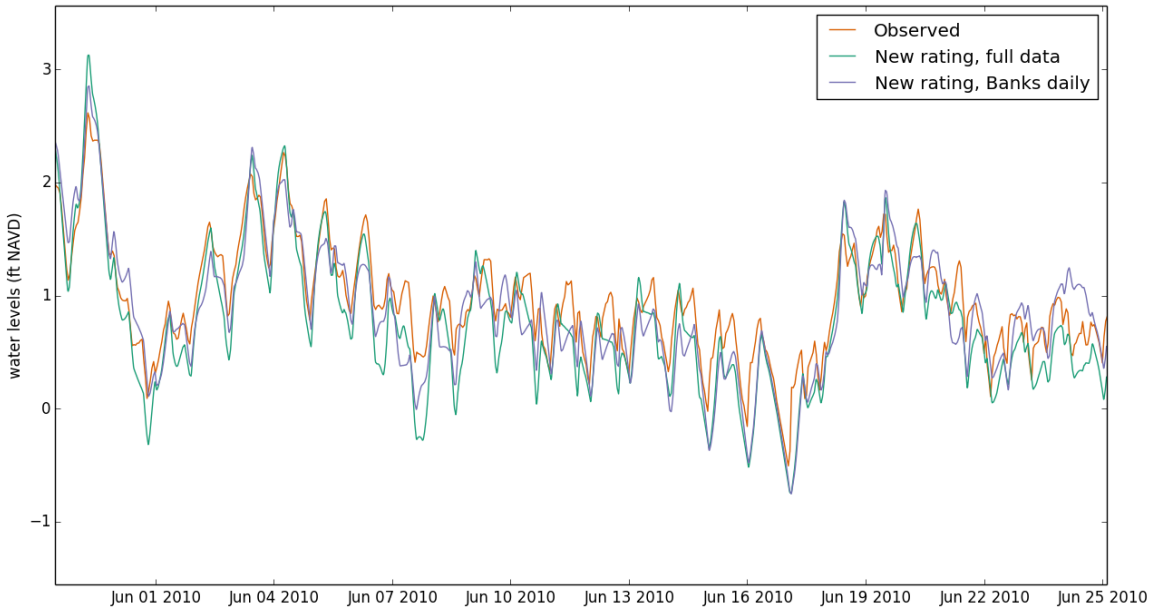

Figure 6-19 Clifton Court Water Levels with New Rating, Instantaneous Gate Heights and Two Granularities of Banks Pumping Data, Instantaneous (full) and Daily

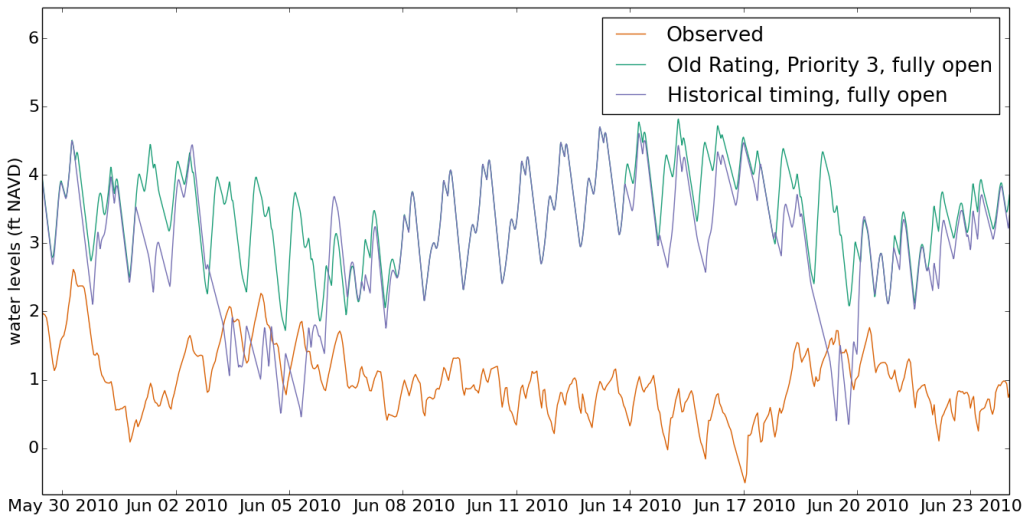

Figure 6-20 Comparison of Scheduled Timing and Actual Historical Gate Timing using DSM2 with the Prior Rating and Gates Treated as Always Open/Closed

6.14 Conclusion

The authors have calibrated a rating that we believe can be successfully applied in operational scheduling and modeling applications. The new rating has a standard error of 400 cfs, or 5 percent, under a fairly wide variety of conditions, and this accuracy can be re-evaluated in a few years as the new Clifton Court intake flow station comes online. Accuracy is much better than the rating curve currently on hand at DFD, and it is somewhat better than the one in DSM2. The new rating is being offered as part of a revised version of DSM2, and is part of the standard package for the 3D Bay-Delta SCHISM model.

Model practices may be at least as important as the rating. Modelers often treat the Clifton Court gates as always being open or closed, and this assumption is enough to cause a large bias in water level results inside the forebay regardless of which gate equation is used. Since the increase in water levels can cause a 30-50 percent change in depth, this would also affect residence time. Furthermore, in the SCHISM model, it changes estimates of local velocity. Most other variables are very robust, including exterior stage and water quality on both sides of the gate.

Modelers often have to proceed with imperfect information when modeling the forebay. Detailed time series of Banks pumping and gate heights are not available for many periods and in planning scenarios. Daily time series are the norm for pumping and timing-without-heights is the norm for gate operations. For most DSM2 applications, gate heights are the component that is really crucial. Given a daily gate flow/allotment and Priority 3 timing, we have provided a formula for estimating gate height that requires no detailed tidal information and reduces most of the objectionable error in water levels. Detailed Banks pumping data is of secondary importance. Instantaneous pumping is required for 2D model or 3D model calculations near pumps or for assessing circulation in the forebay. Consequently, it is not required to produce gross residence time for the forebay or for 1D model studies where focus is on the South Delta or points downstream.

6.15 References

California Department of Water Resources. 1989. O&M Standing Operating Order PC 200.7-A.

Clemmens AJ. 2004. "Avoiding Submergence Transition Zone for Radial Gates in Parallel." In: *Proceedings of the World Water and Environmental Resources Congress.* June 27-July 1, 2004. Salt Lake City (UT). [CD-ROM].

Le K. 2004. "Calculating Clifton Court Forebay Inflow." In: *Methodology for Flow and Salinity Estimates in the Sacramento-San Joaquin Delta and Suisun Marsh. 26th Annual Progress Report*. Sacramento (CA): California Department of Water Resources. Delta Modeling Section.

MacWilliams ML and Gross E. 2013. "Hydrodynamic Simulation of Circulation and Residence Time in Clifton Court Forebay." San Francisco Estuary and Watershed Science. 11(2).

Wah T. and Clemmens A. 2005. "Applying the Energy-Momentum Method to Radial Gate Discharge Calibration*."* Impacts of Global Climate Change. pp. 1-10.

Wahl TL. 2013. "Using WinGate to Develop Practical Discharge Equations for Gated Outlets at Yellowtail Afterbay Dam." USCID Water Management Conference. October 22-25, 2013. Denver (CO): Viewed online at: http://www.usbr.gov/pmts/hydraulics_lab/pubs/PAP/PAP-1098.pdf.

Wilde J. 2006. "Priority 3 Clifton Court Forebay Gate Operations for Extended Planning Studies." In: *Methodology for Flow and Salinity Estimates in the Sacramento-San Joaquin Delta and Suisun Marsh. 26th Annual Progress Report*. Sacramento (CA): California Department of Water Resources. Delta Modeling Section.

Methodology for Flow and Salinity Estimates in the Sacramento-San Joaquin Delta and Suisun Marsh

36th Annual Progress Report
June 2015

Chapter 7
Calibrating the Martinez Boundary Salinity Generator Using PEST

Authors: Prabjot Sandhu and Yu Zhou
Delta Modeling Section
Bay-Delta Office
California Department of Water Resources

Contents

7 Calibrating the Martinez Boundary Salinity Generator Using PEST 7-1
7.1 INTRODUCTION 7-1
7.2 BACKGROUND 7-1
7.2.1 G-Model 7-2
7.2.2 Tidal Signal Incorporation 7-3
7.2.3 Model Calibration and Problems 7-3
7.3 METHODOLOGY AND STUDY CONFIGURATION 7-5
7.3.1 Theory 7-6
7.3.2 Configuration Setup 7-6
7.4 RE-CALIBRATION RESULTS AND DISCUSSION 7-8
7.4.1 Calibration for 1991-1993 7-8
7.4.2 Model Improvement and Re-calibration 7-8
7.4.3 Re-Calibration with Other Periods 7-11
7.5 SUMMARY AND FUTURE WORK 7-12
7.6 REFERENCES 7-13

Figures

Figure 7-1 Salinity at Martinez Boundary of the Bay-Delta 7-1
Figure 7-2 14-day Average Salinity as a Function of 14-day Average Net Delta Outflow (Q) and Antecedent Outflow (G). Data are for Water Year 1968-1986 7-2
Figure 7-3 Tidal Displacement Model as Embedded in the Full Salinity Model 7-3
Figure 7-4 Daily Averaged Salinity Comparison between Historical (blue), Old Salinity Generator (red) (enlarged for 1990-1992, 1993-1995) 7-5
Figure 7-5 Flow Chart for Inverse Problem (parameter estimation) with X as System Configuration 7-6
Figure 7-6 PEST Calibration Process of Martinez EC Generator 7-7
Figure 7-7 Daily Averaged Salinity Comparison Between Historical (blue), Old Generator (red), New Generator (green) Enlarged for 1990-1992, 1993-1995, 2002-2004, 2012-2014 7-9
Figure 7-8 Daily Averaged Salinity Comparison Between Old generator (green, with most of parts overlapped) and Modified Generator (red) 7-10

Tables

Table 7-1 Previous and New Calibration of Parameters of Martinez Salinity Planning Generator 7-4
Table 7-2 Part of Parameter Correlation Coefficient Matrix of Auto-calibration 7-10
Table 7-3 Parameters from Auto-calibration of the Modified Martinez Salinity Planning Generator 7-10
Table 7-4 Parameters of Auto-calibration from Observations of Different Periods 7-12

7 Calibrating the Martinez Boundary Salinity Generator Using PEST

7.1 Introduction

Martinez represents the stage-and-salinity boundary and the location for applying the Delta Simulation Model 2 (DSM2). The salinity at this location is estimated using the Net Delta Outflow (NDO) and stage. This chapter presents a re-calibration effort for the Martinez boundary salinity generator, with a mathematically based calibration software named PEST. This new calibration improves the performance of the model by better matching the historical salinity data, particularly at the higher value range. The performance of the current calibration has been a concern of water resources management, especially in the current drought crisis.

The chapter is organized with section 7.2 describing the background of Martinez boundary salinity generator, section 7.3 explaining methodology and configuration of PEST for model calibration, and section 7.4 presenting some preliminary findings.

7.2 Background

The Sacramento-San Joaquin Delta (Bay-Delta), Figure 7-1, is the nexus of California water system, which provides more than 30 million acre-feet of fresh water pumped to support drinking, agricultural, and industrial-use water. Martinez, with its critical estuarine location and continuous field measurement, serves as the downstream boundary in many modeling tools for this important Bay-Delta domain. The flow-salinity relationship at Martinez is the concern of research, because it could be used in real time or planning practice for various Delta operations and control strategies.

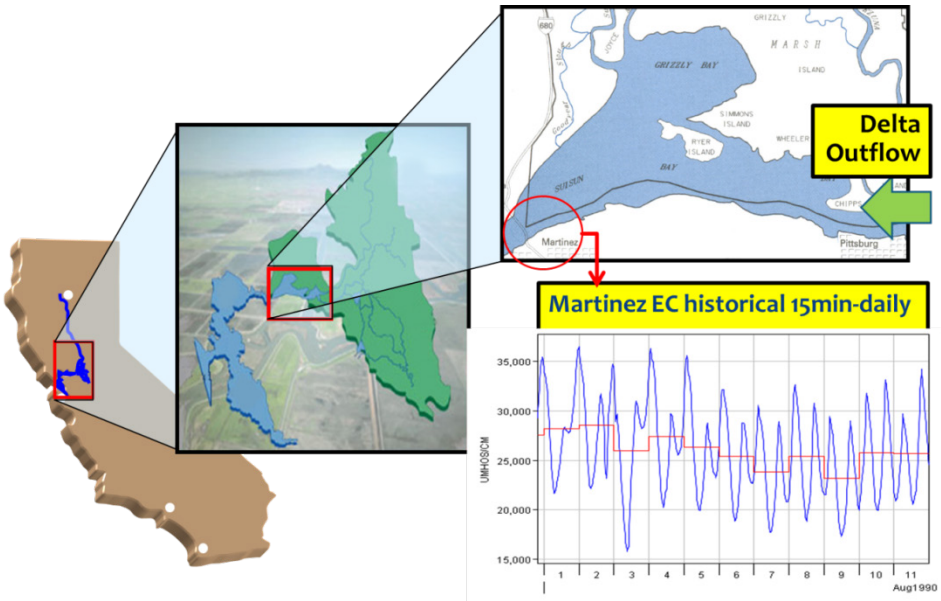

Figure 7-1 Salinity at Martinez Boundary of the Bay-Delta

7.2.1 G-Model

G-model is a conceptual-empirical model of salinity transport along the main stem of the Sacramento River (Ateljevich 2001b). It provides a 1-dimensional advective-diffusion solution for an infinitely long channel with a downstream ocean and an upstream river in its steady state (Denton and Sullivan 1993).

Its mathematical form could be written as an exponential longitudinal salinity profile

$$S(t) = (S_o - S_b) * \exp(-\alpha G^n(t)) + S_b.$$

Where

S_o and S_b are constant ocean and upstream river salinity respectively,

α is a dispersion parameter (consolidating upstream distance),

n is an additional empirical shape parameter,

G is a function representing the flow time-history, aka antecedent flow, with its math form as below

$$\frac{dG}{dt} = \frac{(Q-G)G}{\beta},$$

β is an empirically determined constant depicting system's reaction to Delta outflow,

Q is volumetric flowrate, which is NDO for Martinez,

t is time,

$\frac{dG}{dt}$ is the derivative of G with respect to time.

Figure 7-2 represents the advantages of using *G* over flow *Q* in flow-salinity relationship estimation. Details of the original model may be found in Dr. Denton's report (Denton and Sullivan 1993).

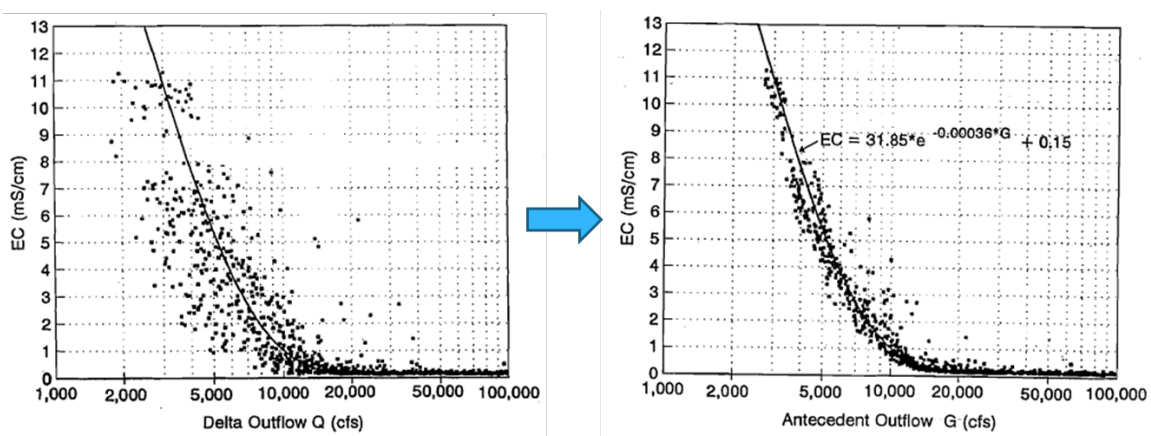

Figure 7-2 14-day Average Salinity as a Function of 14-day Average Net Delta Outflow (Q) and Antecedent Outflow (G). Data are for Water Year 1968-1986

Notice the corrections to NDO to account for both Delta filling and draining and island consumptive use estimates,

$$q_{corrected}(t) = q_{ndo}(t) - A\Delta z(t).$$

A represents the storage area filled by an incremental change in water surface height $\Delta z(t)$.

7.2.2 Tidal Signal Incorporation

To make predictions more accurately in a closer time interval, this salinity model was further developed to incorporate the tidally varying effect from the ocean. The newly applied methodology utilizes a linear filtration to model displacement on lagged values of stage, since the stage signal is directly observable, relatively noise free, and more perfectly harmonic in character (Ateljevich 2001b). The flow chart of the entire nonlinear model is depicted in Figure 7-3, with its full mathematical form modified as below.

$$S(t) = (S_o - S_b) * \exp(-\alpha G^n(t)x(t)) + S_b.$$

Where

x is a harmonic position, reflecting tidal effect, convolution filter,

S_o and S_b are constant ocean and upstream river salinity respectively,

α is a dispersion parameter (consolidating upstream distance),

n is an additional empirical shape parameter,

G is a function representing the flow time-history, aka antecedent flow,

t is time,

exp() is an exponential function.

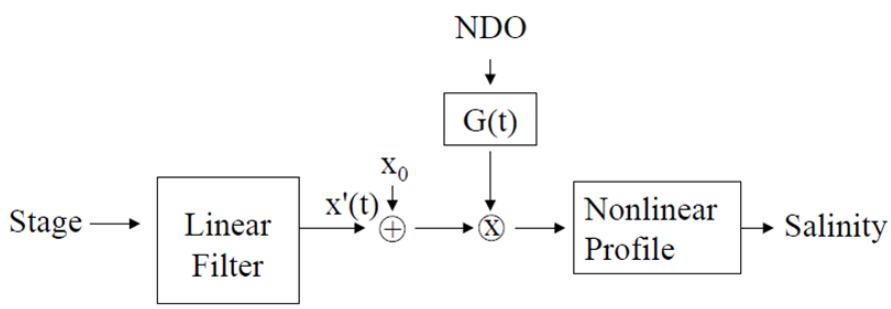

Figure 7-3 Tidal Displacement Model as Embedded in the Full Salinity Model

The final summarized equation is

$$ln\left[E\frac{s(t)-s_b}{s_0-s_b}\right] = \beta_0 + \beta_1 g^n(t) + g(t)\sum_{k=0}^{n_k-1} a_k z(t + k_0\Delta t - k\Delta t).$$

7.2.3 Model Calibration and Problems

The existing model was calibrated for 1991/8/20-1992/9/5 (yellow shaded area in Figure 7-4a), with parameters in the fourth column of Table 7-1 and validated for 1993-1994 (green shaded area in Figure 7-4a). The model output matches the main trend and tidal envelope, with a root mean squared error of 2,828 µs/cm during the validation period (Figure 7-4c).

	Description		Previous calibration	New calibration
Φ	The weighted least squares residuals sum		8.85E+11	4.43E+11
S_o	G-model related	ocean river salinity	32797	35414
S_b		upstream river salinity	200	2333.1
β		system's reaction to Delta outflow	600	419.7845
n		empirical shape parameter	0.75	0.77
A		Correction coefficient of NDO from Delta filling and draining	40000	53662.45
β_0	Tidal coefficient	Convolution filter coefficients for stage	2.76E-03	1.53E-01
β_1			-6.07E-05	-6.00E-05
a_0			1.52E-04	7.40E-05
a_1			-1.05E-05	-1.00E-05
a_2			-2.83E-06	-4.00E-05
a_3			4.96E-05	2.90E-06
a_4			-8.76E-05	-1.00E-04
a_5			7.21E-05	4.60E-05
a_6			-5.18E-05	-1.00E-04

Table 7-1 Previous and New Calibration of Parameters of Martinez Salinity Planning Generator

Newly collected field measurements of last 20 years show that the model underestimates electrical conductivity, (EC), up to 5,000 µs/cm (or the equivalent 5,000 µmhos/cm), at the higher salinity range. Furthermore, this seems to have an upper bound of around 25,000 µs/cm, which is possibly limited by its calibrated parameters.

This salinity underestimation is a concern for water resources operation and planning, especially in the recent continuous drought years. Accordingly, a new thorough and automated calibration is designed in this study.

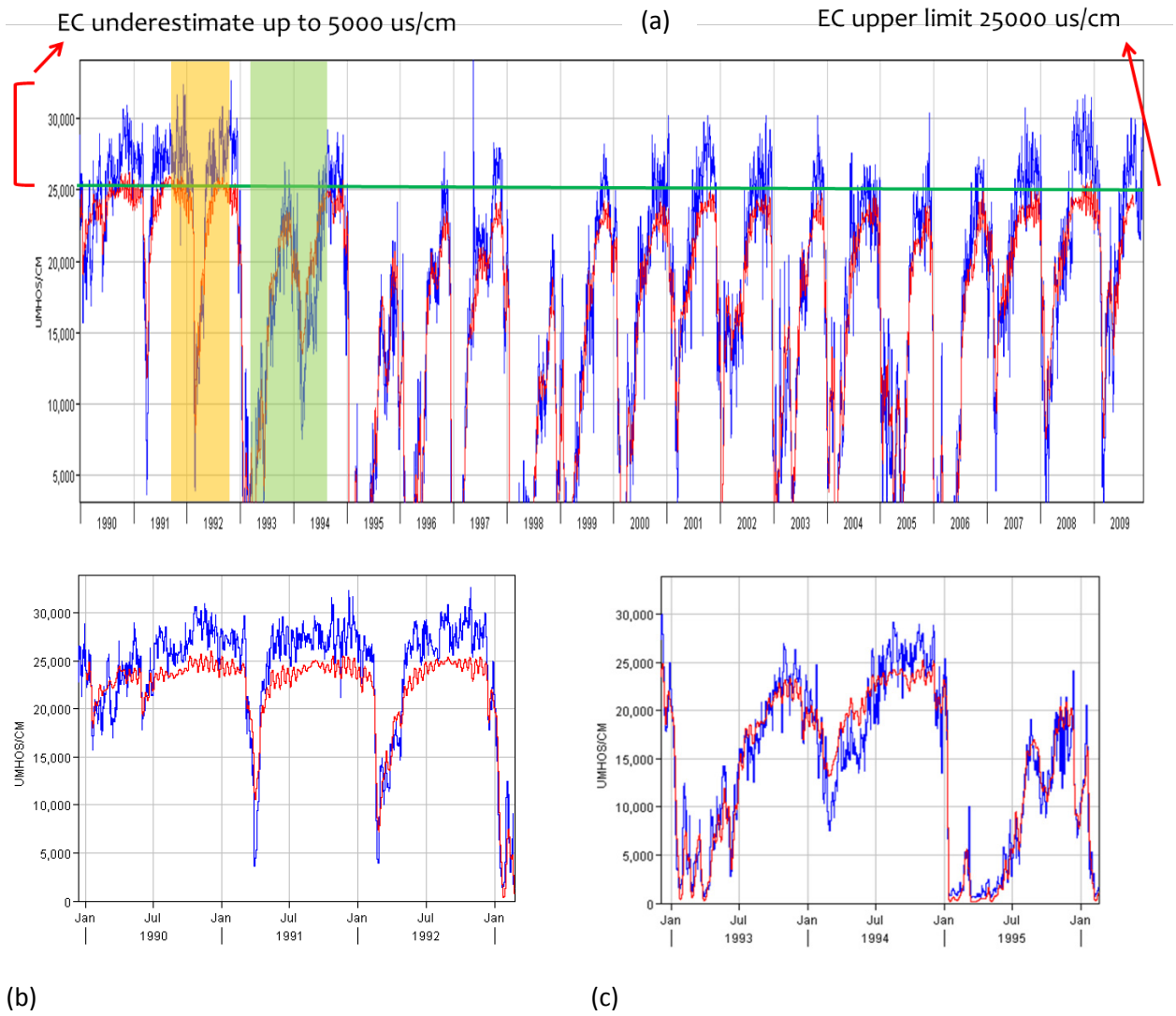

Figure 7-4 Daily Averaged Salinity Comparison between Historical (blue), Old Salinity Generator (red) (enlarged for 1990-1992, 1993-1995)

7.3 Methodology and Study Configuration

PEST, short for Parameter ESTimation, is the industry standard software package for parameter estimation and uncertainty analysis of complex environmental and other computer models, http://www.pesthomepage.org/. It is designed to relieve modelers from manual calibration, which is labor-intensive and subjective (Doherty 2010).

A major feature of PEST is that it is model-independent, so users just need to provide input and output in the required format (Figure 7-5). It has already been used in DWR's Modeling Support Branch for groundwater and surface water model calibrations (Kadir 2006; DiGiorgio 2009; Finch 2014). Details of this methodology and related utility can be found at http://www.pesthomepage.org/.

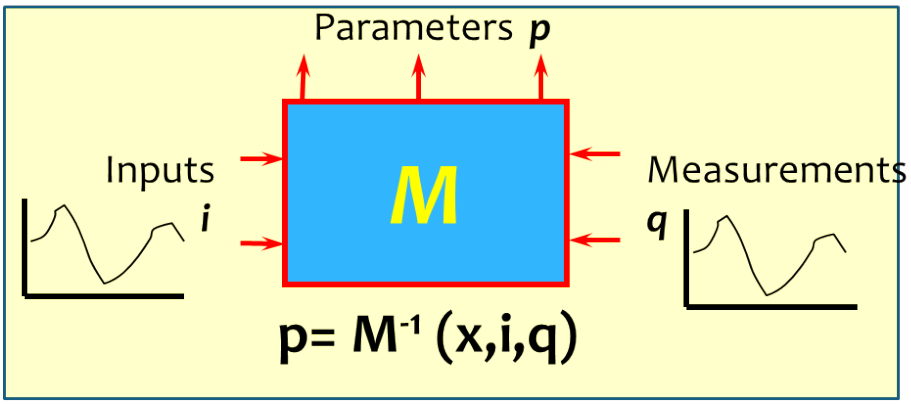

Figure 7-5 Flow Chart for Inverse Problem (parameter estimation) with X as System Configuration

7.3.1 Theory

PEST works by adjusting model parameters to minimize the discrepancies between model outputs and field/laboratory measurements. The discrepancy is formulated below as a single term, weighted least-squares-residuals sum.

$$\text{Objective function: } \Phi = \Sigma\, w_i^2 (q_i - o_i)^2 = \Sigma w_i r_i^2.$$

Where

q as field/lab measurement,

o is model output,

r is residual between field measurement and model output,

w is observation weight,

i is measurement index.

The nonlinear parameter estimation technique PEST uses is called Gauss-Marquardt-Levenberg method (Wikipedia, 2015). It basically constructs the Jacobian matrix of derivatives by using finite differences. It does this by perturbing each parameter independently and running the model to simulate the output at the new value. It then uses a gradient descent method damped by a trust region approach to calculate an updated set of parameters. This process is iterated until an optimal solution is approached.

$$o - o_0 = J\,(p - p_0).$$

$$J_{i,j} = \partial o_i / \partial p_j.$$

Where p is a parameter.

7.3.2 Configuration Setup

There are a couple of versions of the G-Model (described in section 7.2.1) in Bay-Delta Office. One version is used for long-term planning studies. The second version is used for near-term operational simulations. The recalibration described in this chapter using PEST was designed to first study the improvements for long-term planning studies. These improvements and results could be applied in the near-future forecasting G-Model version with Kalman function, which assimilates recent data from neighboring stations to increase the accuracy.

The planning Martinez salinity generator is written in Python scripts, and is included in the DSM2 package. Two of its inputs, Net Delta Outflow (NDO) and stage, are required to be in the format used in the U.S. Army Corps of Engineers' Hydrologic Engineering Center Data Storage System, HEC-DSS. Since PEST uses text files as input and output, wrapping functions are written to enable the data file conversion (Figure 7-6).

- NDO (daily time step) is calculated as the sum of all the Delta boundary flows and exports, with consumptive usage in the Delta Island Consumptive Use (DICU) model version of year 2014, based on California Department of Water Resources (DWR) Bay-Delta Office (BDO) historical data collection.
- Stage (15-minute time step) is the astronomical planning stage at Martinez, also generated by DWR BDO (Ateljevich 2001a).

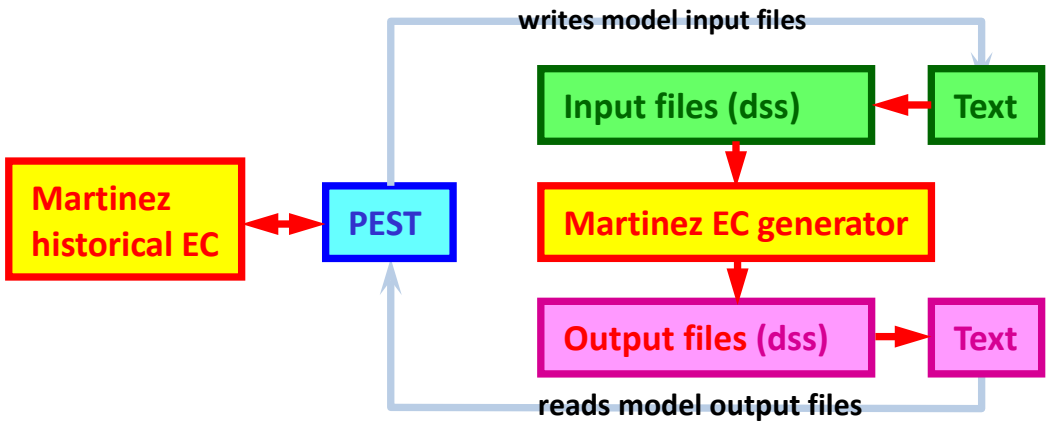

Figure 7-6 PEST Calibration Process of Martinez EC Generator

The model output EC at Martinez (15-minute time step) is compared with the estimation target, its relevant historical data, collected by DWR.

In this study, 14 parameters are determined as adjustable for calibration as shown in Table 7-1. Among which, five parameters are used for G-model daily salinity, and nine parameters are for stage tidal signal. Calibration is conducted first for the former group, with the latter group held constant; then all parameters are calibrated together to match the stage profile. This process is conducted iteratively until a stable result is achieved. Some details of calibration process are:

- Python and Windows-batch scripts have been utilized to develop pre- and post-processors to streamline and automate.
- As a result of the output data limit of the current PEST version, usually the calibration period is selected at less than 2 years and 10 months for 15-minute data.
- Parallel computing utility, BEOPEST, has been utilized on a multicore desktop machine to increase the processing efficiency. Calibration completes in about an hour with typically approximately 20 iterations.
- Different initial values have been tested and do not affect the final convergence much. Details could be referred to the discussion of sensitivity in section 7.4.2.

7.4 Re-Calibration Results and Discussion

The focus of this study is to improve the model suitability at high salinity range, especially the continuous high salinity drought years. Accordingly, 1990-1993 are first selected as the primary calibration period, and the recent 20 years are selected as the validation period.

7.4.1 Calibration for 1991-1993

As shown in Figure 7-7, this study selected 1991/1-1993/9 as the calibration period (yellow shaded area), and 1990-2014 as the validation period. Calibrated parameters are included in Table 7-1. Compared with the old validation outputs (red), the new validation outputs (green) better match the historical data (blue).

- New validation results still match the main trend and tidal envelope well at the moderate-EC range.
- For the low-EC range, new validation results show higher predictions, but this is deliberately ignored as prediction error at the lower range and is not a concern.
- New validation results improve the high-EC range prediction significantly, especially over 25,000 μs/cm (or the equivalent 25,000 μmhos/cm) for most years. Note that in some summers, especially during the recent high-EC period 2012-2014, the predictions from the new calibration still underestimate the observed EC by 2,000-3,000 μs/cm. The reason of this underestimate is still not known, although it is speculated that a more recent calibration data set may result in an improvement.

On the other hand, compared with historical data, model outputs tend to be smoother, while the real data is likely to have more abrupt changes (spikes), especially in the high-EC summer time. This could be caused by local environment variation, like terrain change and weather (e.g., wind) and the current model algorithm cannot represent these details.

7.4.2 Model Improvement and Re-calibration

PEST provides a convenient utility to explore correlation between parameters. Table 7-2 lists part (G-model) of the correlation matrix from calibration of section 7.4.1, with every cell indicating correlation between every two parameters (name of row and column). The closer a value is to 1 or -1, the higher the correlation between those two parameters.

Consequently, this information can be used to achieve parameter parsimony. In this case, S_o has -1 correlation with β_0, totally negatively correlated. It was found that β_0 was introduced with S_o and S_b fixed in the original calibration (Ateljevich 2001b), so it is worthwhile to remove (combine) β_0 to make the model simpler, as shown in the following equation. Calibration was conducted on the modified model. With both Φ and output plot (Figure 7-8) showing that the modified model produces a very similar result, it is safe to claim the validity of β_0 removal.

$$ln\left[\frac{s(t)-s_b}{s_0-s_b}\right] = \beta_1 g^n(t) + g(t)\sum_{k=0}^{n_k-1} a_k z(t + k_0\Delta t - k\Delta t).$$

Where
t is time,
s_0 and s_b are constant ocean and upstream salinities respectively,
β is an empirically determined constant depicting system's reaction to Delta outflow,
g is a function representing the flow-time history,
a, n, and k are convolution filter coefficients.

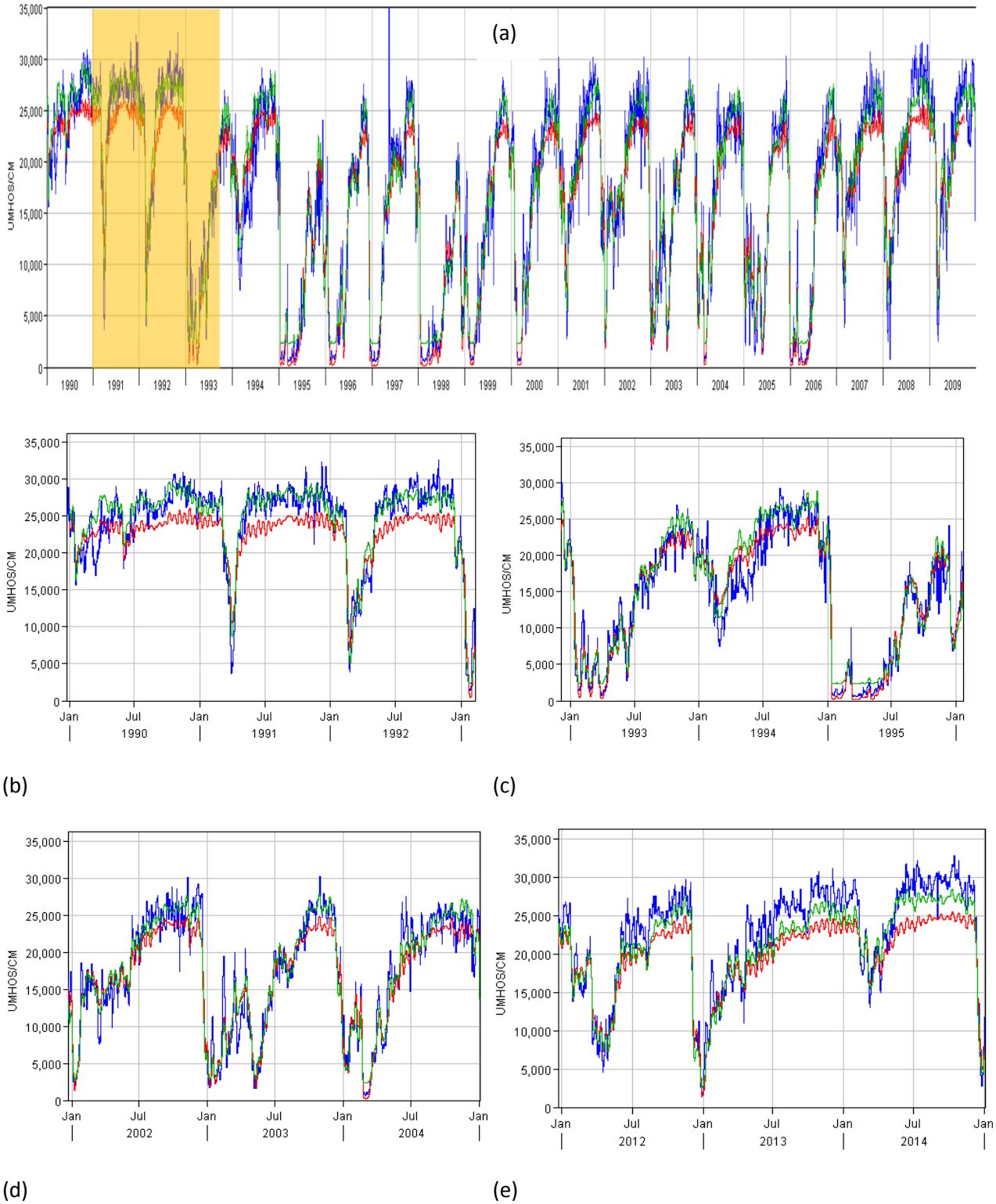

Figure 7-7 Daily Averaged Salinity Comparison Between Historical (blue), Old Generator (red), New Generator (green) Enlarged for 1990-1992, 1993-1995, 2002-2004, 2012-2014

	S_o	S_b	β	n	A	β_0
S_o	1	1.50E-03	-2.11E-04	-3.09E-03	1.90E-04	-1
S_b	1.50E-03	1	-5.88E-02	0.3235	-0.1598	-1.49E-03
β	-2.11E-04	-5.88E-02	1	-4.62E-02	0.2964	2.19E-04
n	-3.09E-03	0.3235	-4.62E-02	1	-0.2933	3.10E-03
A	1.90E-04	-0.1598	0.2964	-0.2933	1	-1.79E-04
β_0	-1	-1.49E-03	2.19E-04	3.10E-03	-1.79E-04	1

Table 7-2 Part of Parameter Correlation Coefficient Matrix of Auto-calibration

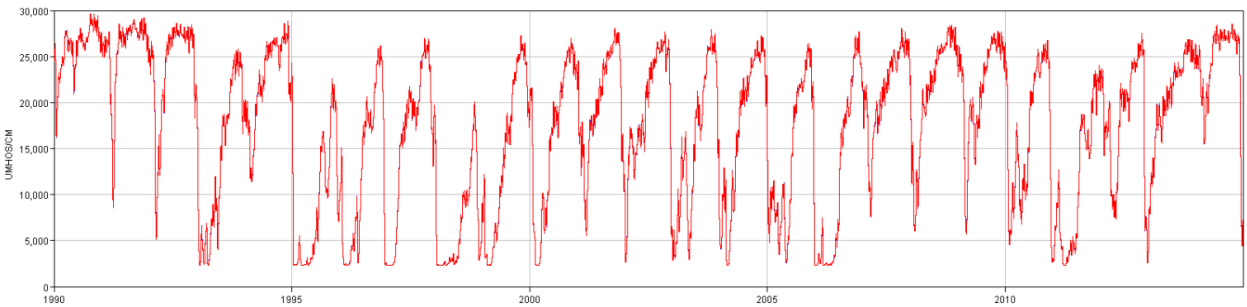

Figure 7-8 Daily Averaged Salinity Comparison Between Old generator (green, with most parts overlapped) and Modified Generator (red)

To quantify the parameters' uncertainty, their 95 percent confidence limits are also calculated, shown in the third and fourth columns of Table 7-3.

	Calibration values	95% percent confidence		Sensitivity	Rel. Sensitivity
Φ	4.46E+11	Lower limit	Upper limit		
S_o	37196	37122.6	3.73E+04	1.91E-03	71.168
S_b	2328.1	2273.29	2382.91	1.72E-03	4.00954
β	420	418.025	4.23E+02	1.90E-02	8.0004
n	0.775	7.69E-01	0.7813	104.992	8.14E+01
A	53411.1	52071.8	5.48E+04	3.91E-05	2.08748
β_1	-6.00E-05	-6.06E-05	-5.94E-05	462591	27.7555
a_0	7.30E-05	6.90E-05	7.70E-05	142668	10.4148
a_1	-1.00E-05	-1.33E-05	-6.74E-06	124834	1.24834
a_2	-3.00E-05	-3.54E-05	-2.46E-05	103390	3.10169
a_3	1.70E-06	-3.37E-06	6.77E-06	106941	0.1818
a_4	-1.00E-04	-1.07E-04	-9.25E-05	126659	12.6659
a_5	4.50E-05	4.09E-05	4.91E-05	122040	5.49179
a_6	-1.00E-04	-1.06E-04	-9.40E-05	110693	11.0693

Table 7-3 Parameters from Auto-calibration of the Modified Martinez Salinity Planning Generator

Correspondingly, the composite parameter sensitivities and relative composite sensitivities are shown in the fifth and sixth columns of Table 7-3. The mathematical definition of composite sensitivity

is shown as below, while the relative composite sensitivity is calculated by multiplying the magnitude of the value of the parameter. The latter represents a measure of the composite changes in model outputs that are incurred by a fractional change in the value of the parameter.

$$s_i = (J^t QJ)_{ii}{}^{1/2}/,$$

Where

J as the Jacobian matrix, and *Q* as the cofactor matrix,

s is sensitivity,

Q is the cofactor matrix.

Those parameters with the much lower sensitivities are regarded as insensitive, e.g., a_3, which corresponds to the larger confidence interval. They reflect that the results of a wider range of calibrated parameter values do not make difference on Φ. On the other side, higher sensitivity represents a narrower range calibrated parameter values, e.g., S_o, n, β_1, are the key parameters and dominate the model performance.

Different initial parameter values were also tested, and their results converge to the same magnitude, although some insensitive parameters, like a_3, may end in different values.

7.4.3 Re-Calibration with Other Periods

Several different calibration periods were selected as comparison groups and the calibrated parameter results are shown in Table 7-4. Some observations are:

- Different target data could result in different calibrated parameters, due to the regression nature of the salinity estimator. Usually high EC is represented by high S_o (ocean salinity boundary).
- These other control groups (2 years 10 months) do not show obvious improvement on objective target ϕ, i.e., match with observed data.
- Since different periods have different target data, they should not be compared directly.

For the purpose of getting a better estimate for high-EC, which is the concern of the study, results of 91/1-93/9 continuous drought period was still used as study target for a general planning estimator.

Calibration period	1991/1-1993/9	1994/1-1996/9	2000/1-2002/9	2006/1-2008/9	2009/1-2011/9	2012/4-2014/12
Φ	4.46E+11	6.06E+11	4.68E+11	7.49E+11	6.58E+11	4.79E+11
S_o	37196	29192	34692	34966	34215	38948
S_b	2328.1	616.58	1082.4	-501.2	988.71	2292.4
β	420	502	386	331	434	407
n	0.775	0.74	0.76	0.73	0.80	0.84
A	53411	51908	60968	39099	73051	48694
β_1	-6.00E-05	-6.0E-05	-6.0E-05	-6.0E-05	-6.0E-05	-8.0E-05
a_0	7.30E-05	1.5E-04	1.0E-04	1.5E-04	8.4E-05	8.0E-05
a_1	-1.00E-05	-1.0E-05	-3.0E-05	-1.0E-05	-4.0E-05	-5.0E-05
a_2	-3.00E-05	-3.0E-06	1.6E-05	-3.0E-06	3.7E-05	6.9E-05
a_3	1.70E-06	5.0E-05	-1.0E-05	5.0E-05	-3.0E-05	-6.0E-05
a_4	-1.00E-04	-9.0E-05	-5.0E-05	-9.0E-05	-2.0E-05	3.6E-05
a_5	4.50E-05	7.2E-05	3.3E-05	7.2E-05	8.7E-06	-2.0E-05
a_6	-1.00E-04	-5.0E-05	-6.0E-05	-5.0E-05	-3.0E-05	-1.0E-06

Table 7-4 Parameters of Auto-calibration from Observations of Different Periods

7.5 Summary and Future Work

In this study, PEST was applied to improve the Martinez salinity generator (G-Model).

- PEST formulates the calibration from manual to systematic automation, relieving people from time-consuming and subjective adjustment.
- PEST newly calibrated parameters produce outputs matching the historical field measurements better than previous calibrated ones.
- This model improvement is important because of its advance in high-EC range, which is the concern in continuous drought years.

Many benefits of PEST have been verified during this study.

- PEST is easy to set up and use for calibration.
- PEST, due to its systematic automation, makes it easy to try different nonlinear additional changes, large number of parameters, and ill-posed problems.
- PEST parallelism performance on modern multicore machines could largely increase efficiency.
- PEST outputs information that helps identify highly correlated parameters.

Future efforts will be spent in the following areas:

- Investigate recent historical information.
- Estimate NDO with another salinity-flow model, DSM2, and with other inputs such as consumptive use, Sacramento River flow, San Joaquin River flow, exports, and gate operations.
- Real-time operation use for forecasting runs.
- Water cost estimations for planning scenarios.

7.6 References

Ateljevich E. 2001a. "Planning Tide at the Martinez Boundary." In: *Methodology for Flow and Salinity Estimates in the Sacramento-San Joaquin Delta and Suisun Marsh*. Chapter 10. Sacramento (CA): California Department of Water Resources.

———. 2001b. "Improving Salinity Estimates at the Martinez Boundary."In: *Methodology for Flow and Salinity Estimates in the Sacramento-San Joaquin Delta and Suisun Marsh. 22nd Annual Progress Report*. Chapter 11. Sacramento (CA): California Department of Water Resources.

Denton R. and Sullivan G. 1993. "Antecedent Flow-salinity Relations: Application to Delta Planning Model. In: *Methodology for Flow and Salinity Estimates in the Sacramento-San Joaquin Delta and Suisun Mars. 34th Annual Progress Report*. Sacramento (CA): California Department of Water Resources.

DiGiorgio CL. 2009. "Data Quality Associated with EC Values in the DICU Model." In: *Methodology for Flow and Salinity Estimates in the Sacramento-San Joaquin Delta and Suisun Marsh. 30th Annual Progress Report*. Chapter 2. Sacramento (CA): California Department of Water Resources.

Doherty J. 2010. *PEST, Model-Independent Parameter Estimation:* 5th Edition. Watermark Numerical Computing.

Finch R. 2014. "Quantitative Calibration of DSM2." In: *Methodology for Flow and Salinity Estimates in the Sacramento-San Joaquin Delta and Suisun Marsh. 35th Annual Progress Report*. Chapter 2. Sacramento (CA): California Department of Water Resources.

Kadir T. 2006. "Estimates for Consumptive Water Demands in the Delta using DETAW.: In: *Methodology for Flow and Salinity Estimates in the Sacramento-San Joaquin Delta and Suisun Marsh. 27th Annual Progress Report*. Sacramento (CA): California Department of Water Resources.

Wikipedia. 2015. Gauss-Marquardt-Levenberg algorithm. Viewed online at:https://en.wikipedia.org/wiki/Levenberg%E2%80%93Marquardt_algorithm. Accessed: 2015.

Methodology for Flow and Salinity Estimates in the Sacramento-San Joaquin Delta and Suisun Marsh

36th Annual Progress Report
June 2015

Chapter 8
Bay-Delta SCHISM Model Developments and Applications

Authors: **Eli Ateljevich, Kijin Nam, Lianwu Liu, Subir Saha, Rueen-fang Wang**
Delta Modeling Section
Bay-Delta Office
California Department of Water Resources

Joseph Zhang
Virginia Institute of Marine Sciences

Contents

8 Bay-Delta SCHISM Model Developments and Applications 8-1
8.1 INTRODUCTION 8-1
8.2 PUBLIC RELEASE 8-1
8.3 APPLICATIONS 8-2
8.3.1 Drought Modeling and Emergency Barriers. 8-2
8.3.2 Temperature Calibration 8-2
8.3.3 Flood Robustification 8-4
8.3.4 Liberty Island and Yolo County 8-4
8.4 ALGORITHMIC IMPROVEMENTS 8-4
8.5 REFERENCES 8-6

Figures

Figure 8-1 From a Study of Circulation Patterns in Franks Tract With and Without Barriers 8-3
Figure 8-2 A Stretch of the San Joaquin River with the Original (left) and Fully Delineated (right) Floodplain 8-4
Figure 8-3 New LSC^2 Mesh with Vanishing Layers and Shaved Cells 8-5

8 Bay-Delta SCHISM Model Developments and Applications

8.1 Introduction

The Bay-Delta SCHISM project is an application of the 3D SCHISM (Semi-Implicit Cross-Scale Hydroscience Integrated System Model) that offers the capability to study cross-scale, multidimensional flow and transport in the Bay-Delta. SCHISM is an open source, 3D computational model derivative from an earlier model, SELFE. We have incorporated into SCHISM practical details needed to model the Bay-Delta, such as agricultural sources and sinks, gates and seasonal gates, and barriers. Work on the model has been collaborative with the Virginia Institute of Marine Science (VIMS) and other users.

The model has been deployed for studies over the full domain for two years by California Department of Water Resources (DWR), and we have begun offering institutional support through workshops. The model has also been used as the estuary hydrodynamic component of multidisciplinary collaborations with National Aeronautics and Space Administration (NASA), National Marine Fisheries/National Oceanic and Atmospheric Administration (NOAA), and San Francisco State University, including the SESAME project, a full life cycle model for fish, and NASA-HICO, a remote sensing and nutrient modeling analysis of human impacts.

Development in the past year has emphasized a public release, drought applications, and algorithm improvements. Progress has been made towards diverse capabilities, such as robust flood modeling and temperature calibration. This report surveys some of the work, much of which is in progress.

Last year we reported the model suite under the name SELFE. Around the time of our workshop, the VIMS branch of development of SELFE was renamed. Developments on this version of the model are publically available under the Apache open source license.

8.2 Public Release

The Bay-Delta application of SCHISM, including input files, tutorials, and numerous support tools are now publically distributed at:
http://baydeltaoffice.water.ca.gov/modeling/deltamodeling/models/bay_delta_schism/.

Links to the executable and VIMS source bundle are also found on this website.

Under the auspices of the California Water and Environmental Modeling Forum (CWEMF), DWR and VIMS conducted managerial and hands-on workshops on SCHISM in December 2014 and January 2015. The purpose of the December workshop was to inform potential stakeholders of the capabilities of the model and to describe possible modes of involvement. The January hands-on workshop spanned nine days over three weeks. It emphasized a review of tidal and mixing processes in the estuary and how they are related to our modeling assumptions, meshing decisions, and algorithmic switches in different parts of the estuary. The DWR computer training capacity of 15 users was fully subscribed, with about half of the participants coming from DWR and half from other agencies.

The biggest barrier to entry operating SCHISM is access to high performance computing (HPC). The mesh resolution of SCHISM is intended to resolve the primary velocity field in major channels. This is really just medium resolution in terms of the physics, but given the extent and complexity of the domain, the problem is computationally burdensome on traditional hardware. Algorithmic improvements described in the next section offer hope that SCHISM will perform meaningful simulations on very high-quality personal computers, at least on shorter time scales.

In the meantime, we and others apply the model over the full Bay-Delta using high performance computing clusters that allow reasonable run times and scaling to larger problems such as the detailed near-scale study of drought barriers. It has not proven difficult for DWR modelers to get used to these types of systems for basic model operation, and such systems are routinely used by oceanographers and coastal modelers. Regardless, only institutional users (DWR, NASA, NOAA, Lawrence Berkeley National Laboratory [LBNL], and some universities) and large consulting firms have regular access to such technologies in-house. Because we have an interest not only in dissemination of the model, but also in establishing redundant platforms for our own use, DWR has tested a small number of commercial cluster services that are available on a commercial basis, including Penguin-on-Demand (POD) and Amazon Web Services (AWS). Of the two, POD offers scientific cluster capabilities that are most compatible with SCHISM and scales up to 128 processing cores with similar performance to our in-house computer. We intend to conduct similar benchmarks on San Diego Supercomputing Center's new Comet supercomputer, which offers time commercially on a discretionary basis. For DWR, these facilities provide redundant capabilities to ensure we can do runs during periods of congested resources For others, they represent a platform to run SCHISM on multi-year studies. We would like to facilitate the sharing of compiled code and data on these systems.

8.3 Applications

8.3.1 Drought Modeling and Emergency Barriers.

The most specific role that SCHISM has played in drought management has been to identify changes in velocities and circulation patterns near the False River Emergency Drought Barrier. Simulations were carried out in 2014 and 2015 to identify locations in Fisherman's Cut, Old River, and Dutch Slough that might be vulnerable to scour if the barriers were installed. In addition, simulations were performed to show how velocity patterns in Franks Tract might be affected by the closure, how this would change the residence time of different areas of the tract and change the likelihood of toxic algal bloom. Example output is shown in Figure 8-1 for a moment after peak flood tide.

SCHISM was extensively recalibrated for drought in 2014; this is the version that is publically available. SCHISM can now model seasonal salinity changes with the barriers in place, including sensitivity to differing models of agricultural consumptive use. The emphasis with SCHISM has been on showing regional changes in circulation, and demonstrating how the False River Emergency Drought Barrier works.

8.3.2 Temperature Calibration

In collaboration with VIMS and using boundary conditions and assumptions supplied by Resource Management Associates (RMA) as part of the calibration of temperature for DSM2, we are most of the way through a temperature calibration for SCHISM. Our partners at VIMS are currently able to model temperature successfully in much of the Bay-Delta, and we are currently working on methods for handling the ocean boundary robustly and accurately. So far, our SESAME partners have supplied boundary conditions from a 3D model of the near coast (CENCOOS ROMS model), and this method holds some promise (e.g., real-time modeling with short-term predictions and hindcasts from the past decade) when this off-shore data modeling data is available. Results in the Delta do not appear to be sensitive to assumptions on the ocean boundary.

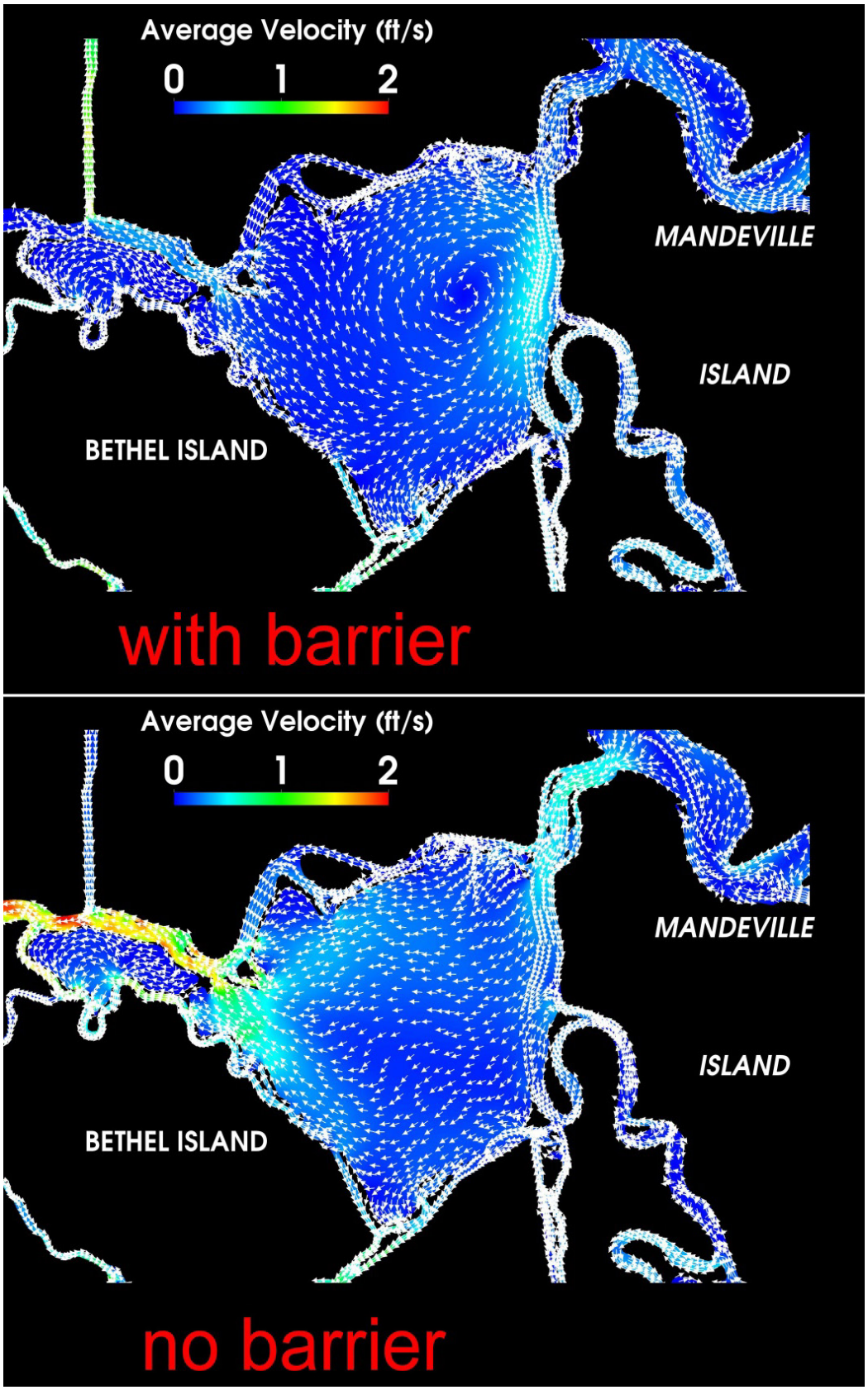

Figure 8-1 From a Study of Circulation Patterns in Franks Tract With and Without Barriers

8.3.3 Flood Robustification

SCHISM was calibrated during 2009-2010, which was a fairly low water period. Because of interest by the DWR Division of Flood Management, in February we began investigating the use of SCHISM for significant storm events and island flooding, using 1997 as a model. Floods require much more thorough delineation of floodplains along the major rivers emptying into the San Joaquin, Old, and Middle rivers (Figure 8-2) than we originally used for general tidal modeling.

This work is still in calibration and will be reported in more detail in coming months. Further work may be necessary to stably model extreme (100-year return period) floods coincident with storm surge.

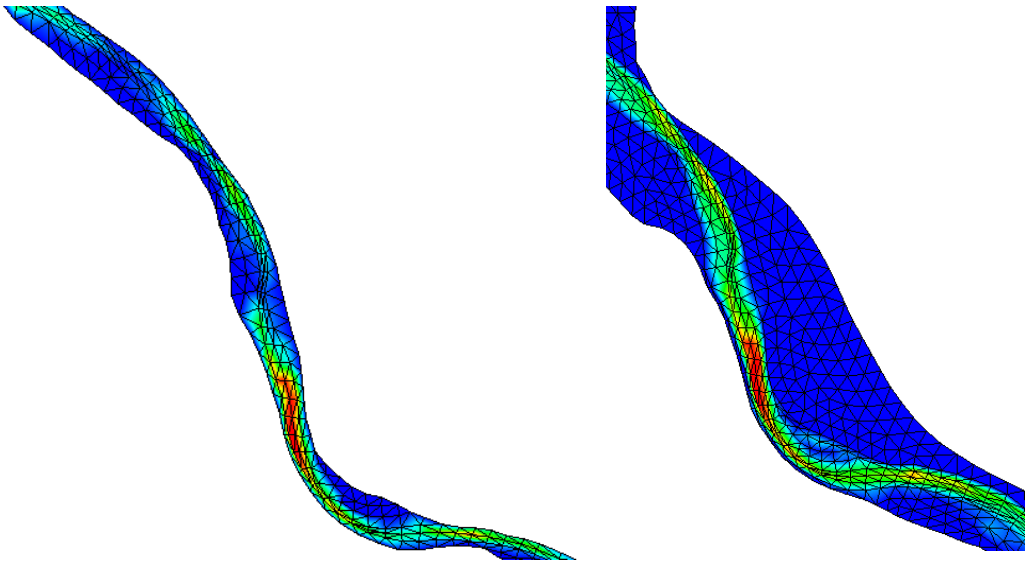

Figure 8-2 A Stretch of the San Joaquin River with the Original (left) and Fully Delineated (right) Floodplain

8.3.4 Liberty Island and Yolo Bypass

For our 1997 flooding project, Yolo Bypass was modeled as a boundary condition, but explicit modeling of the bypass is in development as well. For Yolo Bypass, a key challenge has been gracefully transitioning from the fairly small scale processes of summer flows around Liberty Island and incipient flooding to full floods. We are discussing how insights gained from this project can be used to improve the DAYFLOW index of net Delta outflow.

8.4 Algorithmic Improvements

This year, three improvements to SCHISM will be released that can increase the model's performance and accuracy.

Quadrilateral elements. SELFE and SCHISM were originally restricted to triangular meshes. Quadrilaterals are thought to be a more efficient meshing shape and will allow channelized regions to be covered with the same number of nodes, but roughly half of the elements. The count, after this conversion, is anticipated to be 180,000 elements instead of 250,000, with no loss of fidelity in the bathymetry. Although quadrilaterals have been supported by SCHISM for some time, the transition to quadrilaterals is not anticipated until the end of the year because we have to carefully test and adjust

for its effects on calibration and retool our visualization pre-, and post-processing tools to handle a hybrid triangle-quadrilateral mesh.

Local sigma coordinates with shaved cells (LSC^2). In Zhang et al. (2015), we introduced a new vertical mesh in SCHISM that is still terrain-following, but transitions in the number of layers between regions of deep and shallow terrain. Figure 8-3 shows a section of mesh in steep terrain in the Bay-Delta with the vertical direction greatly exaggerated. Note that vertical layers vanish gradually as the mesh advances into shallower areas. The new mesh remedies some numerical difficulties that nag terrain-following coordinates, such as pressure discretization errors and spurious diapycnal mixing (transport across the density gradient). On a practical note, this innovation will eliminate the restriction under traditional S coordinates that all regions of the estuary have the same number of layers. Since the Delta is mostly shallow, this will result in a vast reduction of nuisance resolution caused by the crowding of S layers in upstream reaches.

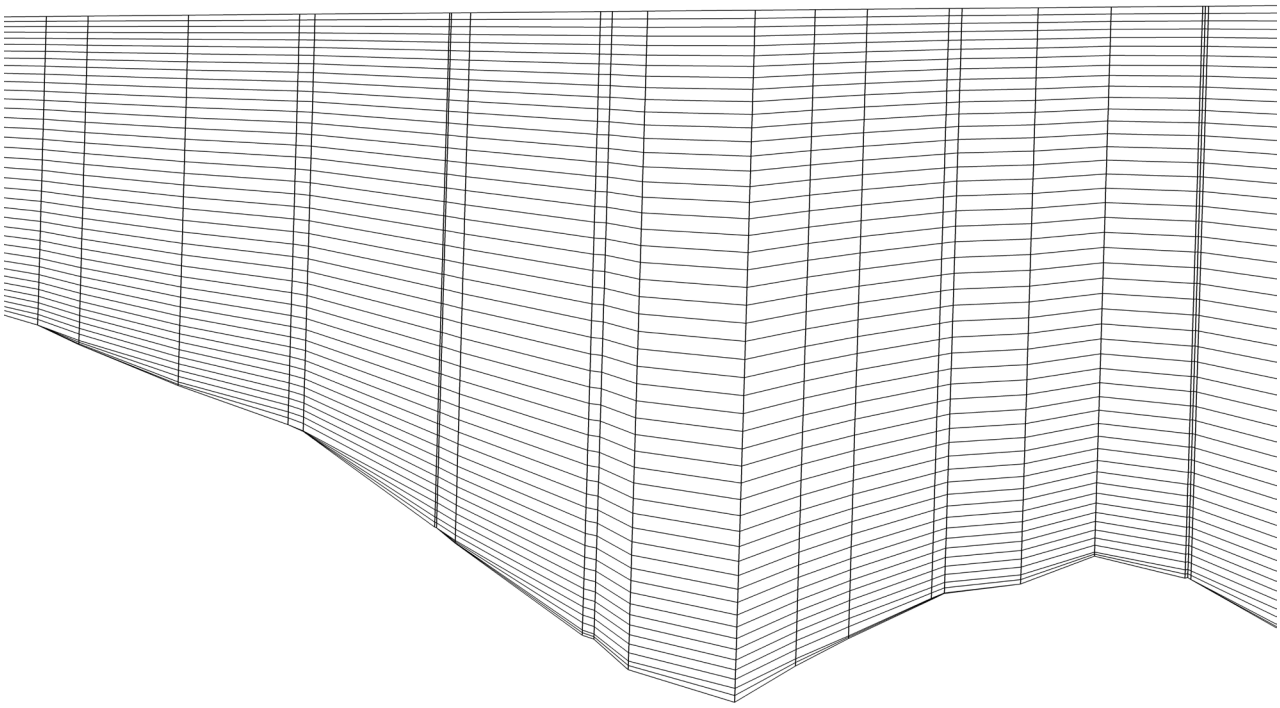

Figure 8-3 New LSC^2 Mesh with Vanishing Layers and Shaved Cells

Note: The apparently variable horizontal lengths of the prism are caused by drawing a straight line across triangles.

Implicit, TVD transport algorithm. Until recently, the high-resolution transport option in SCHISM was adopted from Casulli and Zanolli (2005). When a terrain-following mesh is used, the time-step restrictions of this algorithm can become a costly controlling factor on performance. Recently, Fei Ye of VIMS introduced a new algorithm to SCHISM, based on work by Duraisamy and Baeder (2007), that enjoys accuracy and non-oscillatory behavior at least on par with as the original algorithm, but with more relaxed performance restrictions.

8.5 References

Ateljevich E, Nam K, Zhang Y, Wang R, Shu Q. 2014. "Bay Delta Calibration Overview." In: *Methodology for Flow and Salinity Estimates in the Sacramento-San Joaquin Delta and Suisun Marsh. 35th Annual Progress Report*. Sacramento (CA): California Department of Water Resources.

Casulli V and Zanolli P. 2005. "High Resolution Methods for Multidimensional Advection-Diffusion Problems in Free-Surface Hydrodynamics." Ocean Modelling. pp. 137-151.

Duraisamy K and Baeder J. 2007. "Implicit scheme for Hyperbolic Conservation Laws using Nonoscillatory Reconstruction in Space and Time." SIAM Journal on Scientific Computing. pp. 2607-2620.

Zhang Y, Ateljevich E, Yu, H-C, Wu C-H, Yu J.C.S. 2015. "A New Vertical Coordinate System for a 3D Unstructured-grid Model." Ocean Modelling. 85. pp. 16-31.